Villanova University

The Graduate School

Department of Civil and Environmental Engineering

QUANTIFYING EVAPOTRANSPIRATION IN GREEN INFRASTRUCTURE: A GREEN ROOF CASE STUDY

A Thesis In

Civil and Environmental Engineering

by Meghan Marie Feller

Submitted in partial fulfillment

of the requirements

for the degree of

Master of Science in Civil Engineering

December 2011

QUANTIFYING EVAPOTRANSPIRATION IN GREEN INFRASTRUCTURE: A GREEN ROOF CASE STUDY

By

Meghan Marie Feller

December 2011

12 Dec 2011

Robert G. Traver, Ph.D., P.E., D.WRE — Date
Professor, Department of Civil and Environmental Engineering
Director, Villanova Urban Stormwater Partnership
Director, Villanova Center for the Advancement of Sustainable Engineering

13 Dec 2011

Bridget M. Wadzuk, Ph.D. — Date
Associate Professor, Department of Civil and Environmental Engineering

12/14/11.

Ronald A. Chadderton, Ph.D., P.E., D.WRE — Date
Professor, Department of Civil and Environmental Engineering
Chairman, Department of Civil and Environmental Engineering

12/15/11

Gary A. Gabriele, Ph.D. — Date
Dean of the College of Engineering

TABLE OF CONTENTS

APPENDICES

LIST OF TABLES

LIST OF FIGURES

NOMENCLATURE

d	zero plane displacement height [m]
d_r	inverse relative distance between the Earth and the Sun [dimensionless]
$e°(T)$	saturation vapor pressure [kPa]
e_a	actual vapor pressure [kPa]
e_s	mean saturation vapor pressure [kPa]
$e_s - e_a$	vapor pressure deficit [kPa]
h	vegetation height [m]
k	von Karman's constant, 0.41 [dimensionless]
r_a	aerodynamic resistance [s m^{-1}]
u_z	wind speed at height "z" meters [m s^{-1}]
z	elevation above mean sea level [m]
z_h	height of humidity measurements [m]
z_m	height of wind measurements [m]
z_{oh}	roughness length governing heat and vapor transfer [m]
z_{om}	roughness length governing momentum transfer [m]
C_p	specific heat at constant pressure, 1.013 x 10^{-3} [MJ kg^{-1} °C $^{-1}$]
G_{sc}	solar constant, 0.0820 [MJ m^{-2} min^{-1}]
J	integer between 1 and 365 corresponding to day of the year [dimensionless]
P	atmospheric pressure [kPa]
R	specific gas constant, 0.287 [kJ kg-1 K-1]
R_a	extraterrestrial radiation [MJ m^{-2} day^{-1}]
R_{nl}	net outgoing longwave radiation [MJ m^{-2} day^{-1}]

R_{ns} net shortwave radiation [MJ m^{-2} day^{-1}]

R_s incoming solar radiation [MJ m^{-2} day^{-1}]

R_{so} clear sky radiation [MJ m^{-2} day^{-1}]

RH daily relative humidity [%],

T daily mean air temperature [°C]

T_K absolute temperature [K] (273.16 + T [°C])

T_{kv} virtual temperature given[K]

$T_{max,K}$ maximum absolute temperature during a 24-hour period [K]

$T_{min,K}$ minimum absolute temperature during a 24-hour period [K]

Greek symbols

α albedo or canopy reflection coefficient [dimensionless]

γ psychrometric constant [kPa $°C^{-1}$]

δ solar declination [rad]

ε ratio of the molecular weight of water vapor to that of dry air, 0.622 [dimensionless]

λ latent heat of vaporization [MJ kg^{-1}]

ρ_a density of the air [kg m^{-3}]

σ Stefan-Boltzmann constant, 4.903 x 10-9 [MJ K-4 m-2 day-1]

φ latitude of the site [rad]

ω_s sunset hour angle [rad]

Δ slope of the saturation vapor pressure curve [kPa $°C^{-1}$]

Subscripts

min minimum

max maximum

ABSTRACT

Advancements in the stormwater management field have resulted in a shift to continuous flow monitoring and modeling. While this transition has resulted in more efficiently designed stormwater control measures (SCM), it has necessitated a better understanding of the water budget, particularly an estimation of evapotranspiration (ET), to correctly represent the functioning of these facilities.

The purpose of this research is to quantify the evapotranspiration component of the water budget for a green roof, located on the campus of Villanova University, and determine if current predictive equations for evapotranspiration are applicable in stormwater control measure (SCM) design. This thesis outlines the methods used to quantify ET, including the construction of a weighing lysimeter atop the green roof. Results were compared to several predictive equations commonly used in the agriculture industry, including the Penman and Penman-Monteith equations, to determine their applicability as a predictive design tool.

Based on the data collected, both the Penman and Penman-Monteith equations produced reasonable estimates of ET, with the Penman-Monteith equation providing slightly better results than its foundational counterpart, the Penman equation. The significance of the Penman equation should not, however, be neglected due to its ability to provide reasonable results without calibration.

This paper also illustrates the significance of evapotranspiration as a major component in the water budget of the Villanova Green Roof. Based on the observed lysimeter results and the

Penman and Penman-Monteith equations, this study indicates that over 65% of rainfall on the green roof was mitigated through ET during the 2009 growing season.

Continued research on this and other green roofs across the country and around the world will provide a better understanding of the seasonal and geographic trends in evapotranspiration and the broader applicability of both the Penman and Penman-Monteith equations for estimating ET. These advances will ultimately allow for a tailored design of green roofs to maximize their function as a stormwater mitigation facility.

1 INTRODUCTION

It has become increasingly evident that the preservation of our natural resources, particularly water resources, is one of the most critical concerns of society today. An understanding of the hydrologic cycle is key to the proper design and implementation of water resources management practices. Solar energy and gravitational forces drive the hydrologic cycle. These forces facilitate the transport of water from the earth's surface, via evaporation and transpiration, to the atmosphere where it is transported around the world in the form of water vapor. This water eventually condenses, falling back to earth in the form of rain or snow that is then intercepted by plants and infiltrated into the soil, recharging the groundwater. Precipitation that is not infiltrated generates runoff that enters streams, rivers, lakes and oceans, where the cycle begins again. (Maidment 1993). When an area of land is developed, the cycle is disrupted. These changes can be quantified by the hydrologic budget (water budget) which accounts for the inflow, outflow, and storage of a particular hydrologic system. Water that was previously infiltrated into the soil and reintroduced to the ground water supply can no longer penetrate the newly developed impervious surfaces, and thus results in increased peak runoff rates, runoff volumes, and pollutant loads that erode rivers and streams and degrade their ecosystems. The field of stormwater management aims to alleviate the effects of land development through storage and controlled release or via capture then infiltration (ground water recharge) and/or evapotranspiration of stormwater runoff. Until recently, the primary stormwater management methods focused on large (2 to 100 year) rainfall events via detention facilities. These sites are designed to reduce the peak rate of runoff so that it does not exceed pre-development conditions. While these

facilities target a critical issue in stormwater management, they fail to contribute substantially to volume reductions or water quality improvements and on a watershed basis, are actually capable of increasing the peak flows by altering the timing of the hydrograph and extending the duration of peak flow discharge. (McCuen 1979).

A series of stormwater practices have been proposed and implemented that intend to mimic the natural (pre-development) water budget. These are commonly referred to as stormwater control measures (SCM) and include, but are not limited to, constructed wetlands, bioinfiltration, bioretention, raingardens, permeable pavements, and green roofs. These sites aim to reduce peak flow rates through runoff capture, reduce runoff volume through infiltration and evapotranspiration, and increase pollutant removal through sedimentation and filtration through surface soils. To determine the effectiveness of these SCMs in reducing peak runoff rates and volumes and their ability to enhance water quality, it is important to understand and accurately quantify each component of the water budget. The water budget is a quantification of the inflow (precipitation, runoff), outflow (overflow, infiltration, evapotranspiration), and storage (soil moisture content) of water in a hydrologic system (Viessman and Lewis 2003). This study focuses on the quantification of the evapotranspiration portion of the water budget for a green roof. The SCM studied is a part of the Villanova Urban Stormwater Partnership (VUSP) demonstration park located on the campus of Villanova University in Pennsylvania.

1.1 **Green Roofs**

While the origins of the green roof date back to ancient Mesopotamia (Osmundson 1999), it was not until the 1960s that they were recognized as an effective method to improve the quality of the urban environment. Though research in Germany and other parts of Europe supported the claims of environmental and economic benefits for both the private and public sectors, these technologies were rarely seen in the United States until recently. Based on the type of green roof, some recognized benefits include stormwater runoff reductions, reductions in urban heat islands, building heat and sound insulation, increased roof lifespan, water and air quality improvements, and increases in wildlife habitats.

There are two major types of green roofs, extensive and intensive. Intensive roofs, depending on their application, consist of a soil base-course that can be as shallow as 15-20 centimeters and as deep as 4.5 meters, though, they are typically less than one meter deep. Architectural features can include anything from pathways to water fountains and herbs to small trees. Intensive roofs typically are more costly than external roofs, require periodic maintenance, and require a more robust structural frame on the underlying building. An extensive green roof consists of a base course that is less than fifteen centimeters deep and typically a lightweight growth medium in which sedums and other succulents can grow. These roofs are designed to meet specific engineering and performance criteria. These structures are low cost because they require minimal, if any, added structural support for the underlying building They are also low maintenance because the plant species are drought, disease, and insect resistant, while weeds and other invasive species cannot typically survive in the shallow soils without frequent rainfall.

1.1.1 *The Villanova Green Roof*

The Villanova University Facilities Department, in conjunction with the Civil and Environmental Engineering Department, constructed an extensive green roof as a retrofit to an existing conventional roof in July of 2006. The green roof is located on Villanova's Center for Engineering Education and Research (CEER) building (Figure 1.1 and Figure 1.2).

Figure 1.1. Villanova University Green Roof (May 2007).

The green roof is approximately 53 square meters, capturing only direct precipitation. The existing roof was resurfaced and resealed before an insulation mat and drainage layer were installed. A fabric layer served as a soil and root barrier to the underlying drainage course. Designed to capture the first half-inch of precipitation, three to four inches of growth media and a series of sedums were placed to complete the retrofit. Figure 1.3 is a representative cross section of the layers that comprise a typical extensive green roof.

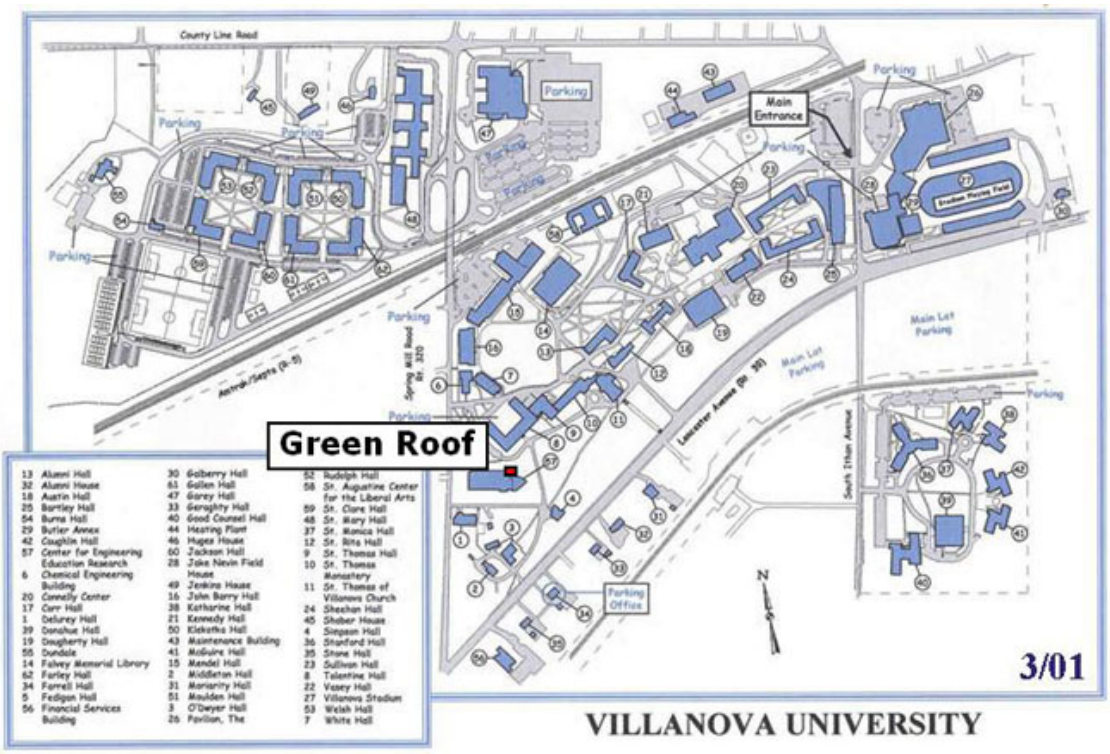

Figure 1.2. Villanova University Green Roof Location

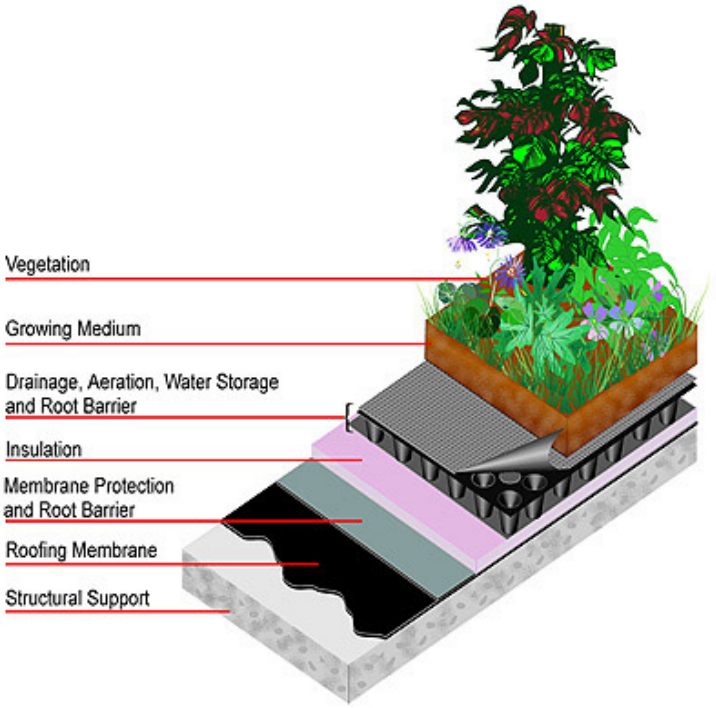

Figure 1.3. Typical Extensive Green Roof Cross Section (Source: American Wick Drain Corporation)

Rooflite® extensive, an engineered growth media created by Skyland USA, LLC, was used on the Villanova Green Roof. This product was chosen because it is lightweight, maintains a good balance (based on FFL standards (FFL 2002)) of water retention and air filled porosity, and provides an ideal growing media for hardy succulents like sedum to prosper while invasive plants cannot. Appendix A provides detailed specifications of the roof media as well as an analysis of performance based on FFL standards.

The vegetation on the Villanova Green Roof consists of a series of sedums; chosen because of their resilience in extreme climates, including heat, direct sunlight, wind, and drought (Villarreal and Bengtsson 2005). These plants are also tolerant of salts and insects as well as resistant to most diseases (Snodgrass 2010). A complete list of the original plant species and the planting scheme used on the Villanova Green Roof is provided in Table 1.1 and Figure 1.4, respectively. These plants have been shown to increase the evapotranspiration rates from a roof (when compared to bare soil media), particularly when water is readily available (several days following a rainfall event) (Berghage, Jarrett et al. 2007).

Table 1.1. Villavova Green Roof Vegetation List

	Scientific Name	Common Name
1	Sedum acre “Aureum”	Golden Stonecrop
2	Sedum album “Murale”	Murale White Stonecrop
3	Sedum album “Coral Carpet”	Coral Carpet Stonecrop
4	Sedum kamtschaticum var. floriferum "Weihenstephaner Gold"	Orange Stonecrop
5	Sedum hybridum "Immergrunchen"	Evergreen Sedum
6	Sedum Reflexum “Blue Spruce”	Jenny’s Stonecrop
7	Sedum sexangulare	Six-sided Stonecrop
8	Sedum spurium “Fuldaglut”	Two-row Stonecrop

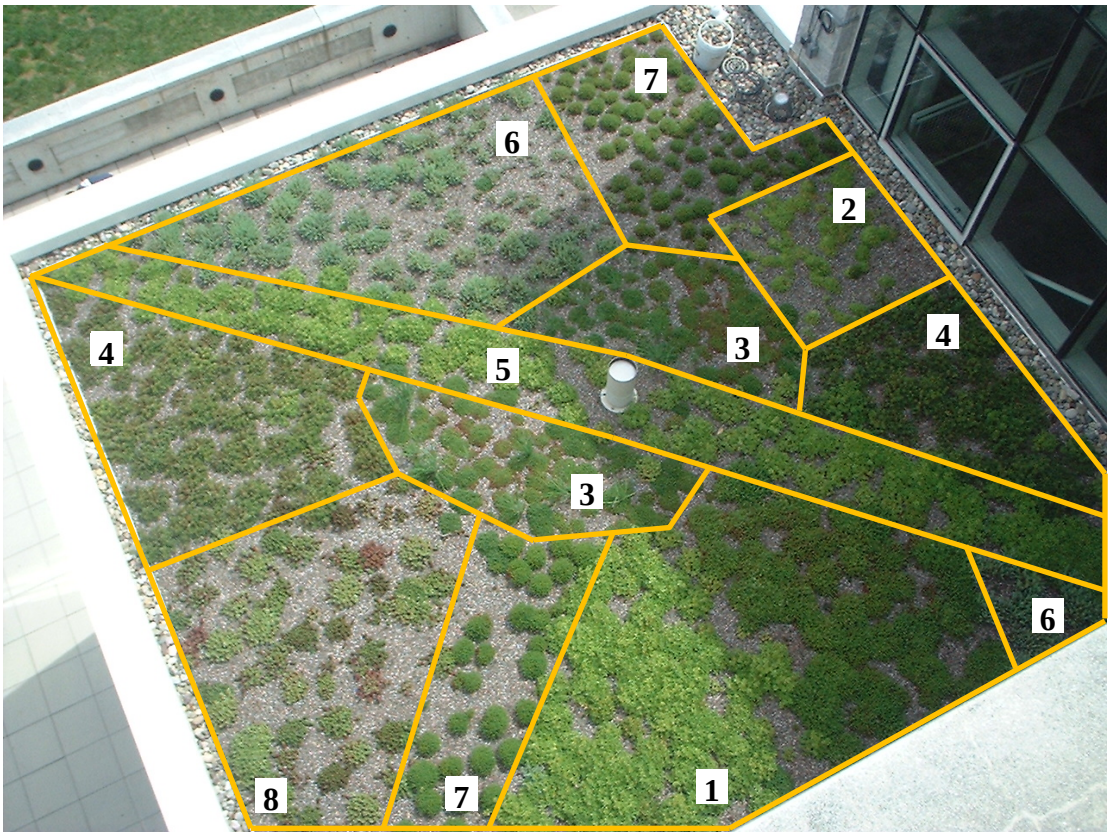

Figure 1.4. Villanova University Green Roof Planting Scheme

This site serves primarily as a research site, and is thus instrumented accordingly. To estimate the quantitative benefits of the green roof, a rain gage and flow meter (located at the overflow structure) are used to measure inflow (precipitation) and overflow

(precipitation in excess of the storage capacity of the green roof), respectively. In an effort to quantify the thermal benefits of the green roof, several temperature sensors were installed, one located on a non-vegetated portion of the roof to serve as a control, one located on the green roof, and two located below the growth medium of the soil. For the purposes of this research, a small weather station was installed on the roof to measure a series of climatological parameters critical to the estimation of evapotranspiration from the green roof. Instrumentation included a temperature and relative humidity probe, solar radiation sensor, and wind speed sensor (not pictured). Figure 1.5 is an aerial photograph of the green roof from (Oct. 2009). Figure 1.6 is a schematic of the instrumented Villanova Green Roof. Further information regarding the instrumentation of the site will be discussed in Chapter 3. Supplementary information regarding the GR can be found in Tokarz (2006) and Rudwick (2008).

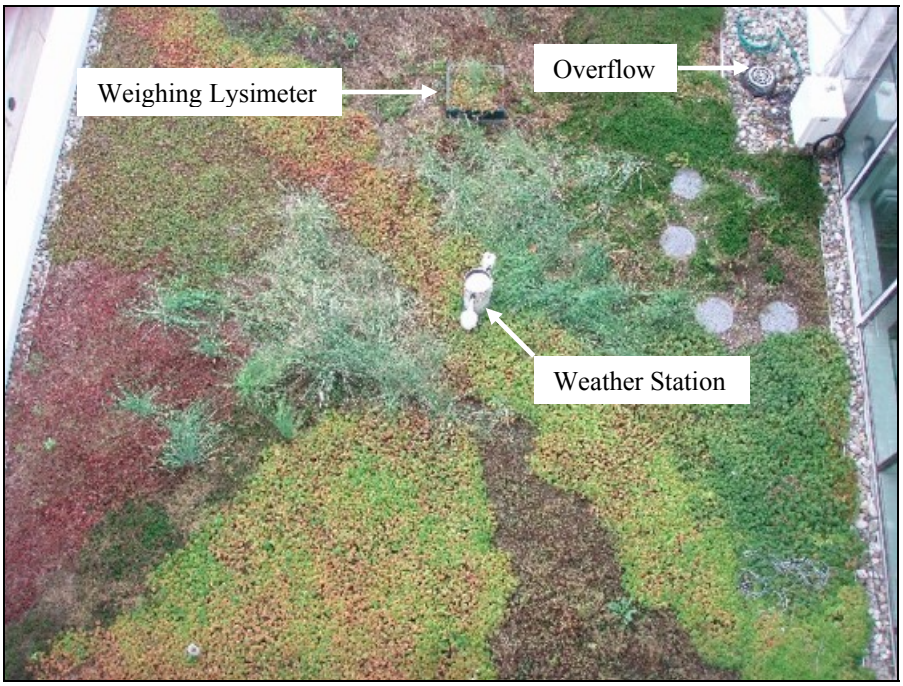

Figure 1.5. Aerial Image of the Villanova Green Roof (October 2009)

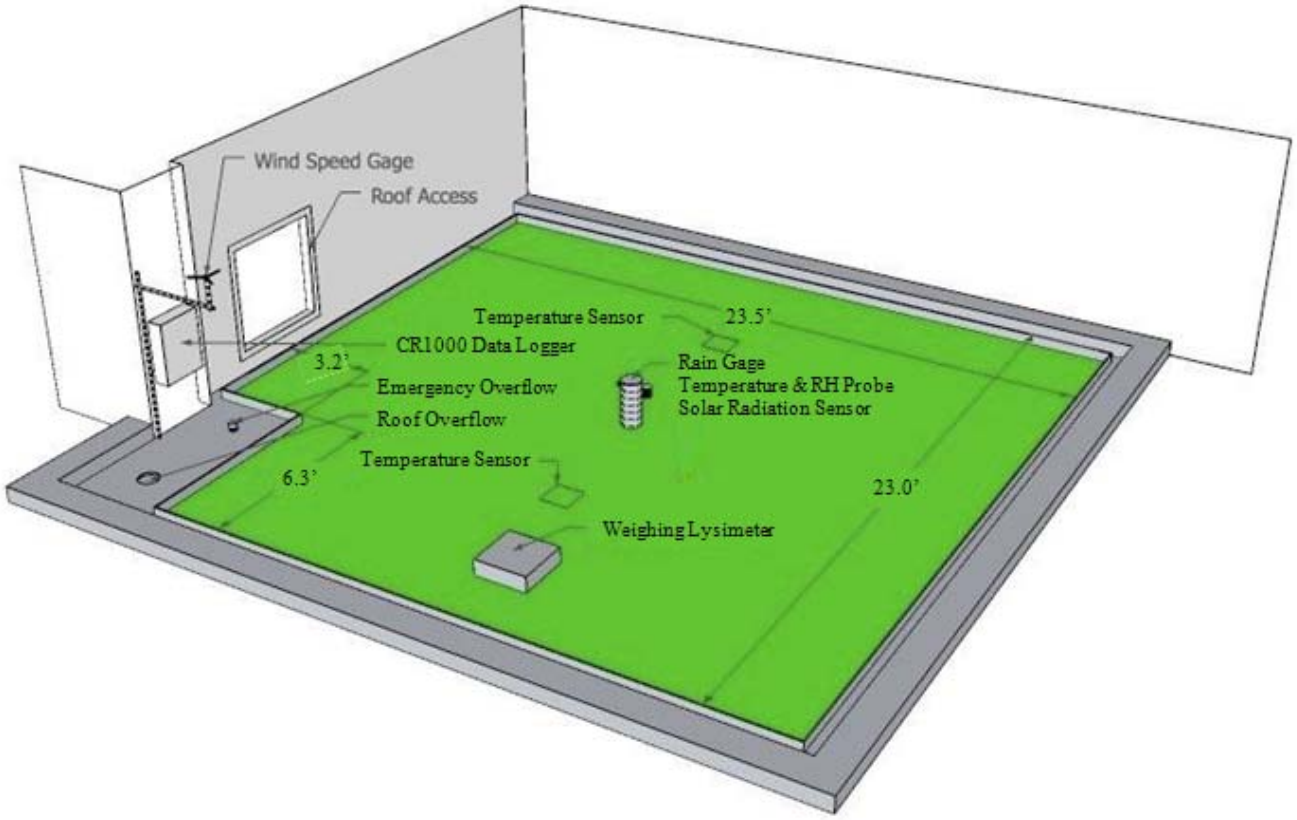

Figure 1.6. Schematic of Green Roof and Current Instrumentation

1.1.2 *Current Green Roof Design Standards*

Current design standards (PA Stormwater BMP Manual) refer designers to a manual by Forschungsgesellschaft Landschaftsentwicklung Landschaftsbau e. V. (FLL). It is a German guideline for planning, installing, and maintaining green roofs. Until the recent publication of several standards (E2398-5 and E2399-5) by the American Society for the Testing of Materials (ASTM), the FLL manual was the only accepted guideline for green roof construction. The FLL manual focuses on the quantification of structural design loads for a building (based on substrate layers and water storage capacity), proper drainage of these systems, and installation aspects of the roof (waterproofing, insulation, vegetation selection, etc.) (FFL 2002). These systems provide great stormwater

management benefits, and often times, in the case of extensive green roofs, these benefits are the sole purpose of implementation. However, they are not represented anywhere in the design standards. The ASTM standards have built on the FLL foundation, following a similar framework, while providing some stormwater design-based guidance. ASTM E2398-11, titled "Standard Test Method for Water Capture and Media Retention of Geocomposite Drain Layers for Vegetative (Green) Roof Systems" (ASTM 2011a), provides guidance for the estimation of water storage capacity of drainage layers for the prediction of dead and live loads, irrigation requirements, and material quantity required to obtain a desired storage volume. ASTM E2399-11, titled, "Standard Test Method for Maximum Media Density for Dead Load Analysis of Vegetative (Green) Roof Systems" (ASTM 2011b), provides guidance for determining the structural needs of the underlying roof by using a theoretical saturation point to estimate the maximum media density, thereby the maximum dead loads on the roof.

1.1.3 ***Role of Evapotranspiration***

While the ASTM methods include a stormwater management component in the design of these systems, it is not time or location sensitive. In other words, if a designer were to estimate the effects of a green roof on the stormwater system, they would assume that the roof at the time of rainfall was dry, thus allowing for virtually all of the storage capacity of the roof to be used by the rainfall event. In reality, the actual roof conditions prior to a rainfall event (a product of the storage capacity of the roof after the previous rainfall, the number of antecedent dry days, and the climate during those dry days) all govern the true storage capacity of the roof. On a single event basis it is difficult to account for these

factors, but as research methods and technology improve the shift is to continuous flow modeling of these stormwater practices, allowing for their inclusion and thus yielding a more accurate portrayal of the efficiency of the SCM. On a continuous flow-modeling basis, therefore, ET becomes an important component because it controls the soil moisture content. Knowledge of the soil moisture content allows for estimates of the available void space in the soil (or available storage for incoming rainfall), which can significantly affect the storage capacity of the roof for the next rainfall event.

1.2 **Research Objectives**

The goals of this research are as follows:

(a) *Quantification of the evapotranspiration portion of the water budget for a green roof.* To quantify the volume and rate of rainwater leaving the green roof due to evapotranspiration, a weighing lysimeter was constructed to mimic the site. The lysimeter is equipped with a series of load cells that measure the change in weight of the system. Subtracting rainfall, any additional weight lost in the system is due to evapotranspiration.

(b) *Determine if evapotranspiration from a green roof is, on a daily basis, a significant portion of the water budget, thus necessitating accurate quantification.* This research aims to prove that the inclusion of the evapotranspiration portion of the water budget is advantageous to the field of stormwater management and has the potential to decrease construction costs by preventing over design of these structural SCMs.

(c) *Determine if current predictive equations for evapotranspiration could be used for the green roof.* Current predictive evapotranspiration equations were developed for, and are primarily used by, the agriculture industry to determine crop watering requirements. The agricultural application lends itself to this sort of analysis because the evaporating surfaces are vast, relatively homogeneous, and irrigated. Conversely, green roofs are primarily an urban environment feature where vast, homogeneous surfaces are rare, making it more difficult to apply the same principles. The equations are typically based on any number of the following climatological parameters: temperature, relative humidity, wind speed, and solar radiation. Each method uses different combinations of the previously stated parameters with varying degrees of accuracy. The most reliable and only recommended method (according to the Federal Agriculture Organization) is the Modified Penman-Monteith method. This method relies on atmospheric conditions to predict the demand for water from a reference surface. A crop coefficient (that relates the actual surface to the reference surface) is then applied to the reference ET value to determine the actual ET. While the Modified Penman-Monteith method may be difficult to apply to green infrastructure (due to lack of research in determining vegetation coefficients for plants common in SCMs), the root Penman-Monteith method as well as the foundational Penman method may still be applicable. The accuracy of the Penman-Monteith method is highly dependent on the ability to predict the surface and aerodynamic resistance parameters. These parameters quantify the resistance to evaporation due to the plant structure and the available soil water, and the resistance to heat and water vapor transfer from the evaporating surface to the surrounding air, respectively. Conversely, the Penman equation does not account for surface resistance

parameters, allowing for a simplified but idealized estimation of ET. To examine the effectiveness of the Penman and Penman-Monteith methods in predicting ET, a weather station was assembled atop the Villanova Green Roof. The station measures precipitation, temperature, relative humidity, wind speed, and solar radiation.

2 LITERATURE REVIEW

2.1 Evapotranspiration

Evapotranspiration is a portion of the hydrologic cycle that is derived from the summation of the evaporation and transpiration from a vegetated surface. Evaporation consists of any water that is returned to the atmosphere from the soil surface, depression storage, or intercepted storage. Transpiration consists of any water that leaves through the vegetated surface via plant stomata.

2.1.1 *Evaporation*

Evaporation is the phase transition of water from a liquid to a gas (water vapor) (Perlman 2008). It drives the water cycle by providing the main mechanism of transport of water from the earth's surface to the atmosphere. Evaporation and the rate of evaporation are dictated by climatological parameters as well as soil water availability. In the case of a surface that is at or near saturation, the climatological parameters almost solely dictate the evaporation rates and thus can be more easily estimated (for instance, Ward and Trimble (2004) suggest ET can be generally estimated as 90% of the potential evaporation when the surface is saturated). However, in stormwater applications it is often the case that the surface is not completely saturated, and thus cannot meet the evaporative demand of the surrounding atmosphere. As a result, evaporation rates are also dictated by the available surface water quantities. (Allen, Pereira et al. 1998).

2.1.2 *Transpiration*

Transpiration is the process by which water from the soil is returned to the atmosphere via plant root uptake. The structure of a plant's leaves allow for water from the plants cells to evaporate within the leaf, increasing the vapor pressure in the intercellular space. This increased vapor pressure results in a vapor pressure gradient between the leaf and the atmosphere, resulting in the diffusion of vapor out of the leaf stomata and into the atmosphere. Once the vapor leaves the leaf, more water is drawn up from the underlying root system bringing with it nutrients to sustain the plant. (Kramer and Boyer 1995) and (Ward and Trimble 2004). The aperture of stomata dictates the rate of vapor exchange. This process is driven by the same climatological factors as evaporation: solar radiation, temperature, wind speed, and relative humidity. Different plants have different transpiration rates and within a single species of plant, transpiration rates can vary as a function of growth stage, environment and maintenance. (Perlman 2008) and (Allen, Pereira et al. 1998). The process is also a function of soil moisture content and soil conductivity, which dictate the amount of water that is available for plant uptake.

2.1.3 *Evapotranspiration*

In practice, evaporation and transpiration are combined into one term: evapotranspiration (ET), because of the difficulty in distinguishing between the two simultaneous processes. The evapotranspiration term is dominated by evaporation when the surface is predominantly bare soil (sparse vegetation), but as vegetation density increases, the soil surface becomes shaded and the plants become more productive, the majority of evapotranspiration losses are from the transpiration process. (Allen, Pereira et al. 1998).

2.1.3.1 *Climatological Effects*

The demand for water from a surface is governed by a series of atmospheric parameters. The resulting evapotranspiration process requires energy, typically in the form of solar radiation, to facilitate the state change of the water molecules from liquid to gas. The amount of energy required is known as the latent heat of vaporization, which decreases slightly as temperature increases. Transfer of water from surface to atmosphere is a function of the vapor pressure deficit (VPD) (Dalton's Law). The VPD is a measure of the difference between the amount of moisture in the air (the actual vapor pressure) and the amount of moisture the air can hold (the saturation vapor pressure). As the vapor pressure deficit decreases, the rate of evaporation slows and the surrounding air becomes more saturated. This process will continue until the point of saturation (when evaporation ceases) unless a mechanism is present to transport the saturated air away from the wet surface and replace it with drier air from the atmosphere. The estimation of each of these effects can be approximately quantified through the measurement or estimation of wind speed, solar radiation, ambient air temperature, and relative humidity. (Allen, Pereira et al. 1998).

2.1.3.2 *Water Availability Effects*

While the atmosphere governs water demand, the soil moisture governs supply. When the soil is saturated, the water supply is unlimited. Gravitational forces are exerted on the water in the soil, causing a portion of the water to drain out of the soil (zone 1, Figure 2.1). The water that remains in the soil via molecular and matric forces is known as the field capacity. The matric forces are generated by the soil particle's adhesive and absorptive molecular attraction to water and the cohesive attraction that water molecules

exert on other water molecules. (Pidwirny 2006). Water moves through soil and plant via capillary action, which only occurs when there is a potential difference resulting in the movement of water is in the direction of decreasing energy, or from areas of low to areas of high matric potential. In a soil and plant system, this means that water moves from wet soil to dry and from soil to plant stomata. (Gardner 1960). As plants draw water from the soil, the matric potential of the soil in close proximity to the root zone increases, drawing in water from the surrounding soil. This process continues until the soil reaches its maximum moisture deficit (see zones 2 & 3, Figure 2.1). Up to this point soil water extraction by the plant is not operating under water stressed conditions, thus water supply to the plant is virtually unlimited. Once the soil water content falls below the maximum soil moisture deficit, it becomes increasingly more difficult for the plant to extract water from the soil. This process ceases completely at the wilting point (Nyvall 2002). It is estimated that the plant can use 50% of the total available soil moisture without operating under water stressed conditions. (Ball 2001) and (Nyvall 2002). Figure 2.1 illustrates the water availability for a range of soil types, including sand, loam, and silty clay loam.

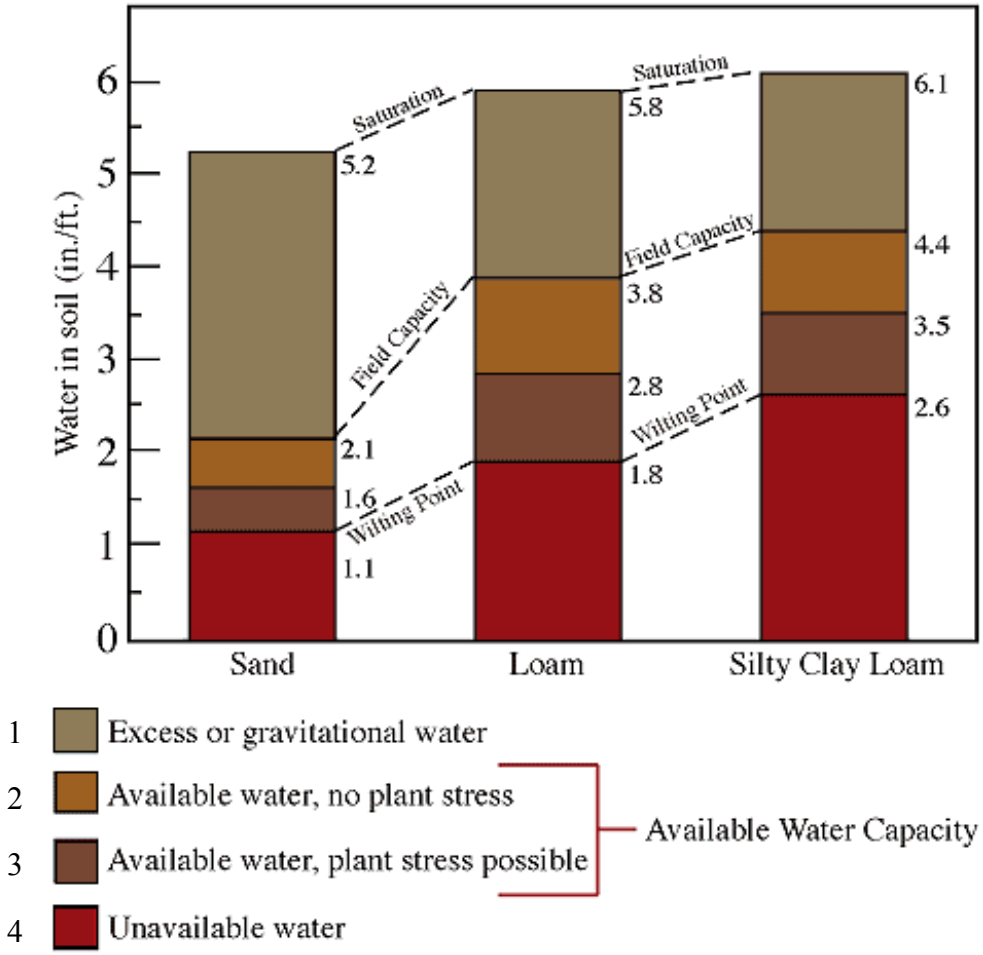

Figure 2.1. Soil Water Capacity taken from Ball (2001)

2.1.3.3 *Actual vs. Potential Evapotranspiration*

It is important to distinguish between the two different classifications of evapotranspiration: actual and potential. Actual ET quantities are a function of surface, subsurface, and meteorological conditions (Anderson 2008). Thus actual ET estimates represent the quantity of water that leaves a given surface based on climatological demand as well as soil water availability and vegetative resistances. Conversely, potential evapotranspiration is a quantification of the amount of water that would leave a surface under a given set of climatological conditions assuming that the surface is well-watered (plants are not water-stressed) and vegetative resistances are negligible. Both

evapotranspiration concepts will be discussed in more detail with regard to the estimation of ET from a vegetated surface later in this chapter.

2.1.4 *Measuring Evapotranspiration*

Evapotranspiration measurements are quantifications of the rate of water vapor loss from a given surface. The rate is a function of solar radiation, wind speed, temperature, vapor pressure, aperture of the plants stomata, soil water content, and soil and plant type, making it a complex parameter to accurately quantify. A water balance approach is an effective way to quantify ET; however, this method is usually only applicable on a watershed basis, or for a longer time scale (monthly or yearly instead of daily). In the case of the green roof, inflow (rainfall) and overflow can be measured, and assuming that storage volume is approximately constant over a month or year, the ET can be calculated as the difference between inflow and overflow. However, this method is not accurate on a daily time step because the storage volume cannot be neglected. Several other methods exist to estimate ET, including potential ET gages that simulate a well-watered leaf and energy balance and mass transfer methods (Bowen ratio and eddy correlation) that measure the water vapor above a canopy. While these methods may provide valid measurements of ET for a green roof, the only direct method of ET measurement, and thus the method chosen for this particular study, is a weighing lysimeter. Any data expressed as "Measured ET" in this document refers to values obtained from a constructed weighing lysimeter, detailed in Chapter 3.

Weighing lysimeters provide one of the most accurate means of quantifying actual evapotranspiration from a vegetated surface (Clawson and Hribal 2009). Often, data from a lysimeter is considered to represent actual ET from a surface and the standard to which the accuracy of other ET estimation methods are gauged. The lysimeter is comprised of a container filled with the soil and vegetation of interest. The entire system is connected to a load cell to track changes in weight, which is equated to actual ET. These systems vary in complexity, from the use of undisturbed soil profiles to different drainage systems, all in an effort to better mimic the current conditions of the area in question. Specific details regarding the design and construction of the Villanova Green Roof lysimeter can be found in Chapter 3.

2.2 **Estimating Evapotranspiration**

The construction and maintenance of a lysimeter is a cost, labor, and time-intensive process that make it an impractical solution for most field investigations and site-by-site design projects. Consequently, predictive equations have been developed to estimate ET based on more readily available field data, including local climatological (from the National Oceanic and Atmospheric Administration (NOAA) or an onsite weather station) and site-specific data (location, etc.).

2.2.1 ***Temperature vs. Combination Methods***

Since the late 1940's, many methods have been proposed to estimate evapotranspiration, each relying on a different set of assumptions and/or empirically based coefficients. The

result is a series of methods that are site specific and are not always universally applicable. There are two major categories of ET quantification methods: temperature methods and combination methods. Temperature methods (Blaney-Criddle, Hargreaves, Turc) rely primarily on temperature measurements but also require some estimation of solar energy. This estimate can be as simple as estimated hours of daylight, or as complex as instrument-measured daily solar radiation (accuracy of data is most often a function of desired output resolution (monthly vs. 10-day vs. daily ET, etc). The Penman equation, also known as the combination equation, provides the foundation for all other combination methods of predicting evapotranspiration. The Penman equation incorporates an energy balance as well as an evaporative function, sometimes referred to as the "drying power of air" [Crago and Crowley (2005), Brutsaert (2005), and Qualls and Gultekin (1997)], to predict evaporation from an open water surface. The Priestley-Taylor, Slatyer-McIlroy, and Penman-Monteith methods are all derivations of the Penman equation. This research focuses on the Penman equation as well as one of the most notable derivations of the equation: the Penman-Monteith equation. The Slatyer-McIlroy predicted ET is also provided throughout this research to serve as a lower bound of daily ET (since the equation assumes minimal advection) under non-water-stressed conditions. Each of the methods mentioned above rely on a slightly different combination of weather inputs to predict ET. These variations are provided in Table 2.1.

Table 2.1. Required Weather Parameters for Common ET Estimation Methods

Method	**Parameter**			
TEMPERATURE	**Solar Radiation**	**Temperature**	**Vapor Pressure**	**Wind Speed**
Blaney-Criddle	O	X	-	-
Hargreaves	O	X	O	-
Turc	-	X	-	-
COMBINATION				
*Penman**	X	X	X	X
*Penman-Monteith**	X	X	X	X
*Slatyer-McIlroy**	X	X	X	-
Priestley-Taylor	X	X	X	-

"X" represents required measured parameters.
"O" represents required estimated parameters
** denotes ET estimation methods used in this research*

2.2.1.1 *The Penman Equation*

The Penman Equation was originally developed to estimate potential ET over open water surfaces; however, Penman and others later established the equations applicability to short vegetated surfaces where there is an unlimited supply of water. The Penman Equation (Penman 1948) is provided as EQ. 2.1.

$$\lambda ET = \frac{\Delta}{\Delta + \gamma}(R_n - G) + \frac{\gamma}{\Delta + \gamma} E_a \qquad \textbf{EQ. 2.1}$$

Where R_n is the net radiation, G is the soil heat flux, Δ is the slope of the saturation vapor pressure curve, γ is the psychrometric constant, and E_a is the "drying power of air". E_a is further defined in Chapter 3, but for the purposes of this discussion, it is a function of wind speed estimates, relative humidity, a wind function (based on roughness or surface turbulence accounting), temperature, and atmospheric pressure.

The Penman Equation is the summation of two terms; the first is the "equilibrium" evaporation, governed only by the energy balance (solar radiation, ground heat flux, temperature, and pressure) while the second term quantifies the divergence from

"equilibrium" and is a bulk transfer estimate (a function of the drying power of the air). At neutral atmospheric stability, which is a reasonable assumption for daily or longer time-steps, the wind function can be estimated using wind speed measurements and estimates of the roughness lengths governing momentum, heat, and vapor transfer (all of which can be estimated if vegetation height is known. (Allen, Pereira et al. 1998). A detailed explanation of the methodology used in this research can be found in Chapter 3.

2.2.1.2 *The Slatyer-McIlroy and Priestley-Taylor Equations*

The Slatyer-McIlroy and Priestley-Taylor equations are based on ET from a wet surface with minimal advection. This occurs when the air above a surface is saturated, due to vapor exchange with the wet surface. As a result, the second term of the Penman Equation (EQ. 2.1), the bulk transfer/drying power of air term, approaches zero. The resultant equation (EQ. 2.2), is the Slatyer-McIlroy Equation (Slatyer and McIlroy 1961), represented by the first term of the Penman equation.

$$\lambda ET = \frac{\Delta}{\Delta + \gamma}(R_n - G) \qquad \textbf{EQ. 2.2}$$

The Slatyer-McIlroy estimate is considered to represent the lower limit of ET from a moist surface (Brutsaert 1982). However, Priestley and Taylor discovered that true equilibrium conditions are rarely attained because the atmospheric boundary layer is never perfectly homogeneous. The results did however demonstrate a proportional relationship between the first term in the Penman equation and the observed ET from advection-free water surfaces and "moist land surfaces with short vegetation". Thus a constant alpha was applied to the first term of the Penman equation. Priestley-Taylor uses an alpha of 1.26 (resulting in EQ. 2.3). (Priestley and Taylor 1972). Based on

other research, it is generally accepted that alpha is, on average, between 1.20 and 1.30 for both surfaces when the water supply is unlimited and the surrounding air is at or near saturation (Brutsaert 2005).

$$\lambda ET = 1.26\left(\frac{\Delta}{\Delta+\gamma}(R_n - G)\right) \qquad \textbf{EQ. 2.3}$$

Preliminary results indicated that the Priestley-Taylor Equation consistently under predicted ET from the Villanova Green Roof. Since Priestley-Taylor ET can be easily obtained from the Slatyer-McIlroy ET prediction if necessary, it has been excluded from further discussion.

2.2.1.3 *The Penman-Monteith Equation*

The Penman-Monteith equation (EQ. 2.4) is a modification of the Penman equation that accounts specifically for vegetated surfaces (incorporates a bulk surface resistance (vegetation resistance) and an aerodynamic resistance term) (Stewart and Howell 2003). The Penman Monteith equation can be used to calculate ET directly because the resistance terms are specific to the vegetation used, thus, as long as the user can accurately define these terms, the Penman-Monteith equation estimations hold true.

$$\lambda ET = \frac{\Delta(R_n - G) + \rho_a c_p \frac{e_s - e_a}{r_a}}{\Delta + \gamma\left(1 + \frac{r_s}{r_a}\right)} \qquad \textbf{EQ. 2.4}$$

Where R_n is the net radiation, G is the soil heat flux, e_s is the saturation vapor pressure, e_a is the actual vapor pressure (these two vapor pressure terms represent the vapor pressure deficit of the air), ρ_a is the mean air density at constant pressure, c_p is the specific heat of

air, Δ is the slope of the saturation vapor pressure curve, γ is the psychrometric constant, r_s is the bulk surface resistance, and r_a is the aerodynamic resistance.

2.2.1.4 *Reference Evapotranspiration*

The reference crop method of estimating evapotranspiration first calculates the potential or reference crop evapotranspiration that represents the climatic demand for water vapor from a surface, then applies an empirical coefficient that, from experimental data, accounts for crop type, growth stage, and soil water availability (Ward and Trimble 2004). This method was established for, and is predominantly used by the agriculture industry because the health of their crops relies so heavily on proper irrigation scheduling. A significant amount of research has been done to develop empirical coefficients for a wide variety of agricultural, vegetated surfaces to make this method practical. The reference crop method, as defined by the Federal Agriculture Organization (FAO), is estimated by the FAO Penman-Monteith method and is recognized as the sole standard method for estimating reference crop ET. This method assumes a uniform reference surface of crop height 0.12 meters, an albedo of 0.23, and a surface resistance of 0.70 s m^{-1} (Allen, Pereira et al. 1998) and (Maidment 1993). Albedo is a term that describes the reflectivity of a surface. It quantifies the proportion of total solar radiation that is reflected versus the total incident radiation. This value is an important part of the local and global climate because it dictates the amount of Earth-absorbed shortwave radiation that occurs. The energy that is absorbed is then used to heat the earth and drive the hydrologic cycle. (Budikova, Hall-Beyer et al. 2008). High albedos are associated with high reflectivity, thus the objects appear bright. Low albedos have low reflectivity (meaning that the light, thus energy, is being absorbed), thus the object appears dark.

Albedo is dependent on a number of factors, but has been estimated by land cover type for this report. Table 2.2 provides typical albedo values for a range of cover types.

Table 2.2. Reflectivity Values for Broad Land Cover Classes Taken from Maidment (1993).

Land Cover Class	Short-Wave Radiation Reflection Coefficient α
Open water	0.08
Tall forest	0.11-0.16
Tall farm crops (e.g. sugarcane)	0.15-0.20
Cereal crops (e.g. wheat)	0.20-0.26
Short farm crops (e.g. sugar beet)	0.20-0.26
Grass and pasture	0.20-0.26
Bare soil	0.10 (wet) - 0.35 (dry)
Snow and ice	0.20 (old) - 0.90 (new)

Note: Albedo can vary widely with time of day, season, latitude, and cloud cover. In the absence of knowledge of crop cover the value α = 0.23 is recommended.

The reference method relies on a simplified representation of the vegetated surface as well as established crop coefficients to generate an estimate of ET. In the field of stormwater management, there is not a set of generally accepted crop coefficients to estimate ET from stormwater control measures. While the development of such coefficients is possible for SCMs, the nature of these sites (relatively small footprint, not easily represented by a homogeneous surface, not extensively studied for the development of crop coefficients, etc) makes it increasingly difficult to do so, potentially rendering this method impractical. Instead, this research evaluates the effectiveness of current predictive equations to estimate ET from the Villanova Green Roof without the use a crop coefficient. It should be noted that the applicability of the methods provided in this research are specific to the Villanova Green Roof, but the results indicate that further research is warranted to establish the applicability of these methods to other green roofs, and ultimately, other SCMs.

3 RESEARCH METHODS

The four major components of this research are addressed in this section. They are as follows:

1. Measurement of evapotranspiration from the Villanova green roof via a weighing lysimeter.
2. Prediction of ET from the green roof through the use of the Penman equation and derivatives of the Penman equation, including the Penman-Monteith and Slatyer-McIlroy equations.
3. Calibration of predictive equations on days without rainfall (due to measurement constraints).
4. Application of predictive equations to all days in the dataset to allow for water budget assessment.

3.1 Measuring Evapotranspiration - Green Roof Weighing Lysimeter

In an effort to quantify evapotranspiration volumes, a weighing lysimeter was used to simulate the water budget of the Villanova green roof. The weighing lysimeter (Figure 3.1) was designed to measure the changes in weight of an 18" by 18" by 5" waterproof CPVC box, which contained a replicate cross-section of the green roof, including a synthetic storage layer, soil media, and sedum vegetation. Three (3) compression load cells were used to measure changes in weight of the lysimeter, which reflected changes in soil water content of the system. Detailed information regarding the load cell can be found in Appendix B.

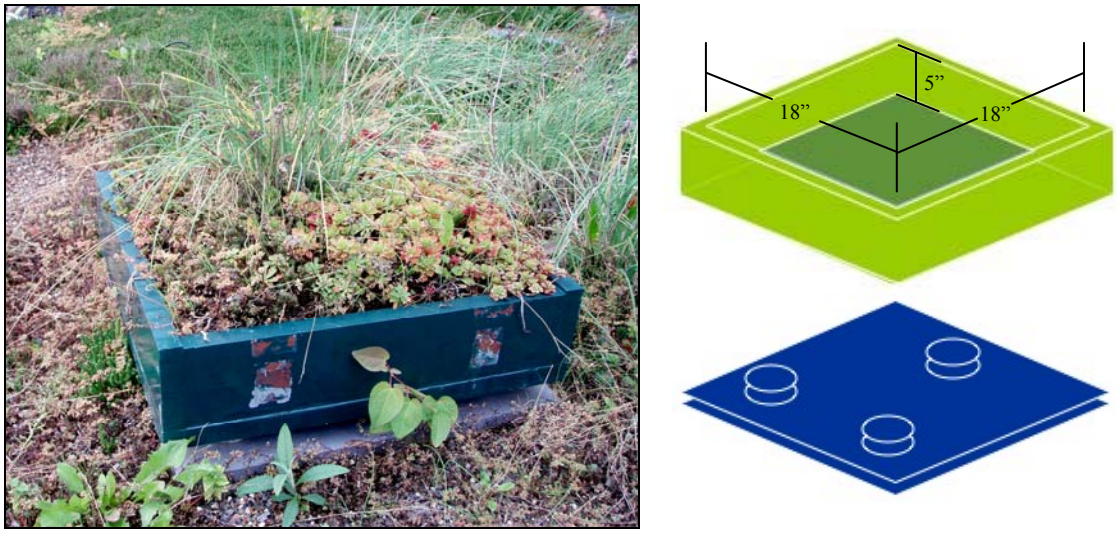

Figure 3.1. Villanova Weighing Lysimeter

3.1.1 *Load Cell Error*

While the load cells used in this study were calibrated to manufacturer standards by Sentran, LLC, the conditions of the roof are unique, thus warranting further examination of the associated error. To test the precision of the load cells, they were subjected to a constant load of approximately 66 kg for 23 days and the results were observed. The mean load cell output for the 23-day period (5-minute data increments) was 66.27 kg. It was assumed that the data was an approximately normal distribution, thus a t-distribution was used along with EQ. 3.1, yielding an error of +/- 0.27 kg.

$$+/- Error = t * s + CL \qquad \textbf{EQ. 3.1}$$

Where,

t = critical value from the t - distribution
s = standard deviation of the sample population
CL = Confidence Level

In this case, t = 1.645 (0.05 critical value with infinite degrees of freedom), s = 0.16 kg, and CL = 0.004 kg (95% confidence level). Application of the error resulted in 90% of the data (at 95% confidence) falling between 66.00 and 66.55 kg. The error associated with these daily fluctuations is shown in Figure 3.2.

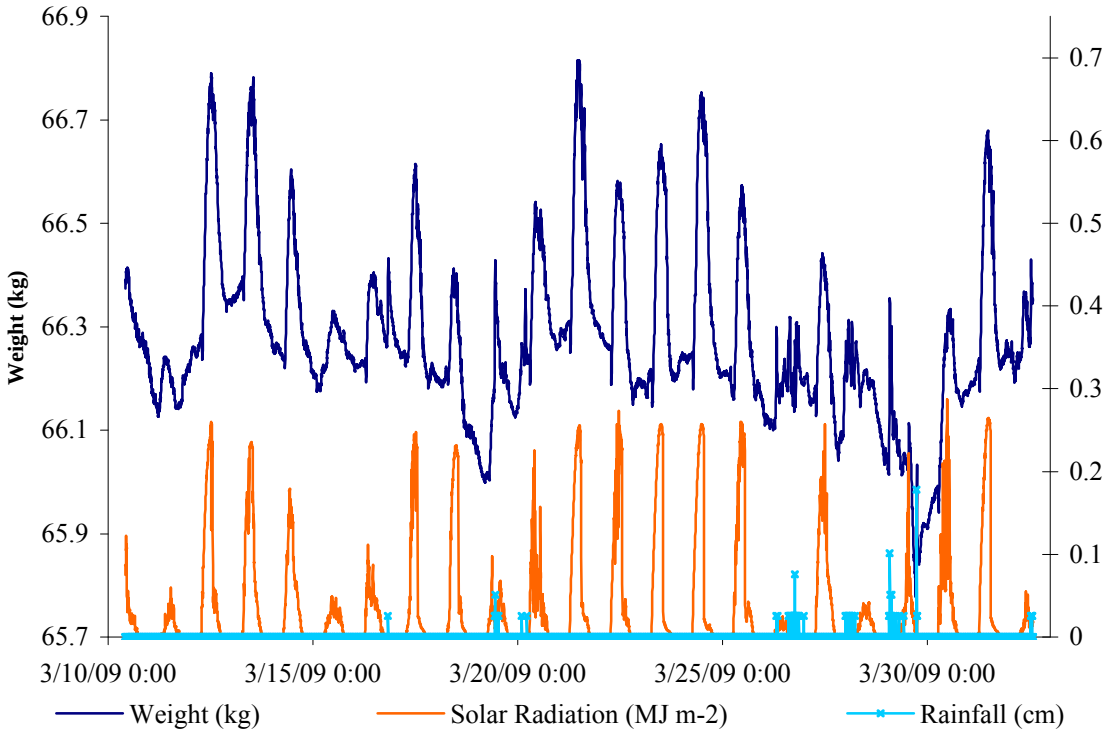

Figure 3.2. Diurnal Variation of Load Cell Output Under a Constant Load

Preliminary results showed skewness in the data during daytime hours, which is possibly a function of radiation, leading to the uneven heating of the load cells (see Figure 3.2). In an effort to reduce the error associated with load cell output, the daily data was eliminated from the data set, utilizing the more stable nighttime values. This was done by observing a discrete data point at midnight (0:00) each night and comparing it to the previous midnight data point to determine ET values for a particular day. Though this

drastically reduced the sample size (from n =5063 to n=23), the resultant error was reduced to +/- 0.19 kg (via EQ. 3.1). Mean load cell output for the 23-day period (using only midnight data) was 66.20 kg, with a standard deviation of 0.09 kg, and a 95% confidence level of 0.04 kg. Application of the error resulted in 90% of the data (at 95% confidence) falling between 66.01 and 66.39 kg. This interval is shown in Figure 3.3 as the error associated with the midnight data.

The comparison above was completed to determine which method (either use of all of the data or use of only midnight data) resulted in a lower associated load cell error. Because of the reduced error associated with using only midnight readings (+/-0.27 kg using 5-minute data versus +/-0.19 kg using midnight values), this method was chosen and applied to the remaining dataset to determine daily evapotranspiration from the lysimeter. The actual error associated with the change in weight of the lysimeter from midnight to midnight was calculated by observing the load cell output (expressed in mm of water) under a constant load. The mean change in weight for the 23-day period (n = 22) was 0.01 mm, with a standard deviation of 0.50 mm, yielding an error of +/- 1.04 mm of water (+/-0.22 kg). This error was then applied to the entire data set (April 2009 - November 2009).

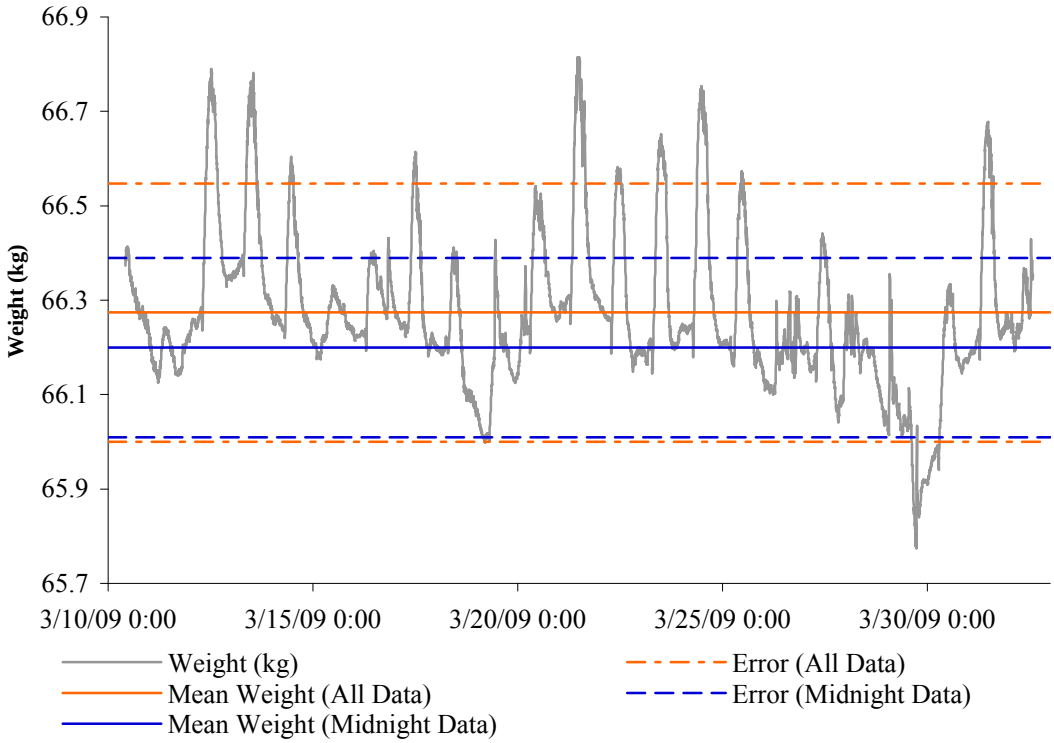

Figure 3.3. Comparison of the Error Associated with the Use of All Data versus the Use of Instantaneous Data from Midnight Each Day

3.2 **Predicting Evapotranspiration**

This research focuses on three predictive equations, all based on climatological parameters, which are used to estimate ET leaving the green roof on a daily basis. The equations include the Penman, Penman-Monteith, and Slatyer-McIlroy equations. Penman-Monteith and Slatyer-McIlroy are both modifications of the foundational Penman Equation.

3.2.1 ***Climatological and Site-Based Inputs***

The predictive equations used in this research rely on some combination of measurements or estimations of temperature, vapor pressure, solar radiation, wind speed, site location,

elevation, and vegetative cover to estimate ET. Table 3.1 provides the relevant permutations of the measured data parameters used in this study.

Table 3.1. Required Measured Weather and Site Data

Parameter	Parameter Definition	Units
T_{min}	Minimum daily air temperature	°C
T_{max}	Maximum daily air temperature	°C
T_{avg}	Average daily air temperature	°C
RH_{min}	Minimum daily relative humidity	%
RH_{max}	Maximum daily relative humidity	%
u_z	Average daily wind speed at height z	$m\ s^{-1}$
R_s	Incoming solar radiation	$MJ\ m^{-2}$
z	Elevation above mean sea level	m
J	Number of day in the year (1 to 365)	-
φ	Site latitude	rad
h	Vegetation height	m
α	Albedo (surface reflectance)	-

For this research, a weather station was installed atop the roof (see Figure 3.4) in an effort to minimize error associated with spatial variations in weather data. Table 3.2 provides a detailed description of the instrumentation used at the weather station. Daily summarized weather data inputs can be found in Appendix C.

Figure 3.4. Villanova Green Roof Weather Station Including a Temperature and Relative Humidity Probe, Rain Gauge, and Pyranometer (left), and Anemometer (right).

Table 3.2. Green Roof Weather Station Instruments

Parameter	Product No [a]	Instrument
Temperature	HMP50	Vaisala Temperature and RH Probe
Relative Humidity	HMP50	Vaisala Temperature and RH Probe
Wind Speed	014A	Met One Anemometer
Solar Radiation	LI200X	LI-COR Silicon Pyranometer
Rainfall	2149	American Sigma Rain Gauge
Datalogger	CR1000	Campbell Scientific Measurement and Control System

a. Corresponds to Campbell Scientific product numbers.

3.2.2 *The Penman Equation*

The Penman equation (EQ. 3.2) was originally developed by Howard Penman in 1948 to describe evaporation from an open water surface.

$$\lambda ET = \frac{\Delta}{\Delta + \gamma}(R_n - G) + \frac{\gamma}{\Delta + \gamma}E_a \qquad \textbf{EQ. 3.2}$$

Where R_n is the net radiation, G is the soil heat flux, Δ is the slope of the saturation vapor pressure curve, γ is the psychrometric constant, is the latent heat of vaporization, and E_a

is the "drying power" of air. All of these parameters can be calculated or estimated given the local climatological (temperature, relative humidity, solar radiation, and wind speed) and site-specific (latitude, longitude, elevation, and vegetation height) data. Table 3.3 contains the required weather inputs for each parameter in the Penman Equation.

Table 3.3. Penman Required Weather Inputs by Parameter

Parameter	Parameter Definition	Weather Inputs
R_n	Net radiation	T_{min}, T_{max}, RH_{min}, RH_{max}, R_s, φ, z, J, α
G	Soil heat flux	-
Δ	Slope of the saturation vapor pressure curve	T_{avg}
γ	Psychrometric constant	T_{avg}, z
E_a	"Drying power" of air	T_{min}, T_{max}, T_{avg}, RH_{min}, RH_{max}, u_z, z, h
λ	Latent heat of vaporization	T_{avg}

3.2.2.1 *Net Radiation (R_n)*

Net radiation (R_n) is derived from the pyranometer data output. However, the pyranometer accounts only for incoming solar radiation while the Penman equation requires an estimate of daily net radiation to determine a daily ET value. Allen, Pereira et al. (1998) proposed a method to estimate the net solar radiation using measured incoming solar radiation in combination with site geographic location and time of year. Net radiation, as expressed by EQ. 3.3, is the difference between incoming and outgoing radiation.

$$R_n = R_{ns} - R_{nl} \qquad \textbf{EQ. 3.3}$$

Where R_{ns} is the net shortwave radiation [MJ m^{-2} day^{-1}] and R_{nl} is the net outgoing longwave radiation [MJ m^{-2} day^{-1}]. R_{ns} and R_{nl} are given by EQ. 3.4 and EQ. 3.5, respectively.

$$R_{ns} = (1-\alpha)R_s \qquad \textbf{EQ. 3.4}$$

Where α is the albedo or canopy reflection coefficient [dimensionless] and R_s is the incoming solar radiation [MJ m^{-2} day^{-1}]. R_s was measured in the field[1]. For the purposes of this research, an albedo value of 0.23 was selected in accordance with Table 2.2.

$$R_{nl} = \sigma\left[\frac{T_{\max,K}^4 + T_{\min,K}^4}{2}\right](0.34 - 0.14\sqrt{e_a})\left(1.35\frac{R_s}{R_{so}} - 0.35\right) \qquad \textbf{EQ. 3.5}$$

Where R_{nl} is the net outgoing longwave radiation [MJ m^{-2} day^{-1}], σ is the Stefan-Boltzmann constant, 4.903 x 10-9 [MJ K-4 m-2 day-1], $T_{max,K}$ and $T_{min,K}$ are the maximum and minimum absolute temperatures during a 24-hour period [K], e_a is the actual vapor pressure [kPa], R_s is the solar radiation (measured) in [MJ m^{-2} day^{-1}], and R_{so} is the clear sky radiation [MJ m^{-2} day^{-1}]. R_{so} is estimated from EQ. 3.6. (Allen, Pruitt et al. 1996).

$$R_{so} = (0.75 + 2*10^{-5}z)R_a \qquad \textbf{EQ. 3.6}$$

Where z is the elevation of the site above sea level [m] and R_a is the extraterrestrial radiation estimated for daily periods by EQ. 3.7 [MJ m^{-2} day^{-1}].

---

[1] If not able to measure in the field, the FAO provides ways of estimating the solar radiation component (see Allen, Pereira et al. (1998)).

$$R_a = \frac{24(60)}{\pi} G_{sc}\, d_r \left[\omega_s \sin(\varphi)\sin(\delta) + \cos(\varphi)\cos(\delta)\sin(\omega_s)\right] \qquad \textbf{EQ. 3.7}$$

Where R_a is the extraterrestrial radiation [MJ m^{-2} day^{-1}], G_{sc} is the solar constant, 0.0820 [MJ m^{-2} min^{-1}], d_r is the inverse relative distance between the Earth and the Sun (given by *EQ. 3.8*), δ is the solar declination [rad] (given by *EQ. 3.9*), ω_s is the sunset hour angle [rad] (given by EQ. 3.10), and φ is the latitude of the site [rad].

$$d_r = 1 + 0.033\cos\left(\frac{2\pi}{365} J\right) \qquad \textbf{EQ. 3.8}$$

$$\delta = 0.409\sin\left(\frac{2\pi}{365} J - 1.39\right) \qquad \textbf{EQ. 3.9}$$

Where J is the Julian date (an integer between 1 and 365).

$$\omega_s = \frac{\pi}{2} - \arctan\left[\frac{-\tan(\varphi)\tan(\delta)}{X^{0.5}}\right] \qquad \textbf{EQ. 3.10}$$

Where,

$$X = 1 - \left[\tan(\varphi)^2\right]\left[\tan(\delta)^2\right]$$
$$X = 0.00001 \; if \; X = 0 \qquad \textbf{EQ. 3.11}$$

3.2.2.2 *Soil Heat Flux (G)*

The soil heat flux is the quantity of thermal energy that passes through an area of soil per unit of time (Sauer and Horton 2005). The soil heat flux is positive when the soil is being heated and negative while the soil is cooling. Although the soil heat flux is part of the overall energy balance, it is relatively small in comparison to the net radiation and thus can be neglected on a daily time-step (Allen, Pereira et al. 1998).

3.2.2.3 *Psychrometric Constant (γ)*

The psychrometric constant relates the partial pressure of water vapor in the air to the actual air temperature, allowing for the derivation of actual vapor pressure from dry and wet bulb thermometer readings, or in this case, dry bulb and relative humidity measurements. *EQ. 3.12* defines the psychrometric constant. (Brunt 1952).

$$\gamma = \frac{c_p P}{\varepsilon \lambda} \qquad \textbf{EQ. 3.12}$$

Where γ is the psychrometric constant [kPa °C^{-1}], λ is the latent heat of vaporization [MJ kg $^{-1}$] (given by EQ. 3.16), C_p is the specific heat at constant pressure, 1.013 x 10^{-3} [MJ kg^{-1} °C $^{-1}$], ε is the ratio of the molecular weight of water vapor to that of dry air, 0.622, and P is the atmospheric pressure [kPa] given by EQ. 3.13.

$$P = 101.3\left(\frac{293 - 0.0065z}{293}\right)^{5.26} \qquad \textbf{EQ. 3.13}$$

Where z is the elevation above mean sea level [m]. This equation is a derivation of the ideal gas law assuming that the temperature at the reference surface is 20 °C (for the generic form of this equation, see Burman et al. (1987)). While atmospheric pressure is measured relatively easily, for the purposes of this study, an estimate based on site location above mean sea level is sufficient.

3.2.2.4 *Slope of the Saturation Vapor Pressure Curve (Δ)*

The slope of the saturation vapor pressure curve is expressed as the ratio of the change in vapor pressure to the change in temperature from saturated surface conditions to actual surface conditions. The initial inclusion and definition of this parameter by Penman was

a crucial step in his analysis. For this study, the Tetens (1930) form of the equation (EQ. 3.14) was used to estimate the slope of the saturation vapor pressure curve (as recommended and demonstrated by the Federal Agriculture Organization in Allen, Pereira et al (1998)).

$$\Delta = \frac{4098\left[0.6108\exp\left(\frac{17.27T}{T+237.3}\right)\right]}{(T+237.3)^2} \qquad \textbf{EQ. 3.14}$$

Where Δ is the slope of the saturation vapor pressure curve [kPa $°C^{-1}$] at air temperature, T [°C].

3.2.2.5 *Drying Power of Air (Ea)*

The drying power of air term in the Penman Equation is defined by a wind function and the vapor pressure deficit (the difference between the actual and saturation vapor pressures). However, there is no generally accepted formulation of the wind function. For the purposes of this study, a fundamental approach, provided by Brutsaert (2005)) was used and is provided by EQ. 3.15. This formulation is based on turbulence similarity (see Brutsaert (2005)) and assumed neutral atmospheric conditions (typically a reasonable assumption for daily time-steps)[2].

[2] For hourly time-steps, a different form of the drying power of air equation (such as the form provided by Brutsaert (1982)) should be used to account for variable atmospheric stability. An example of this application is provided by Parlange and Katul (1992).

$$E_a = \lambda \frac{0.41^2 u_z \rho_a \frac{0.622}{P}(e_s - e_a)}{\ln\left(\frac{z_m - d}{z_{om}}\right)\ln\left(\frac{z_h - d}{z_{oh}}\right)} \qquad \textbf{EQ. 3.15}$$

Where λ is the latent heat of vaporization [MJ kg^{-1}] (given by EQ. 3.16), u_z is the wind speed [m s^{-1}] at height z [m], ρ_a is the density of the air [kg m^{-3}], P is the atmospheric pressure [kPa], $(e_s - e_a)$ is the vapor pressure deficit, d is the zero plane displacement height [m], z_{om} is the roughness length governing momentum transfer [m], z_{oh} is the roughness length governing heat and vapor transfer [m], z_m is the height of wind measurements [m], and z_h is the height of humidity measurements [m]. For the green roof weather station, $z_m = 2$ and $z_h = 0.5$. The mean saturation vapor pressure (e_s) is defined by EQ. 3.18 (Allen, Pereira et al. 1998).

3.2.2.6 *Latent Heat of Vaporization (λ)*

The latent heat of vaporization, given by EQ. 3.16 (Harrison 1963), is the amount of energy (typically in the form of solar radiation) required to facilitate a state change of water molecules from a liquid to a gas.

$$\lambda = 2.501 - \left(2.361 * 10^{-3}\right)T \qquad \textbf{EQ. 3.16}$$

Where T is the daily mean air temperature [°C].

3.2.2.7 *Saturation Vapor Pressure ($e°(T)$)*

The saturation vapor pressure is a quantification of the portion of atmospheric pressure associated with the maximum water vapor content of air at a given temperature. As air temperature increases, the saturation vapor pressure also increases as a result of the

increased water storage capacity of the air. (Allen, Pereira et al. 1998). The saturation vapor pressure is defined by EQ. 3.17 (Tetens 1930).

$$e^{\circ}(T) = 0.6108 \exp\left[\frac{17.27T}{T + 237.3}\right] \qquad \textbf{EQ. 3.17}$$

Where e°(T) is the saturation vapor pressure [kPa] at air temperature, T [°C]. The mean saturation vapor pressure should be calculated using the daily minimum and maximum temperature rather than the daily mean temperature (as shown in EQ. 3.18). This prevents underestimation of the daily saturation vapor pressure and thus, underestimation of the daily vapor pressure deficit (as recommended by the Federal Agriculture Organization (Allen, Pereira et al. 1998)).

$$e_s = \frac{e^{\circ}(T_{\max}) + e^{\circ}(T_{\min})}{2} \qquad \textbf{EQ. 3.18}$$

Where e_s is the mean saturation vapor pressure [kPa], and $e°(T_{max})$ and $e°(T_{min})$ are the saturation vapor pressures that correspond with the daily maximum and minimum air temperatures [kPa], respectively. $e°(T_{max})$ and $e°(T_{min})$ can be calculated using EQ. 3.17. (Allen, Pereira et al. 1998).

3.2.2.8 *Actual Vapor Pressure (e_a)*

The actual vapor pressure is a quantification of the pressure exerted by the water in the air. Though it is not possible to directly measure this pressure, it is often derived from available humidity or dew point data. (Allen, Pereira et al. 1998). For the purposes of this research, the actual vapor pressure was calculated using available relative humidity data as shown in EQ. 3.19.

$$e_a = \frac{e^{\circ}(T_{\min})\frac{RH_{\max}}{100} + e^{\circ}(T_{\max})\frac{RH_{\min}}{100}}{2} \qquad \textbf{EQ. 3.19}$$

Where e_a is the actual vapor pressure [kPa], and RH_{max} and RH_{min} are the maximum and minimum daily relative humidity readings [%], respectively.

3.2.2.9 *Mean Air Density (ρ_a)*

Air density [kg m^{-3}] can be calculated by considering the ideal gas law, as shown in EQ. 3.20. (Smith, Allen et al. 1991).

$$\rho_a = \frac{P}{T_{kv}R} \qquad \textbf{EQ. 3.20}$$

Where P is the atmospheric pressure [kPa] estimated by EQ. 3.13, T_{kv} is the virtual temperature given by EQ. 3.21, and R is the specific gas constant, 0.287 [kJ kg-1 K-1].

3.2.2.10 *Absolute Temperature (T_{kv})*

$$T_{kv} = T_K\left(1 - 0.378\frac{e_a}{P}\right)^{-1} \qquad \textbf{EQ. 3.21}$$

Where T_K is the absolute temperature [K] (273.16 + T [°C]), e_a is the actual vapor pressure [kPa] given by EQ. 3.19, and P is the atmospheric pressure as estimated by EQ. 3.13.

3.2.2.11 *Aerodynamic Parameters*

Aerodynamic parameters include the zero plane displacement height (d), the roughness length governing momentum transfer (z_{om}), and the roughness length governing heat and

vapor transfer (z_{oh}). For a wide range of vegetated surfaces, these parameters can be estimated via EQ. 3.22, EQ. 3.23, EQ. 3.24, respectively (Allen, Pereira et al. 1998).

$$d = \frac{2}{3} h \qquad \textbf{EQ. 3.22}$$

$$z_{om} = 0.123\, h \qquad \textbf{EQ. 3.23}$$

$$z_{oh} = 0.1\, z_{om} \qquad \textbf{EQ. 3.24}$$

Where h is the vegetation height [m].

3.2.3 *The Slatyer-McIlroy Equation*

As previously discussed in Chapter 2, the Slatyer-McIlroy equation (EQ. 3.25) is represented by the first term of the Penman equation. This equation is considered to represent the lower limit of ET from a wet surface. It remains in this research as a highly conservative approach to ET estimation.

$$\lambda ET = \frac{\Delta}{\Delta + \gamma}\left(R_n - G\right) \qquad \textbf{EQ. 3.25}$$

The slope of the saturation vapor pressure curve (Δ) is defined by EQ. 3.14, the psychrometric constant (γ) by EQ. 3.12, and the net radiation (R_n) by EQ. 3.3. The ground heat flux, G, is again, assumed to be zero.

3.2.4 *The Penman-Monteith Equation*

The Penman-Monteith equation (EQ. 3.26) was used to estimate ET leaving the green roof on a daily basis.

$$\lambda ET = \frac{\Delta(R_n - G) + \rho_a c_p \frac{e_s - e_a}{r_a}}{\Delta + \gamma\left(1 + \frac{r_s}{r_a}\right)} \qquad \textbf{EQ. 3.26}$$

Where R_n is the net radiation given by EQ. 3.3, G is the soil heat flux, e_s is the saturation vapor pressure (EQ. 3.18), e_a is the actual vapor pressure (EQ. 3.19) (these two vapor pressure terms represent the vapor pressure deficit of the air), ρ_a is the mean air density at constant pressure (EQ. 3.20), c_p is the specific heat of air (EQ. 3.27), Δ is the slope of the saturation vapor pressure curve (EQ. 3.14), γ is the psychrometric constant (EQ. 3.12), r_s is the bulk surface resistance, and r_a is the aerodynamic resistance (EQ. 3.28). Table 3.4 contains the required weather inputs for each parameter in the Penman Equation.

Table 3.4. Penman-Monteith Required Weather Inputs by Parameter

Parameter	Parameter Definition	Weather Inputs
R_n	Net radiation	T_{min}, T_{max}, RH_{min}, RH_{max}, R_s, φ, z, J, α
G	Soil heat flux	-
Δ	Slope of the saturation vapor pressure curve	T_{avg}
γ	Psychrometric constant	T_{avg}, z
E_a	"Drying power" of air	T_{min}, T_{max}, T_{avg}, RH_{min}, RH_{max}, u_z, z, h
λ	Latent heat of vaporization	T_{avg}
e_s	Saturation vapor pressure	T_{min}, T_{max}
e_a	Actual vapor pressure	T_{min}, T_{max}, RH_{min}, RH_{max}
r_s	Bulk surface resistance	-
r_a	Aerodynamic resistance	u_z, z, h

3.2.4.1 *Specific Heat of Air (c_p)*

$$c_p = \frac{\gamma \varepsilon \lambda}{P} \qquad \textbf{EQ. 3.27}$$

3.2.4.2 *Aerodynamic Resistance (r_a)*

The aerodynamic resistance term, r_a, governs the transfer of heat and water vapor (via turbulent mixing) from the evaporating surface (the green roof) to the air above. In general, this parameter follows two phenomenon; first, as wind speed approaches zero, the aerodynamic resistance approaches infinity and second, as the canopy surface roughness increases, so too does the turbulent mixing, resulting in a smaller aerodynamic resistance term (Davie 2002). This research relies on surface similarity theory, (logarithmic windspeed profile) proposed by, and presented here in EQ. 3.28, to estimate aerodynamic resistance. (Allen, Jensen et al. 1989).

$$r_a = \frac{\ln\left[\frac{z_m - d}{z_{om}}\right] \ln\left[\frac{z_h - d}{z_{oh}}\right]}{k^2 u_z} \qquad \textbf{EQ. 3.28}$$

Where r_a is the aerodynamic resistance [s m^{-1}], z_m is the height of wind measurements [m], z_h is the height of humidity measurements [m], d is the zero plane displacement height [m] (EQ. 3.22), z_{om} is the roughness length governing momentum transfer [m] (EQ. 3.23), z_{oh} is the roughness length governing transfer of heat and vapor [m] (EQ. 3.24), k is von Karman's constant, 0.41, and u_z is the wind speed at a height of "z" meters [m s^{-1}].

3.2.4.3 *Bulk Surface Resistance (r_s)*

The bulk surface resistance (sometimes referred to as canopy resistance) describes the resistance of water vapor movement through vegetation and soil media on the evaporating surface. The term is a function of many parameters including, but not limited to: vegetation type, growth stage, and soil water availability. The number, variety and complexity of contributing variables make the bulk surface resistance a difficult parameter to quantify.

4 RESULTS

The results of this research are presented in accordance with the research objectives outlined in Chapter 1. As previously discussed, a weighing lysimeter was constructed and used to measure evapotranspiration on the Villanova green roof. The lysimeter data was used to gauge the effectiveness of current predictive equations (the Penman, Penman-Monteith, and Slatyer-McIlroy equations) in estimating ET. Estimated, Penman and Slatyer-McIlroy ET was compared directly to measured lysimeter ET. Estimated, Penman-Monteith ET was first calibrated (via optimization of a single value for both bulk surface and aerodynamic resistance based on lysimeter ET (as discussed below)) then compared to the measured ET. Both of these comparisons used data only from days without rainfall due to lysimeter constraints (primarily lack of overflow measurements from the lysimeter prevented a complete water balance during precipitation events). Once the accuracy of these equations was established, the Penman and calibrated Penman-Monteith methods were extrapolated to include days with rainfall, thus representing ET values for the entire dataset. Using rain and non-rain days allowed for an estimation of monthly total and monthly average ET, and ultimately, the ability to assess the effects of ET on the water budget of the green roof.

4.1 Calibration Routine for Predictive Equations

While the Penman-Monteith equation can provide extremely accurate estimates of actual ET, it relies on several parameters, namely the aerodynamic resistance and bulk surface resistance terms, which are difficult to quantify. This research proposed the use of a

calibration coefficient to account for uncertainty in the bulk surface resistance term of the Penman-Monteith equation. During calibration, it was determined that applying a coefficient to the bulk surface resistance term alone does not explain enough of the error in the predicted Penman-Monteith ET. As a result, a calibration coefficient was also applied to the aerodynamic resistance term (r_a). The calibration included minimizing the sum of the square error of the Penman-Monteith, predicted ET, to the measured, lysimeter ET, on days without rainfall. The result was a single calibration factor for aerodynamic resistance (x = 0.61) and a single value for bulk surface resistance (r_s = 83) unique to the Villanova green roof. The aerodynamic calibration coefficient, x, was applied as a direct multiplier to r_a values from EQ. 3.28, as illustrated in EQ. 4.1, below.

$$r_{a,\,calbrated} = x\left(r_{a,\,EQ.3.28}\right) \qquad \textbf{EQ. 4.1}$$

Since no equation was used to establish preliminary estimates of bulk surface resistance, this term was optimized based on the routine described above, resulting in a bulk surface resistance of 83 for the dataset.

4.2 **Applicability of Predictive Equations on Days without Rainfall**

4.2.1 ***Graphical Evaluation***

To examine the applicability of the Penman and calibrated Penman-Monteith equations for ET estimation on the green roof, each was plotted against the lysimeter measured ET and the results were observed. From these plots, days where the Penman or calibrated Penman-Monteith equation diverged from lysimeter measured ET (particularly values outside of the lysimeter measurement error) were identified. For clarity, the data was

separated by month and displayed below. The first plot for each month (Figure "A" in the series (e.g., Figure 4.1) compares the Penman, calibrated Penman-Monteith, and Slatyer-McIlroy equations to the lysimeter measured ET. Slatyer-McIlroy estimates have been included to provide an approximate lower bound for ET based on the corresponding climatological conditions (as outlined in Chapter 3). This estimate is based solely on an energy budget, thus it neglects any effects on ET rate due to vapor pressure deficits, transport fluxes, soil water content, or vegetative cover. This is not, however, an absolute lower bound, but rather a lower bound based on atmospheric demand assuming an unlimited water supply. In the event the supply is limited or negligible, ET from the roof would approach zero.

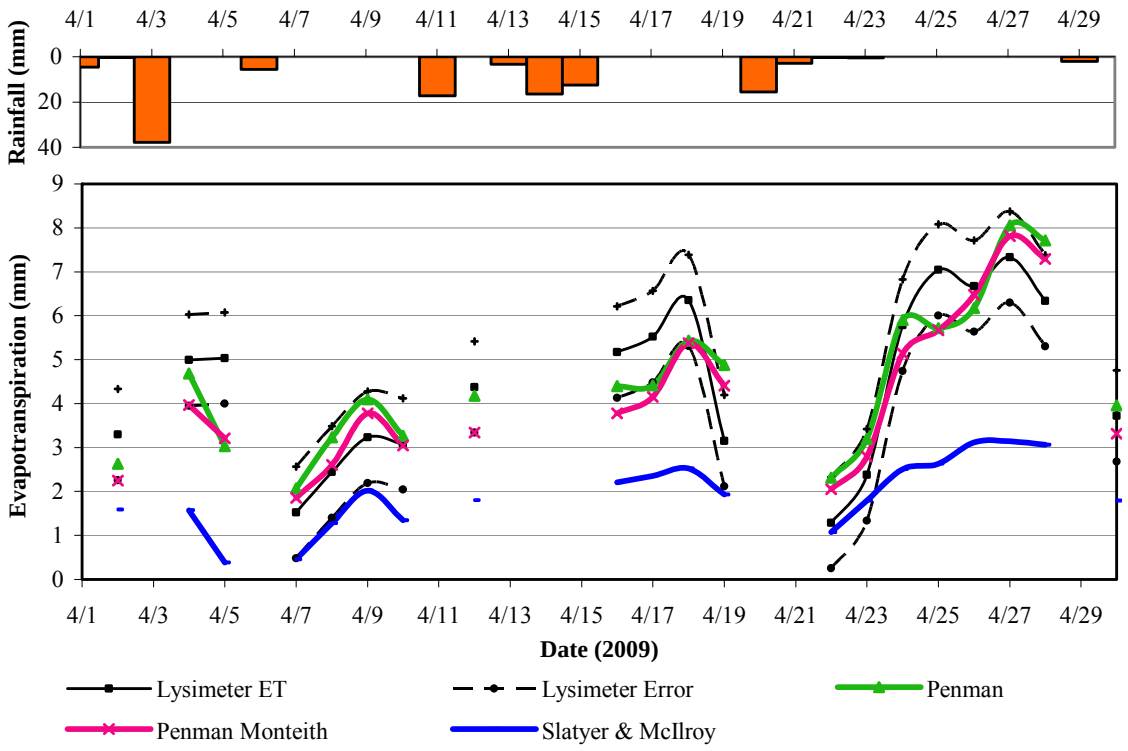

Figure 4.1. April 2009. "A" A comparison of measured and estimated ET

The second plot in the series, Figure "B" (e.g., Figure 4.2), represents the Penman and calibrated Penman-Monteith estimated ET versus lysimeter measured ET, with the

Penman ET shown as a closed circle and the calibrated Penman-Monteith ET as an open circle. If the predictive equations exactly represented the lysimeter measured ET, every data point would fall on the one-to-one line (also shown in Figure "B"). However, lysimeter measurement error coupled with inherent error in the estimation equations result in some scatter in the data. As a result, both the Penman and calibrated Penman-Monteith data sets were fitted with a linear regression best-fit line. This allowed for the comparison (visual and numerical) of the monthly trends in each estimation method relative to one another as well as to the one-to-one line.

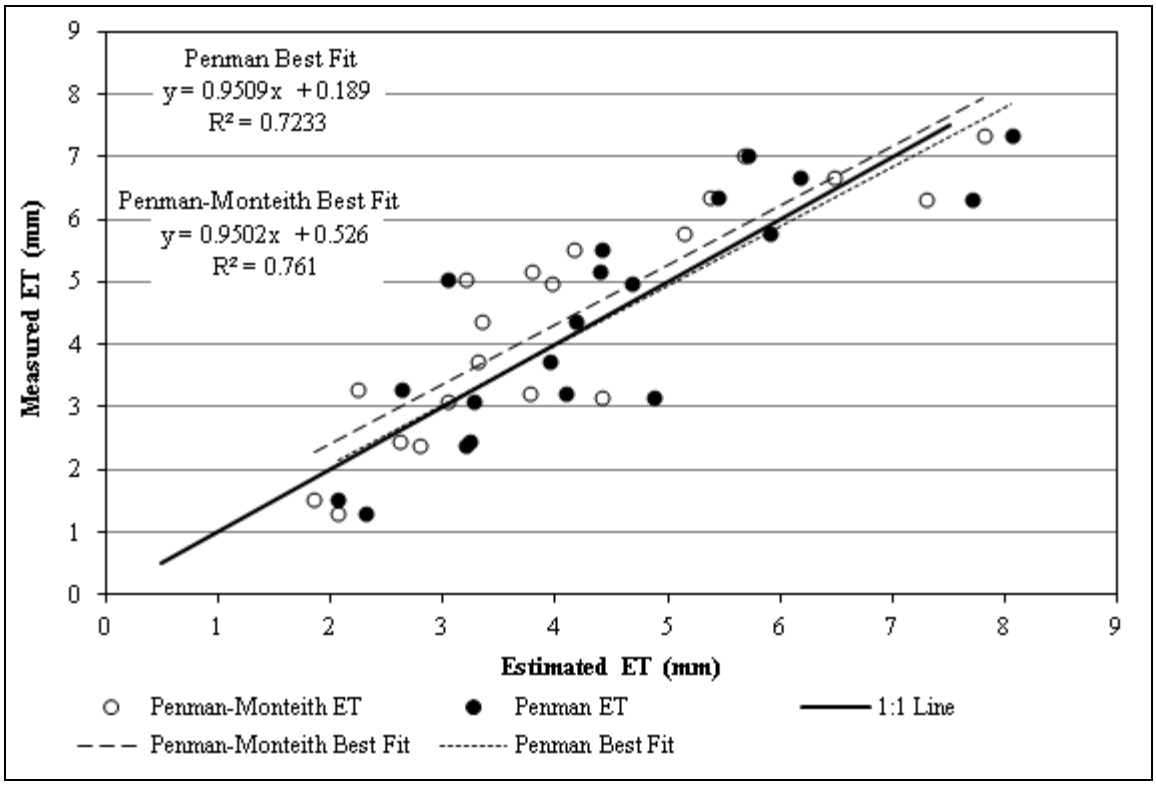

Figure 4.2. April 2009. "B" Penman and Penman-Monteith estimated versus lysimeter ET

The remaining plots, Figures "C" and "D" (e.g., Figures 4.3 and 4.4, respectively), represent the individual variability of each data point for Penman estimated ET and calibrated Penman-Monteith estimated ET, respectively. To determine if the estimated

ET values represent the actual ET occurring on the roof (within the range of measurement error), the appropriate error bars (as calculated in Chapter 3) were applied to each day, then compared to the one-to-one line. If the one-to-one line fell within the error bars, the ET estimates for that day were considered to be acceptable. Data points that failed to encompass the one-to-one line in their error bars (denoted with an "X" in Figures "C" and D") represent days in which the estimation equations failed to sufficiently explain the evapotranspiration process occurring on the roof.

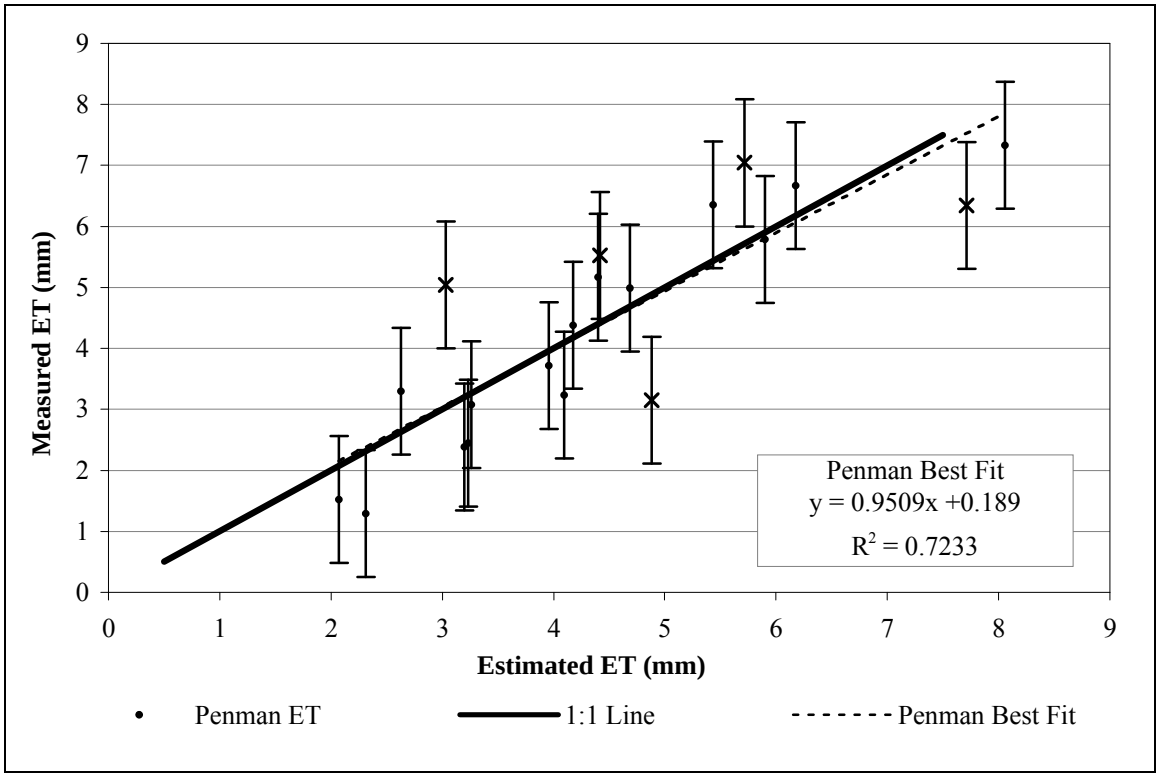

Figure 4.3. April 2009. "C" Measured versus Penman estimated ET

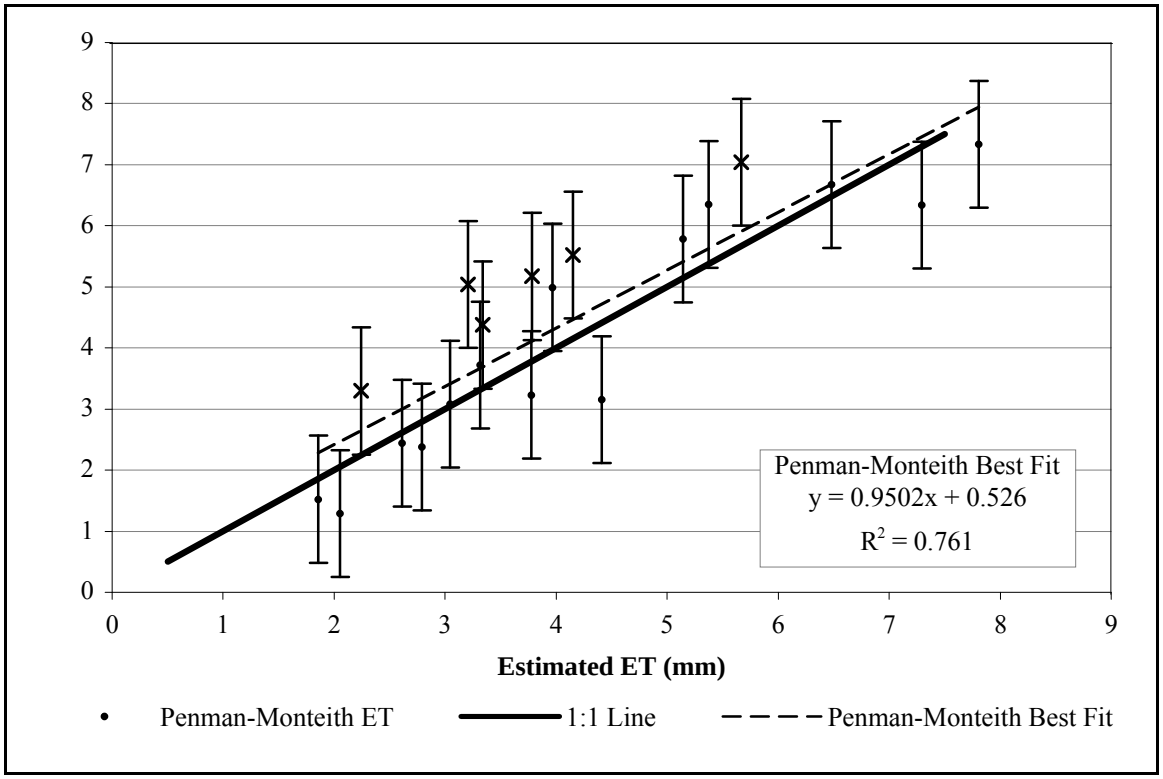

Figure 4.4. April 2009. "D" Measured versus Penman-Monteith estimated ET

The figures that follow (Figure 4.5 through Figure 4.32) depict the resultant relationships of the Penman and Penman-Monteith equations for the remaining months in this study (May through November 2009). Each month has been evaluated using the same routine outlined above (April 2009).

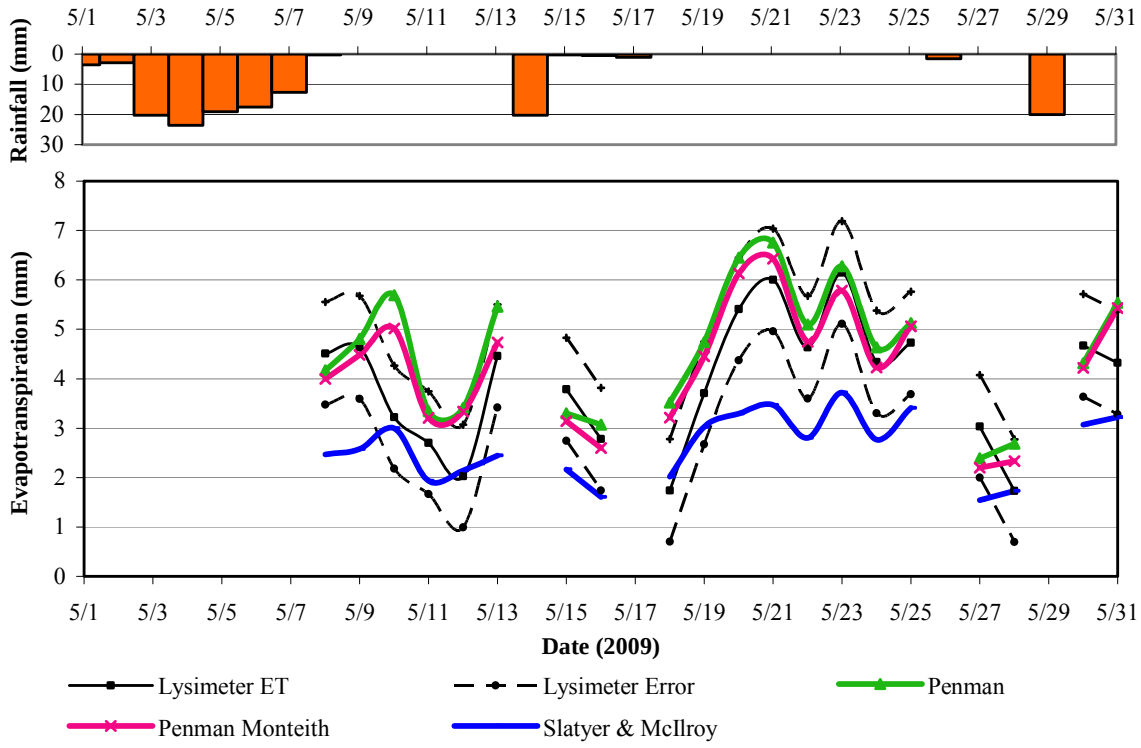

Figure 4.5. May 2009. "A" A comparison of measured and estimated ET

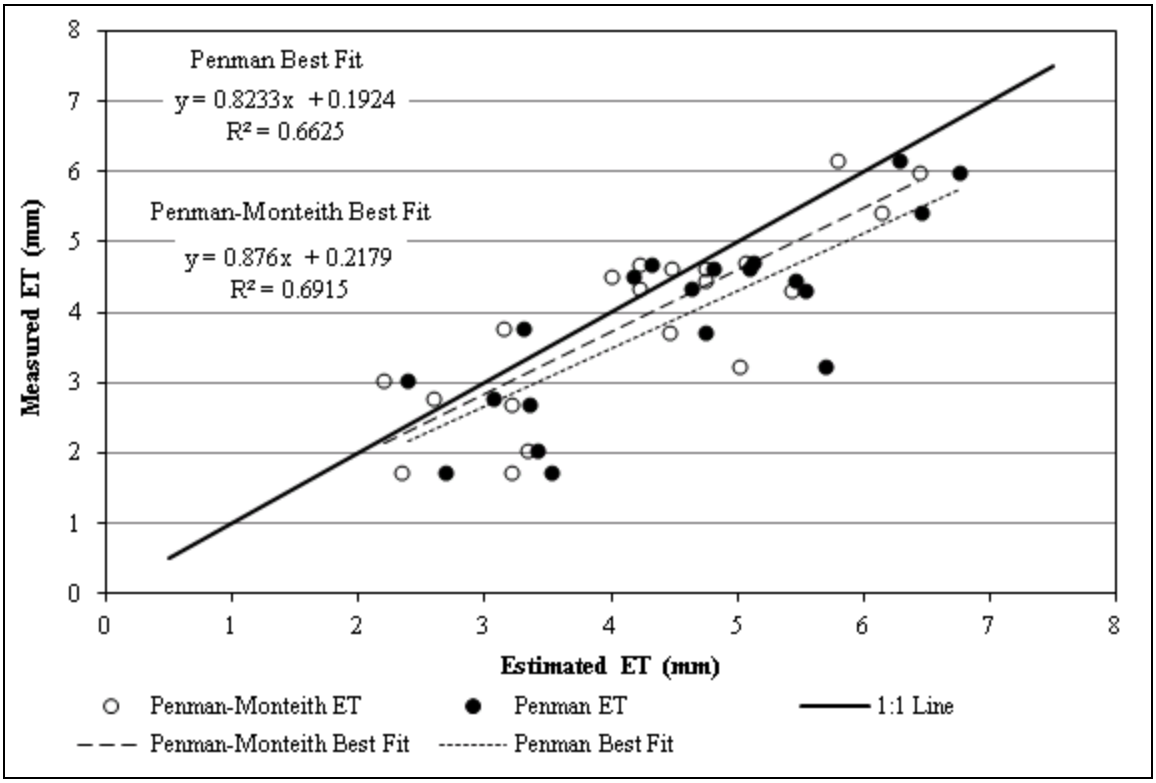

Figure 4.6. May 2009. "B" Penman and Penman-Monteith estimated versus lysimeter ET

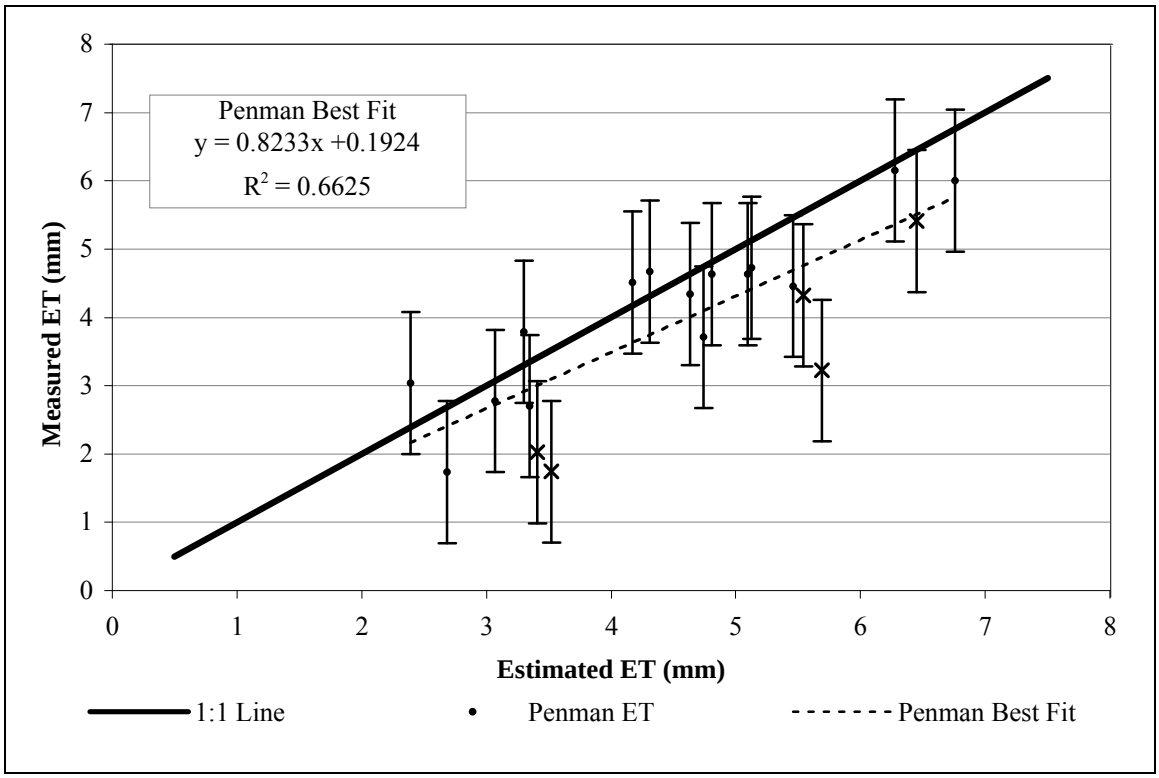

Figure 4.7. May 2009. "C" Measured versus Penman estimated ET

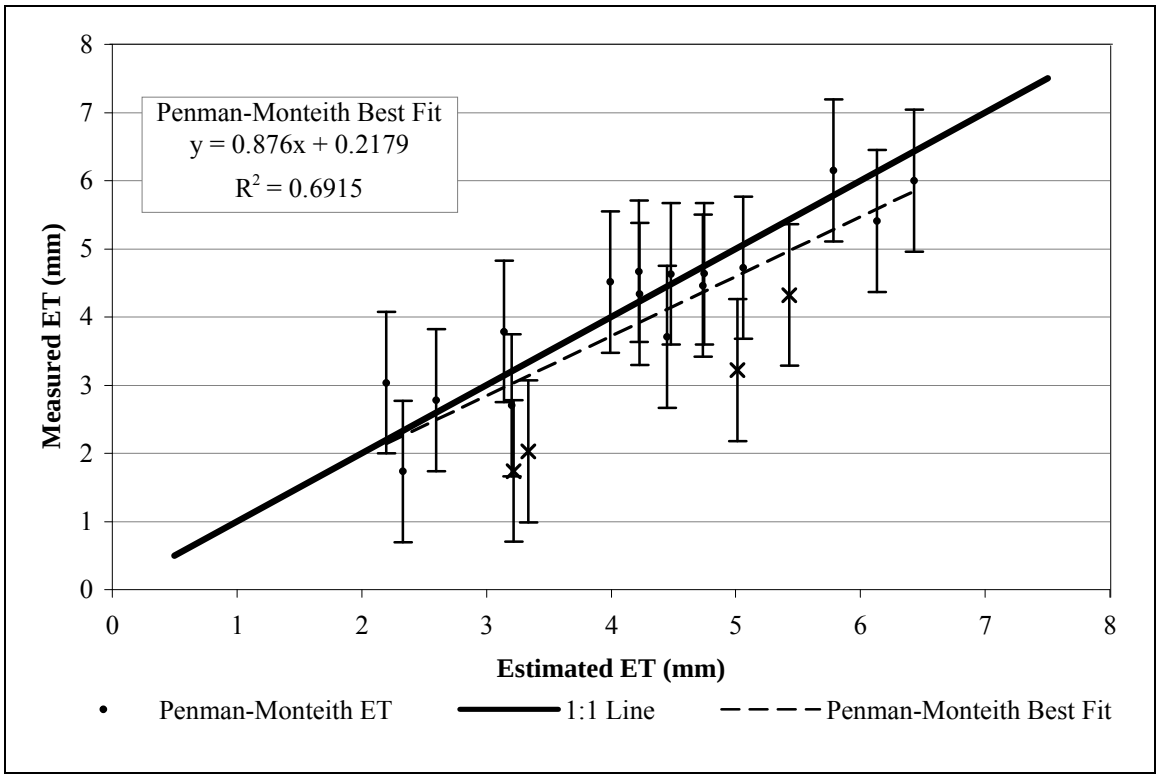

Figure 4.8. May 2009. "D" Measured versus Penman-Monteith estimated ET

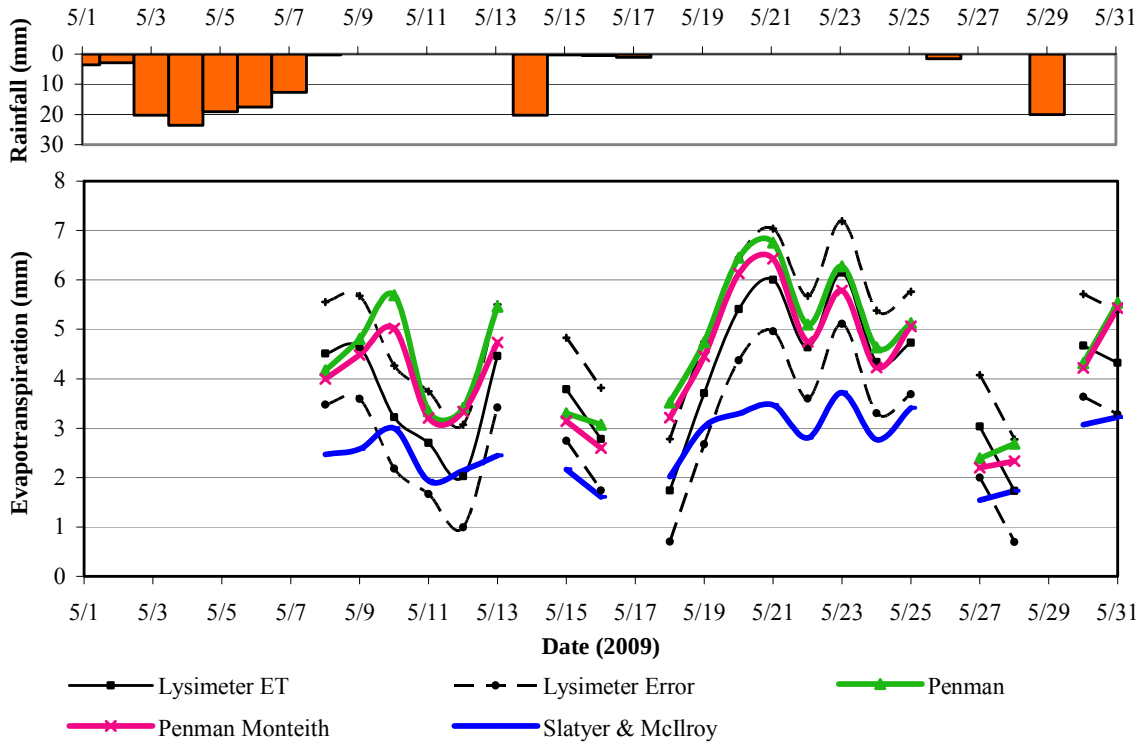

Figure 4.5. May 2009. "A" A comparison of measured and estimated ET

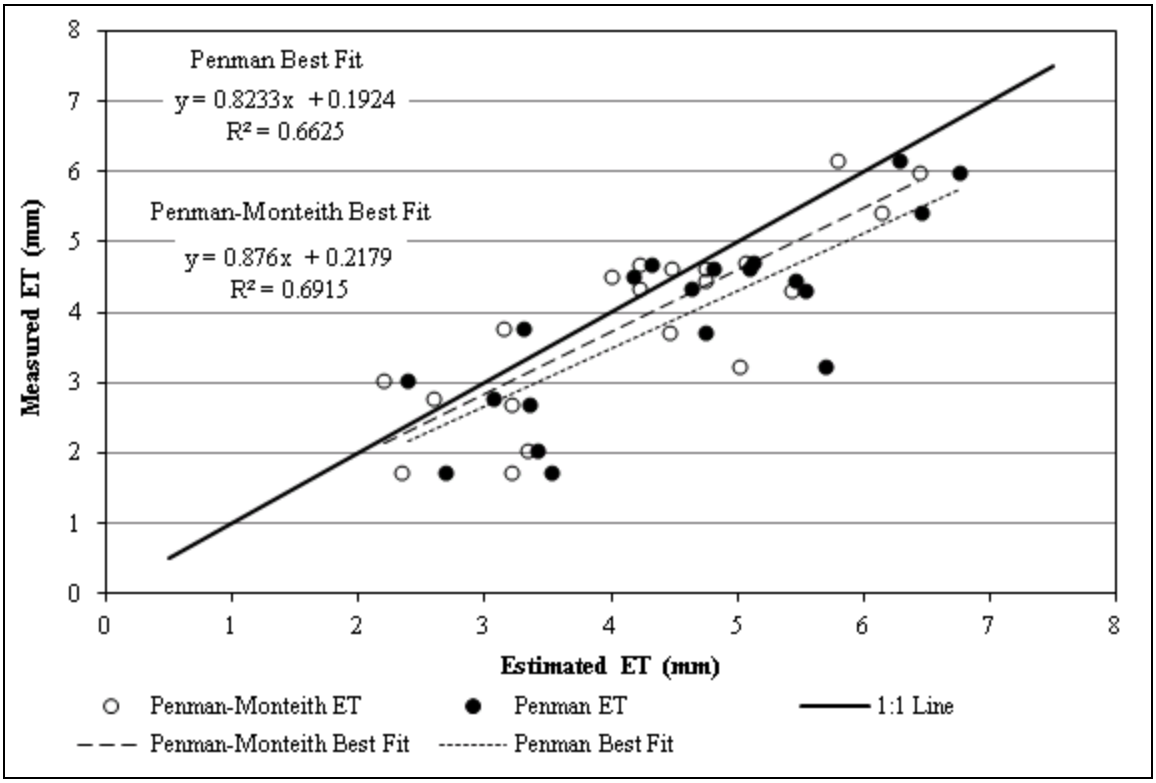

Figure 4.6. May 2009. "B" Penman and Penman-Monteith estimated versus lysimeter ET

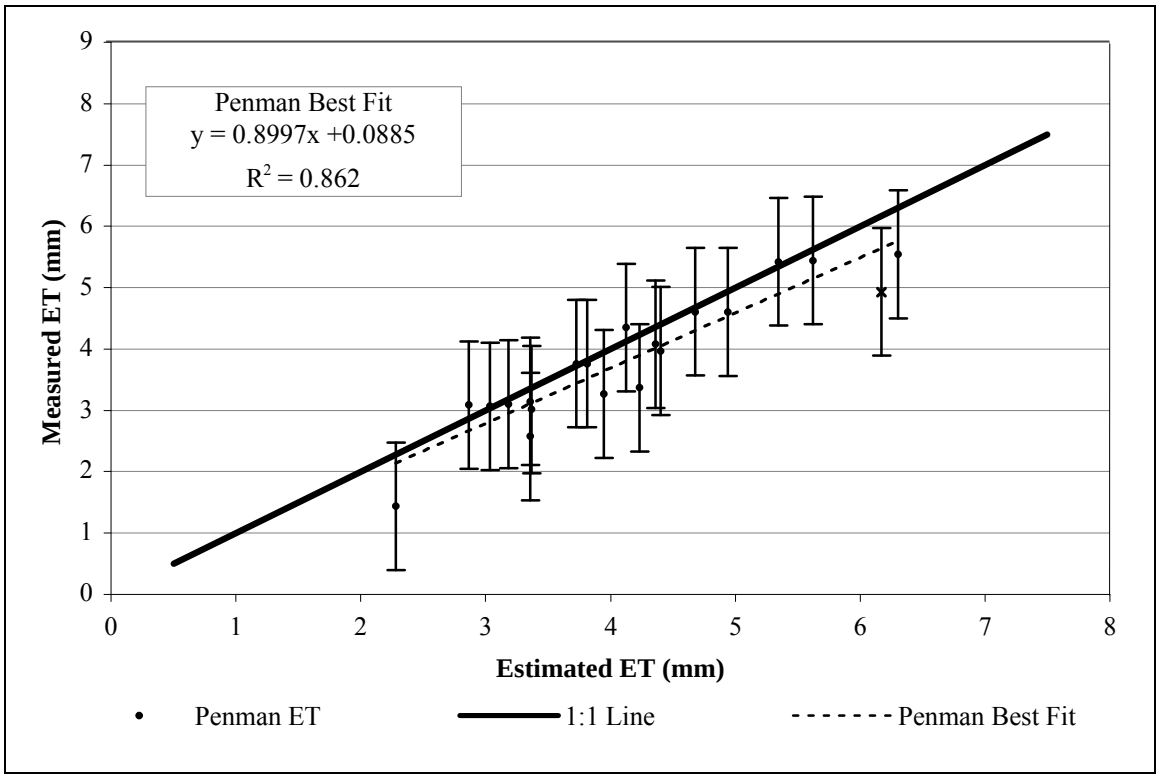

Figure 4.11. June 2009. "C" Measured versus Penman estimated ET

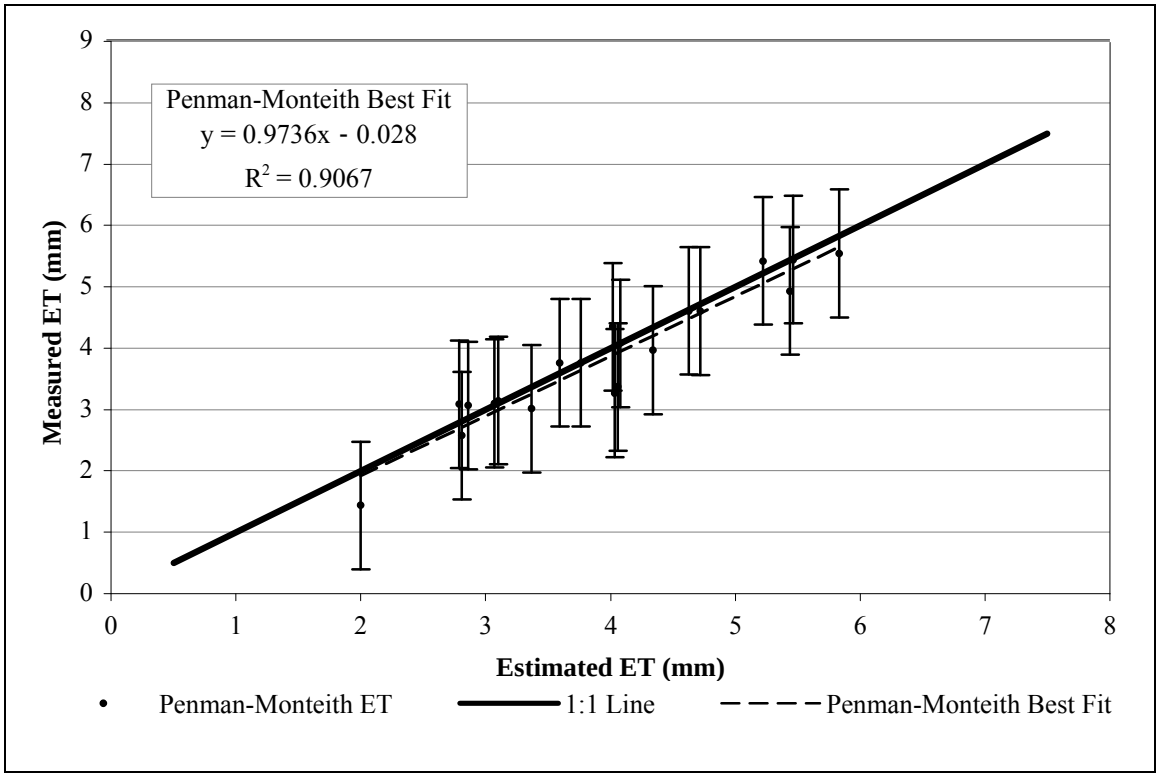

Figure 4.12. June 2009. "D" Measured versus Penman-Monteith estimated ET

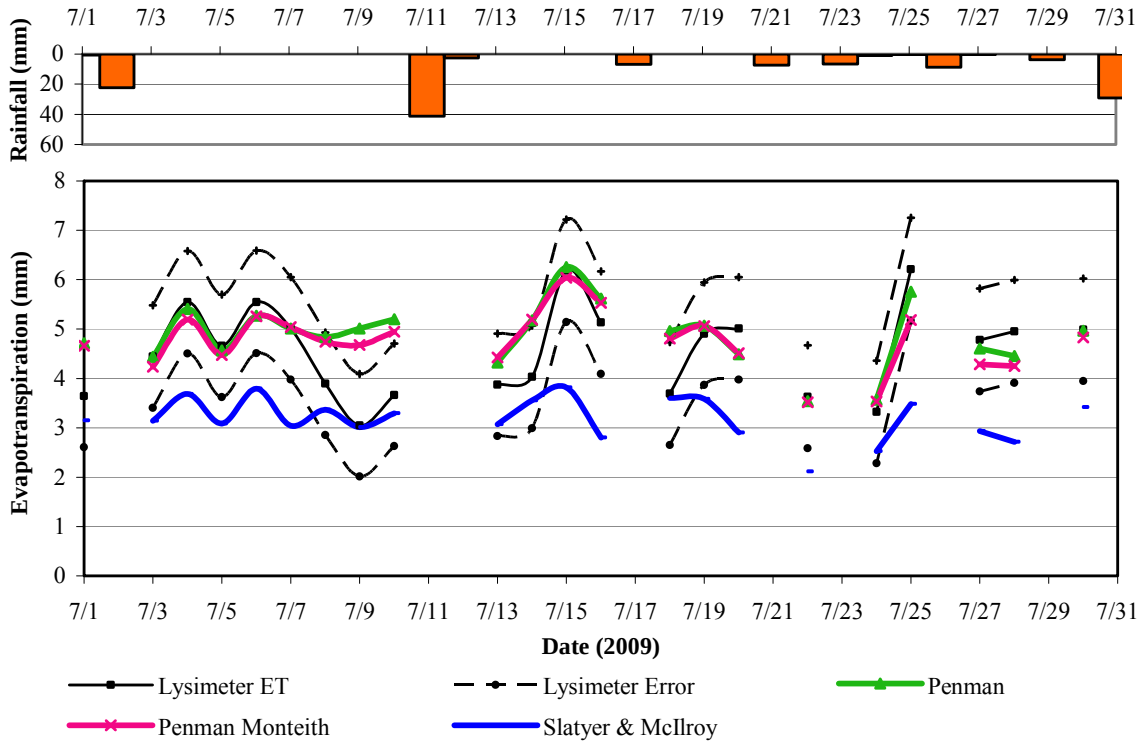

Figure 4.13. July 2009. "A" A comparison of measured and estimated ET

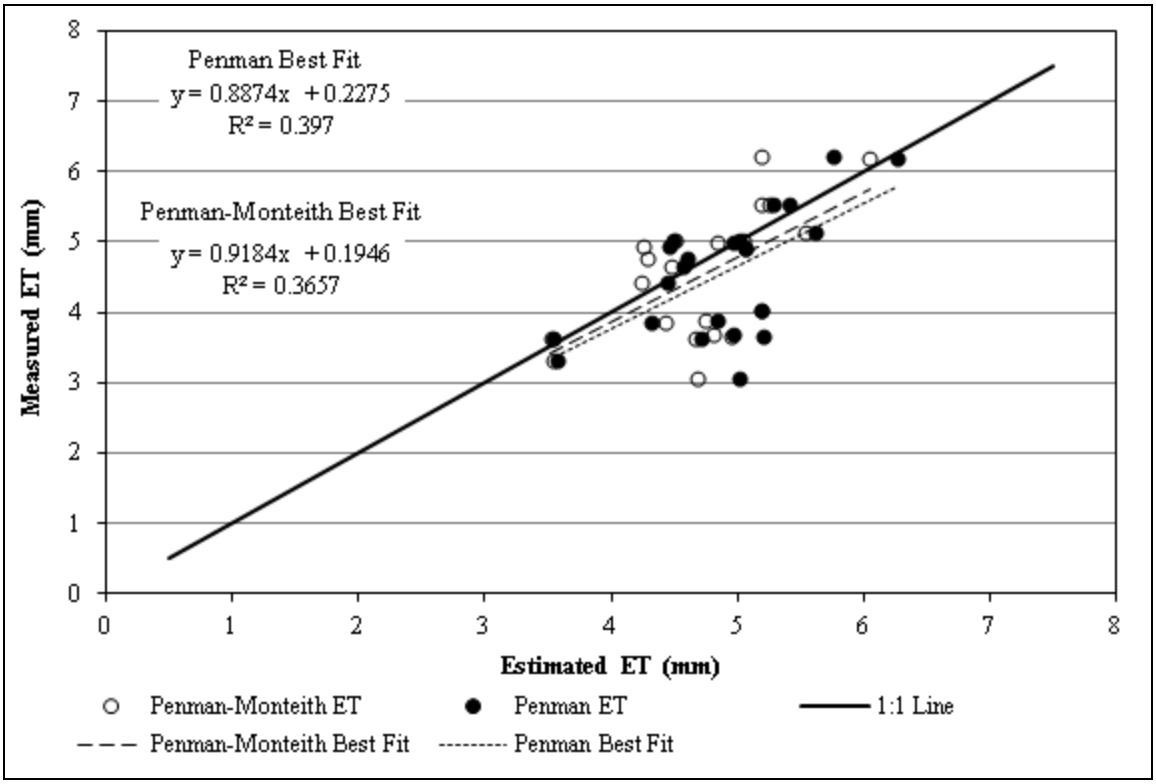

Figure 4.14. July 2009. "B" Penman and Penman-Monteith estimated versus lysimeter ET

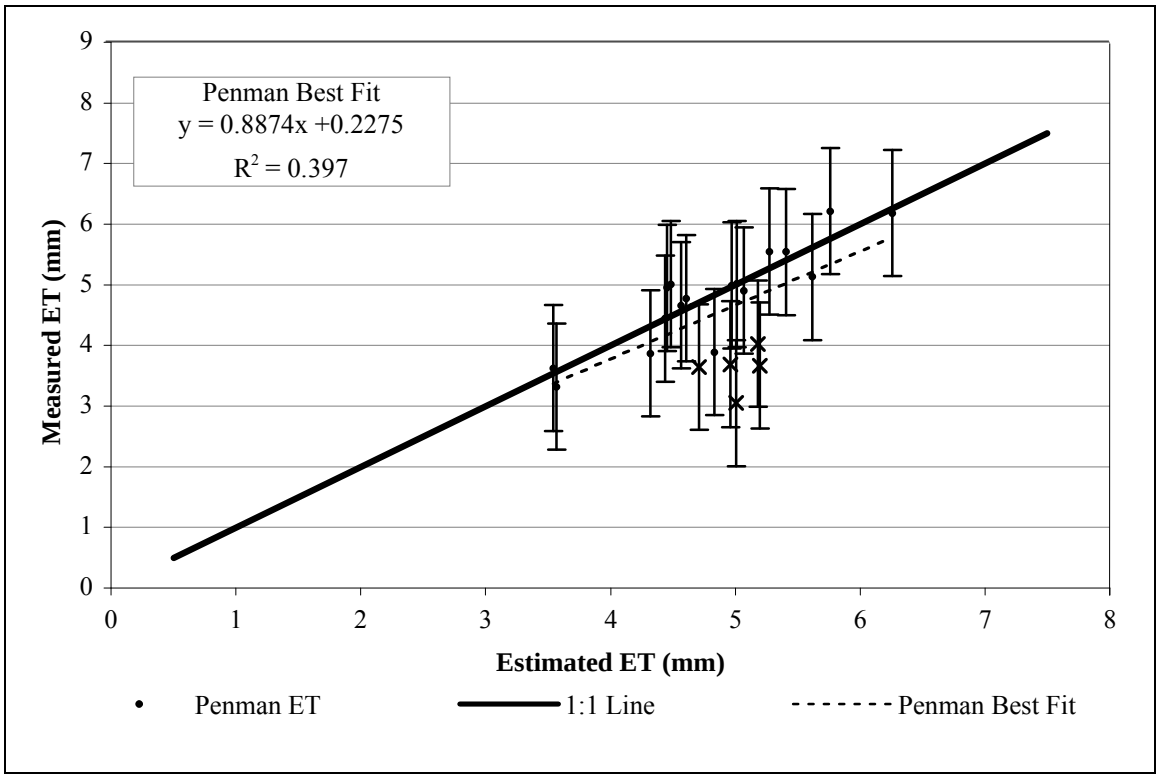

Figure 4.15. July 2009. "C" Measured versus Penman estimated ET

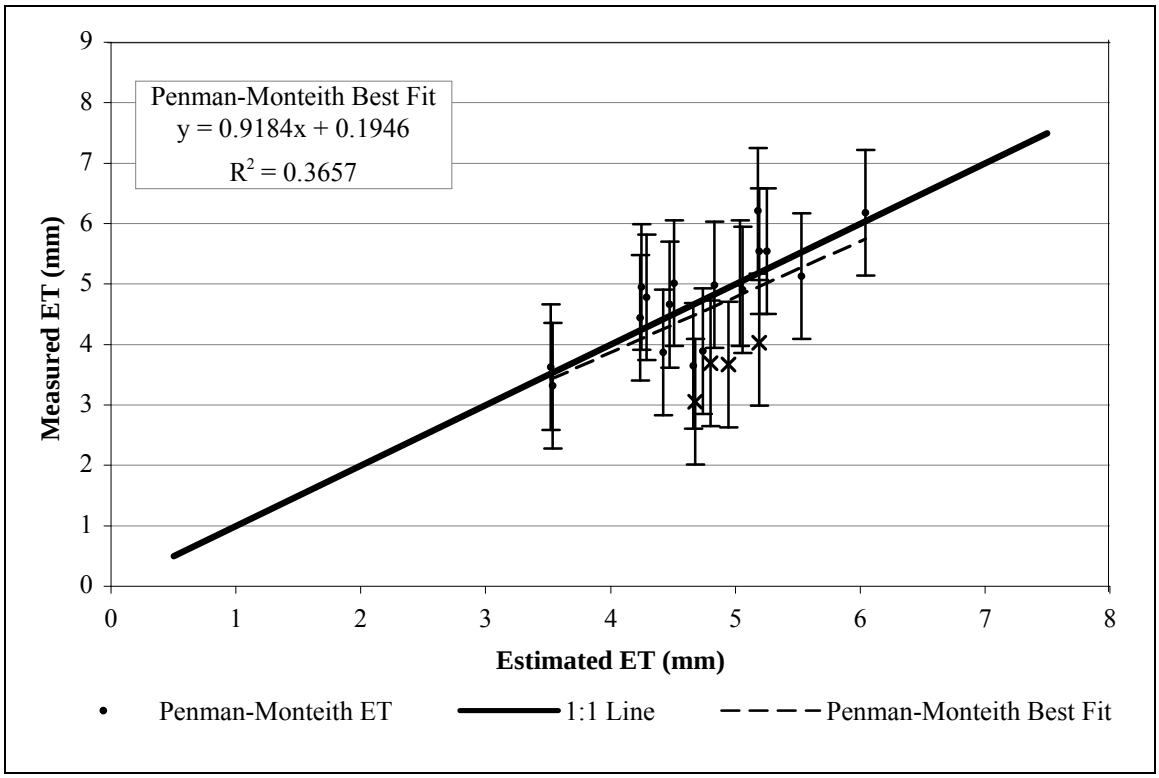

Figure 4.16. July 2009. "D" Measured versus Penman-Monteith estimated ET

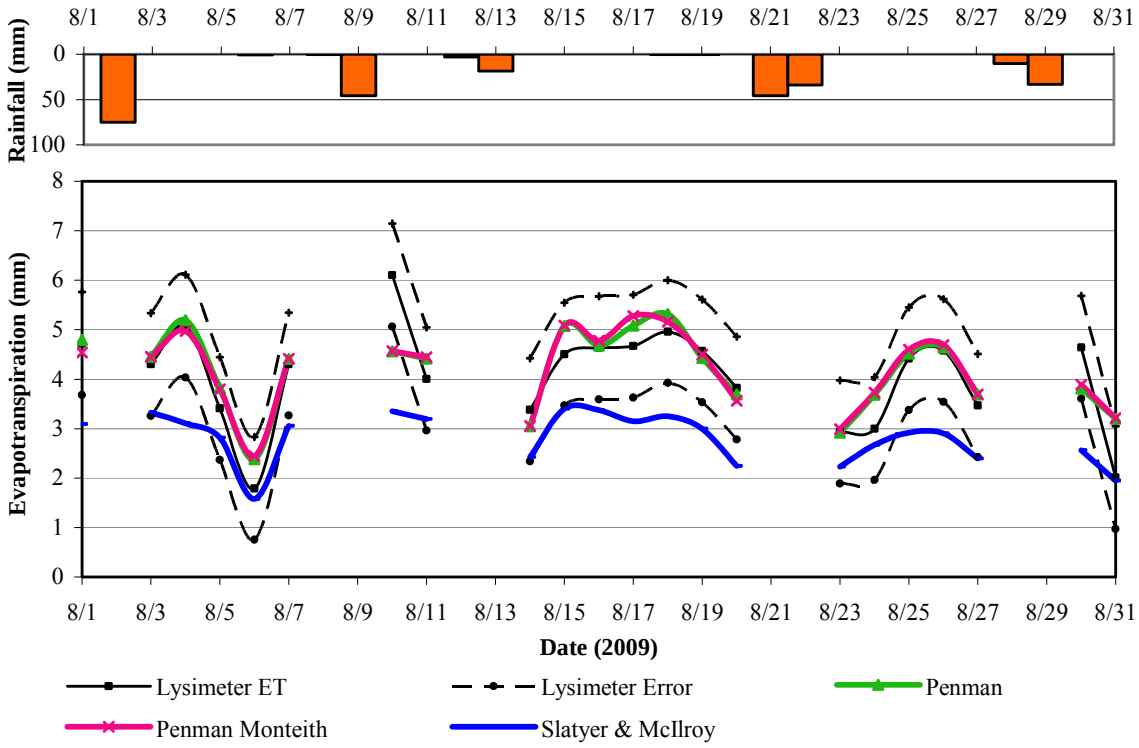

Figure 4.17. August 2009. "A" A comparison of measured and estimated ET

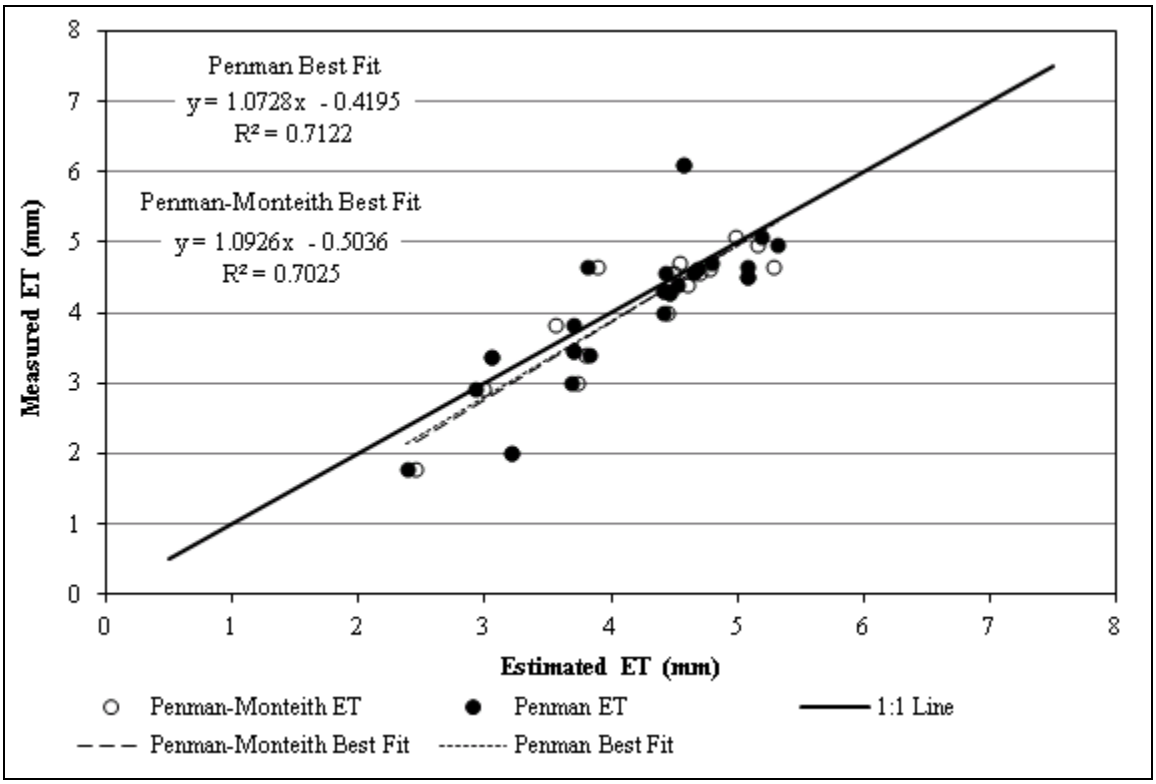

Figure 4.18. August 2009. "B" Penman and Penman-Monteith estimated versus lysimeter ET

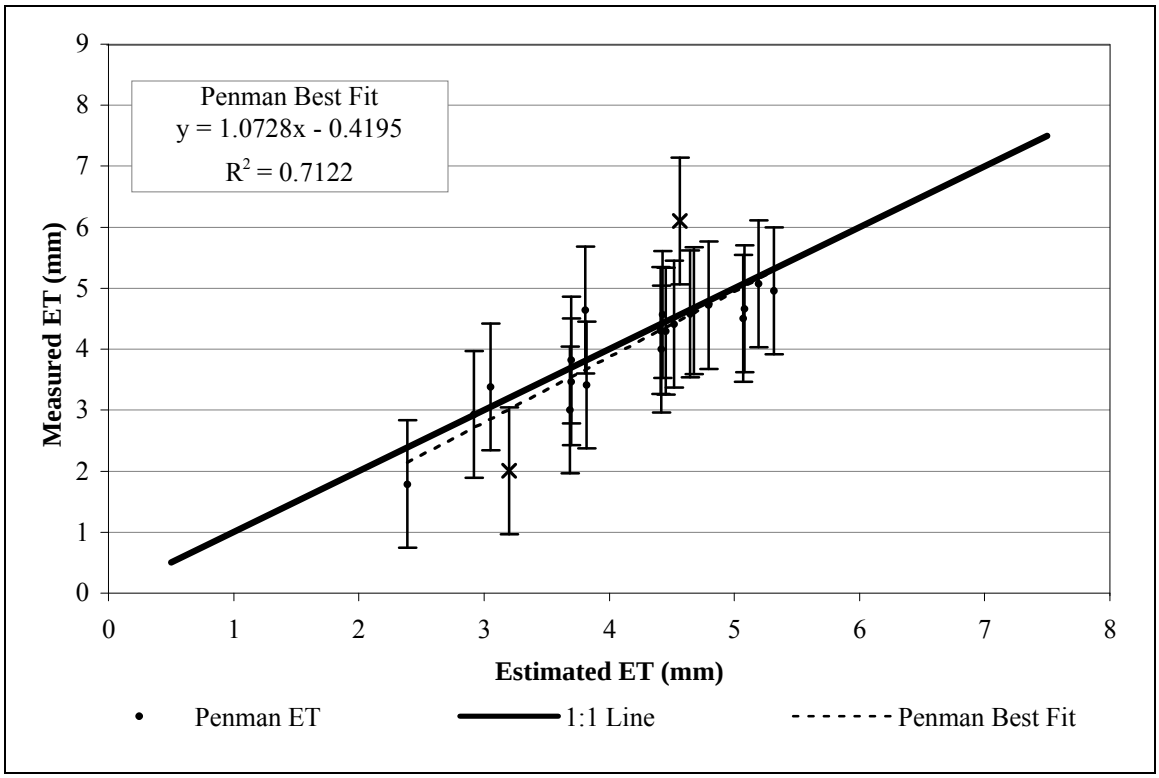

Figure 4.19. August 2009. "C" Measured versus Penman estimated ET

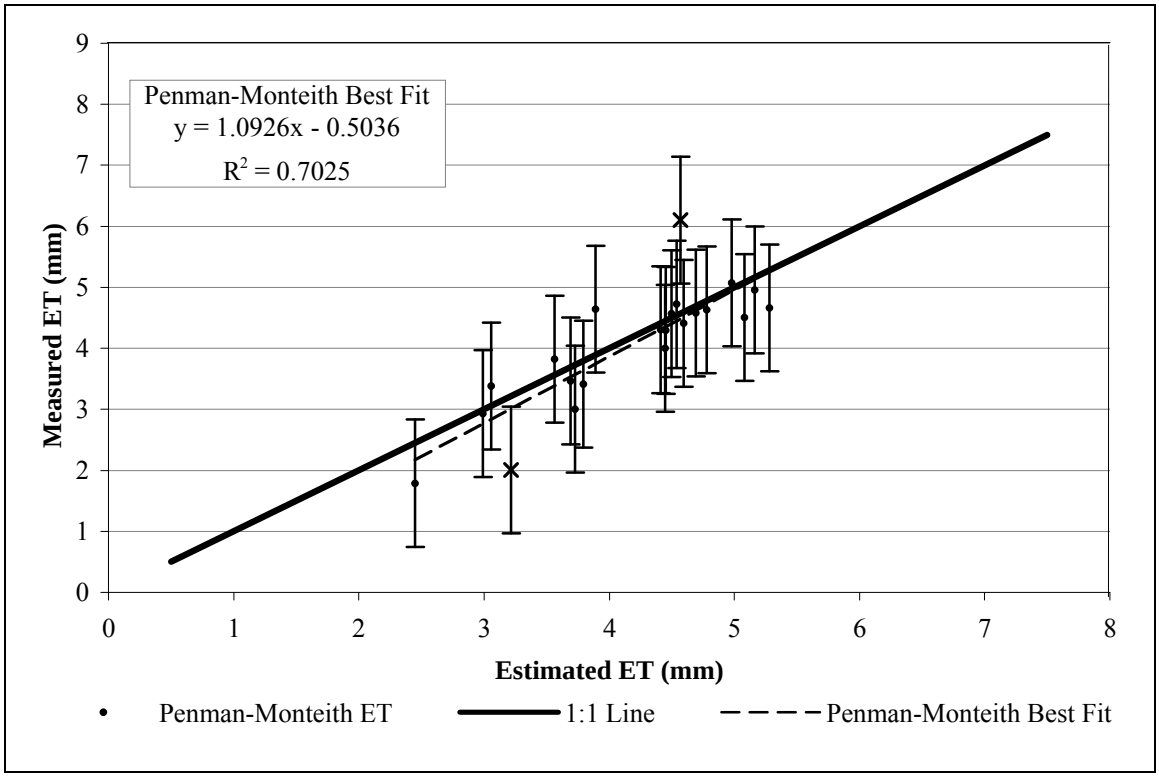

Figure 4.20. August 2009."D" Measured versus Penman-Monteith estimated ET

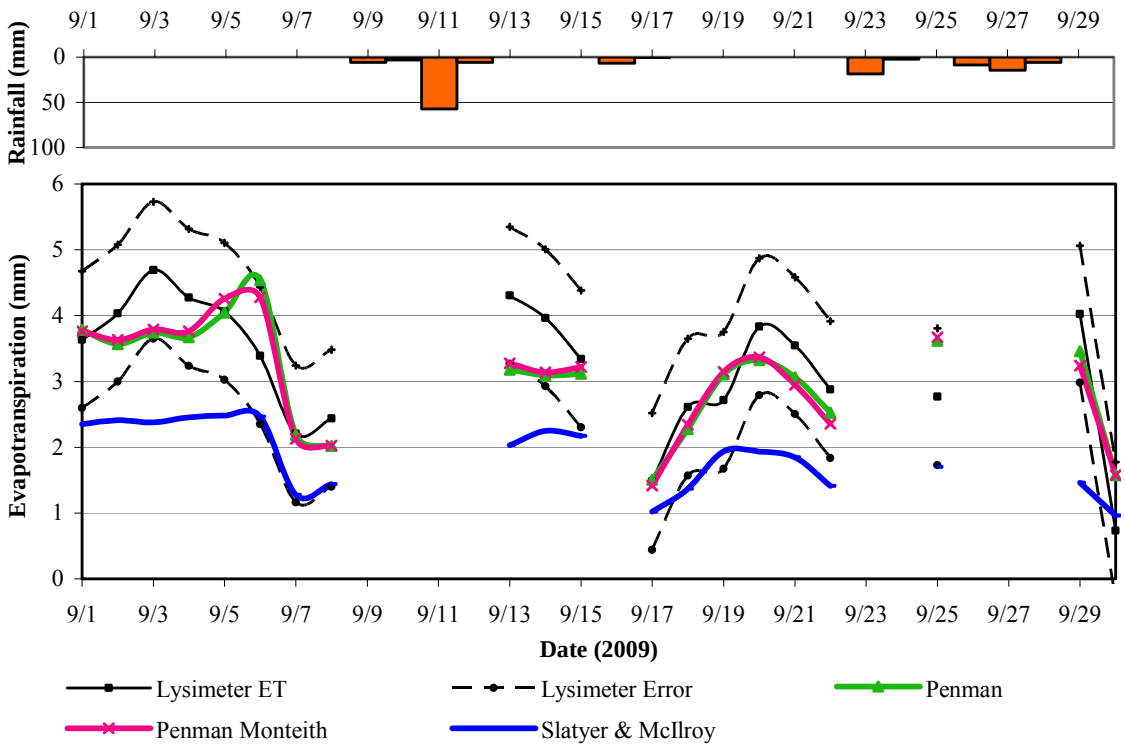

Figure 4.21. September 2009. "A" A comparison of measured and estimated ET

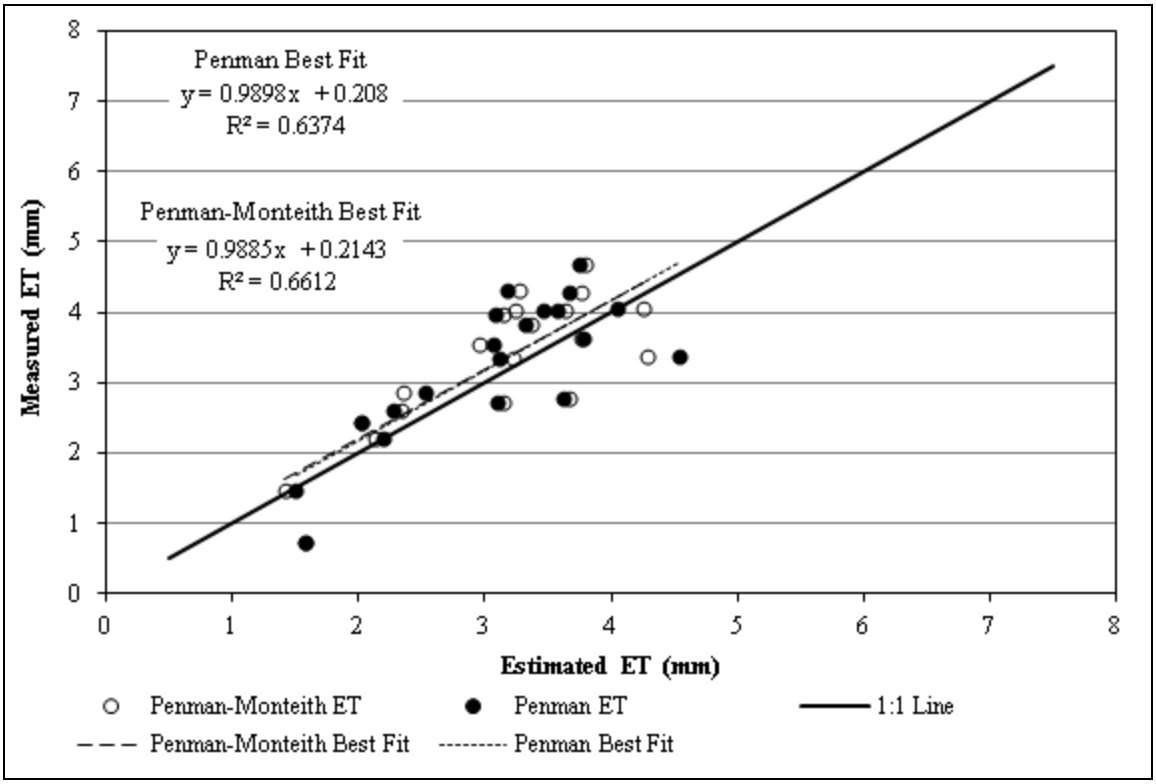

Figure 4.22. September 2009."B" Penman and Penman-Monteith estimated versus lysimeter ET

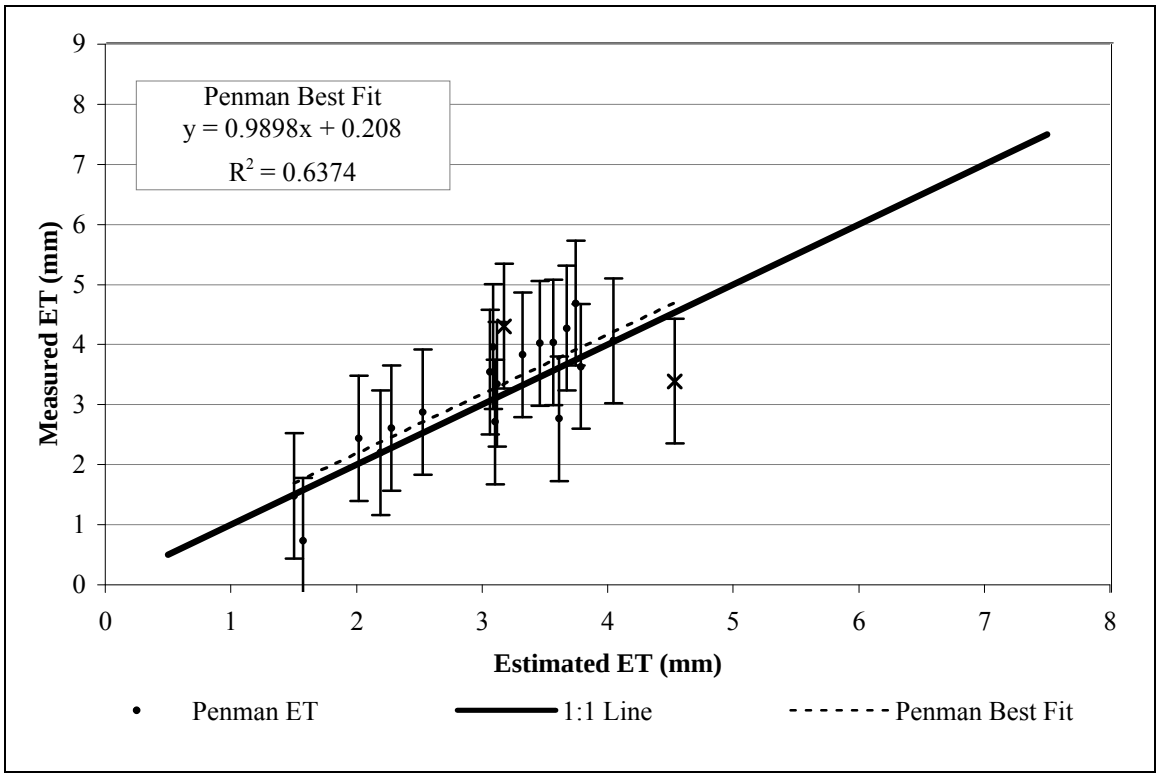

Figure 4.23. September 2009. "C" Measured versus Penman estimated ET

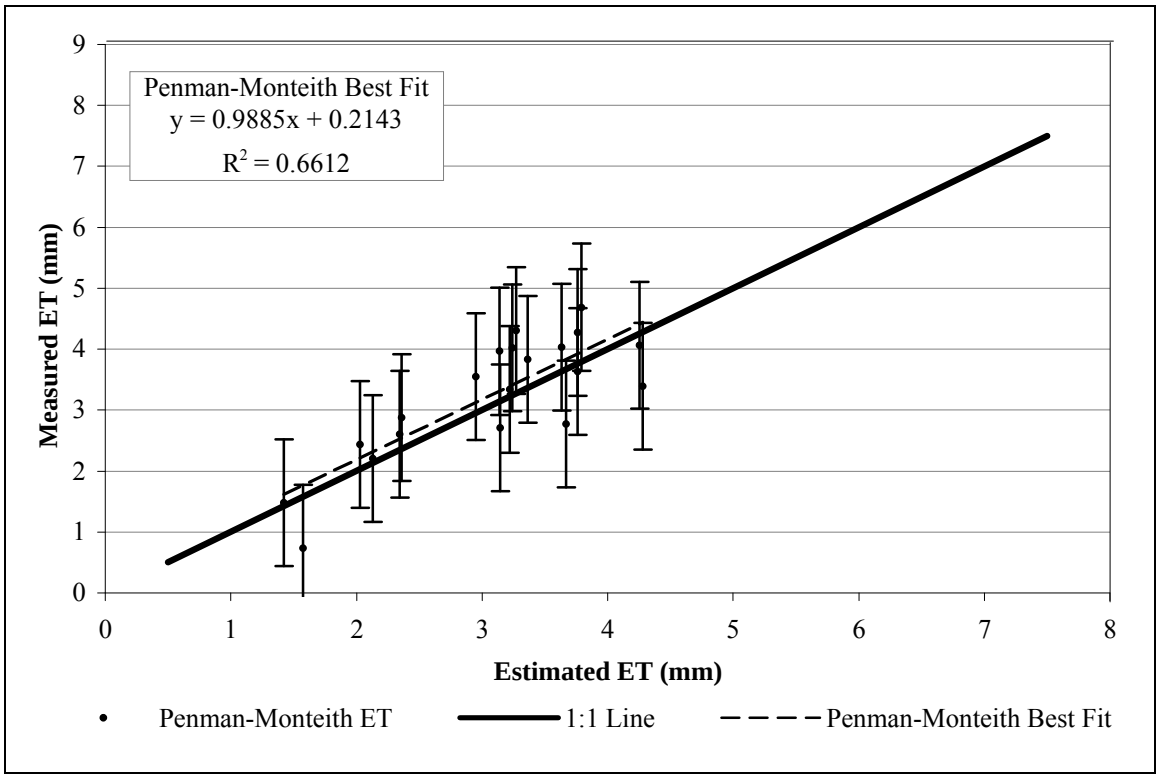

Figure 4.24. September 2009. "D" Measured versus Penman-Monteith estimated ET

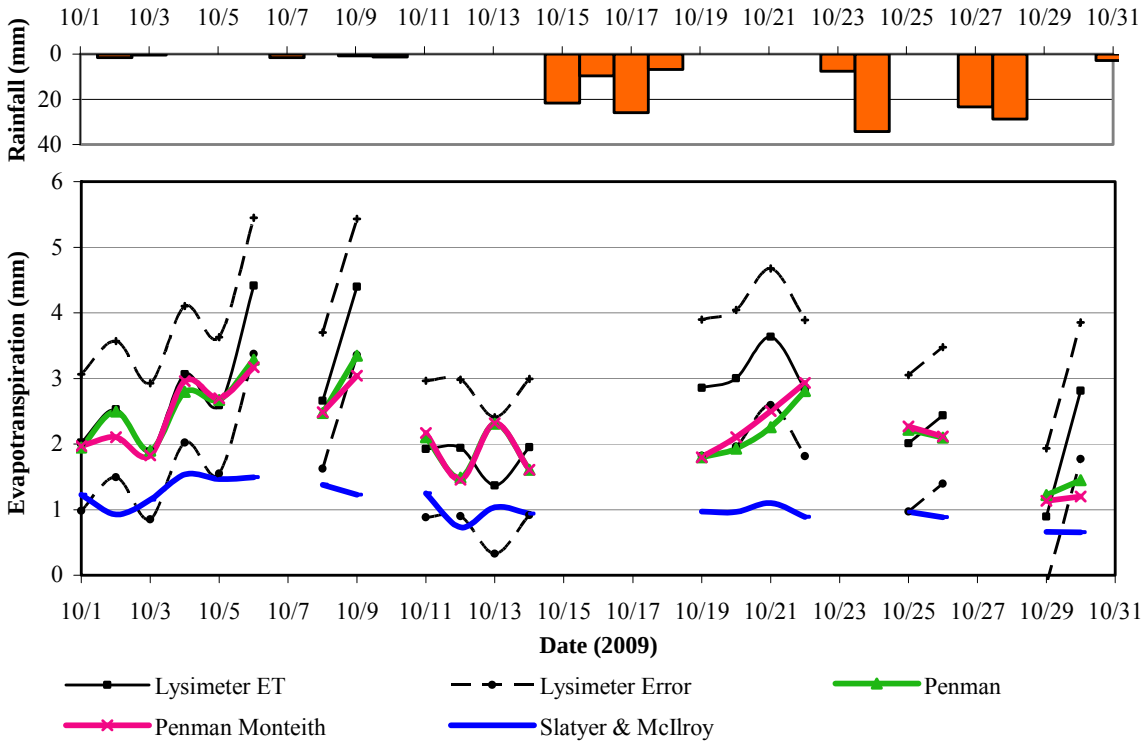

Figure 4.25. October 2009. "A" A comparison of measured and estimated ET

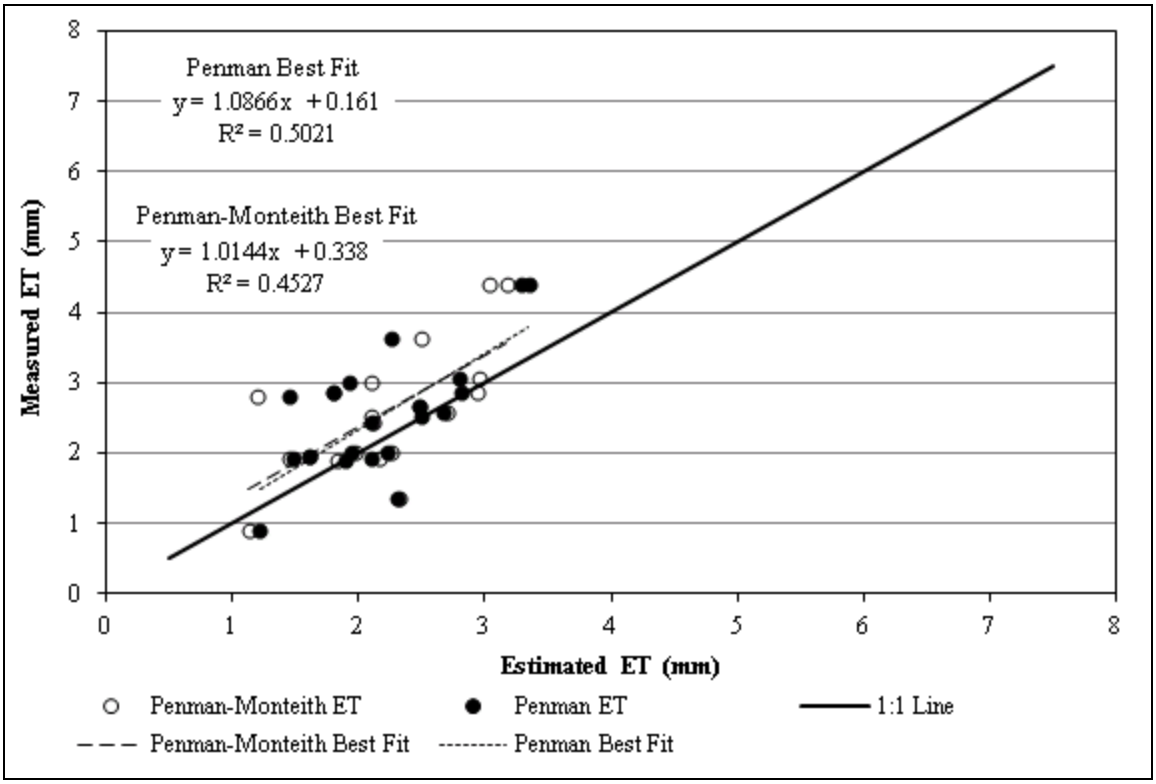

Figure 4.26. October 2009. "B" Penman and Penman-Monteith estimated versus lysimeter ET

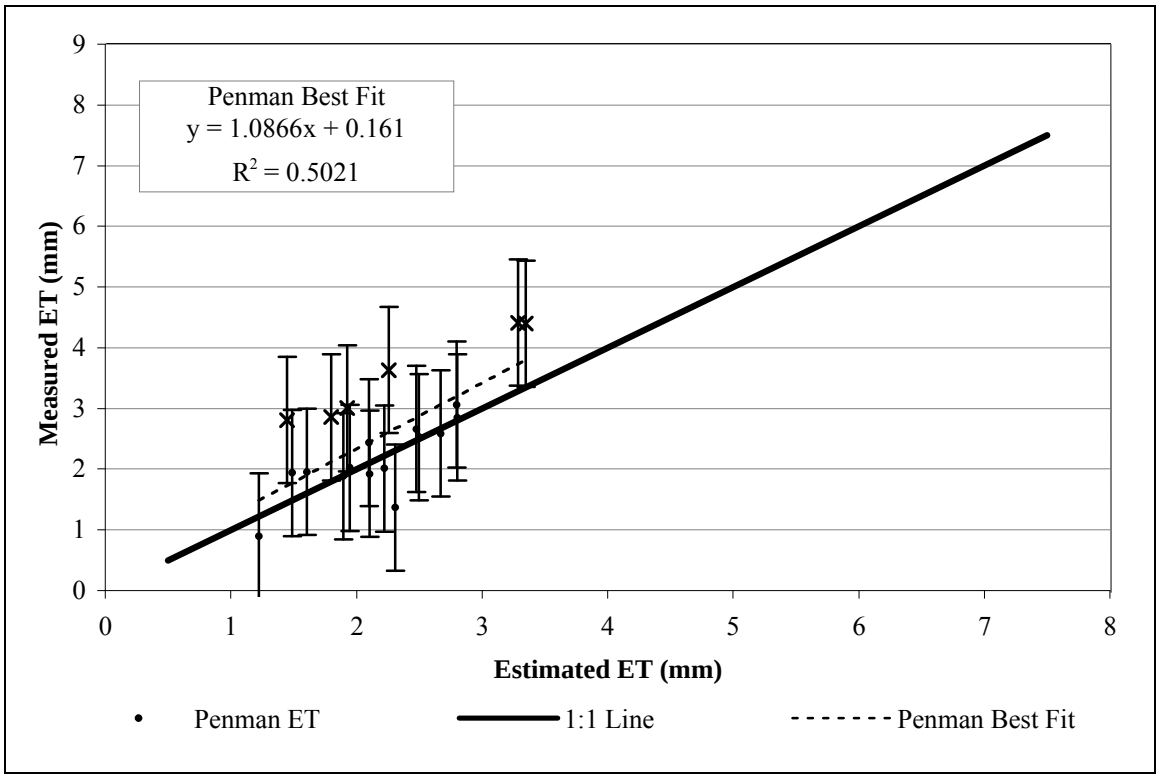

Figure 4.27. October 2009. "C" Measured versus Penman estimated ET

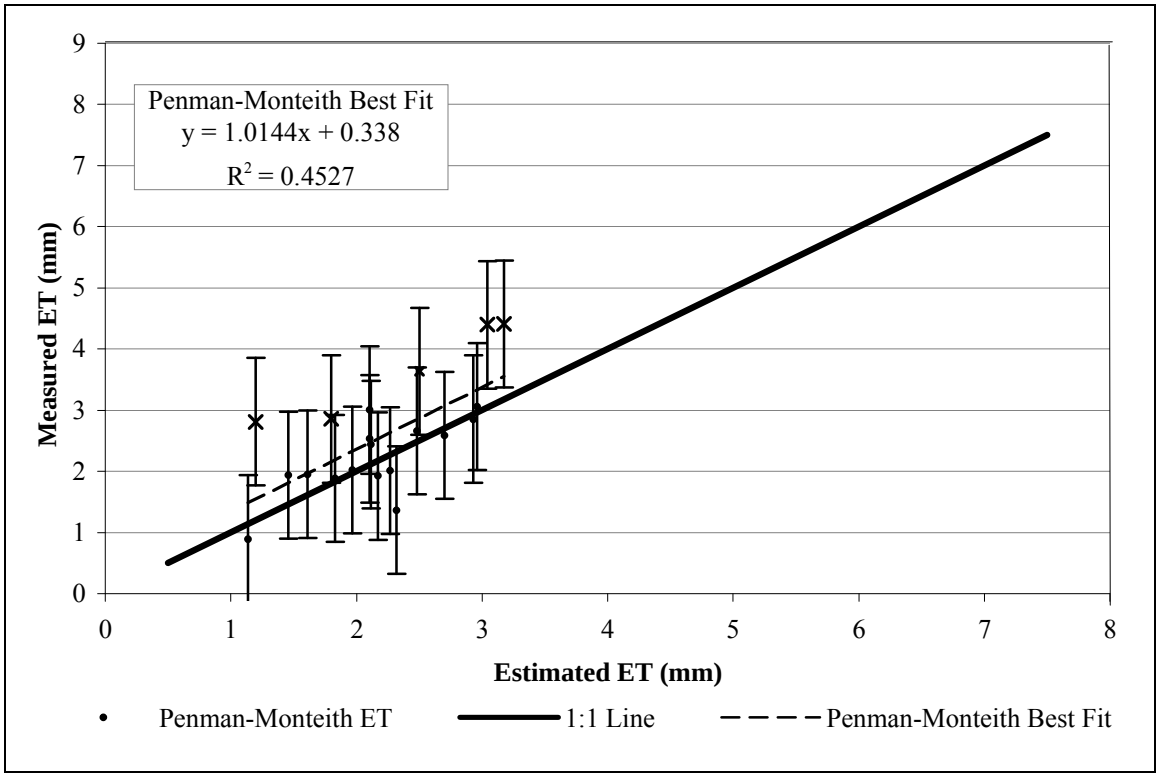

Figure 4.28. October 2009. "D" Measured versus Penman-Monteith estimated ET

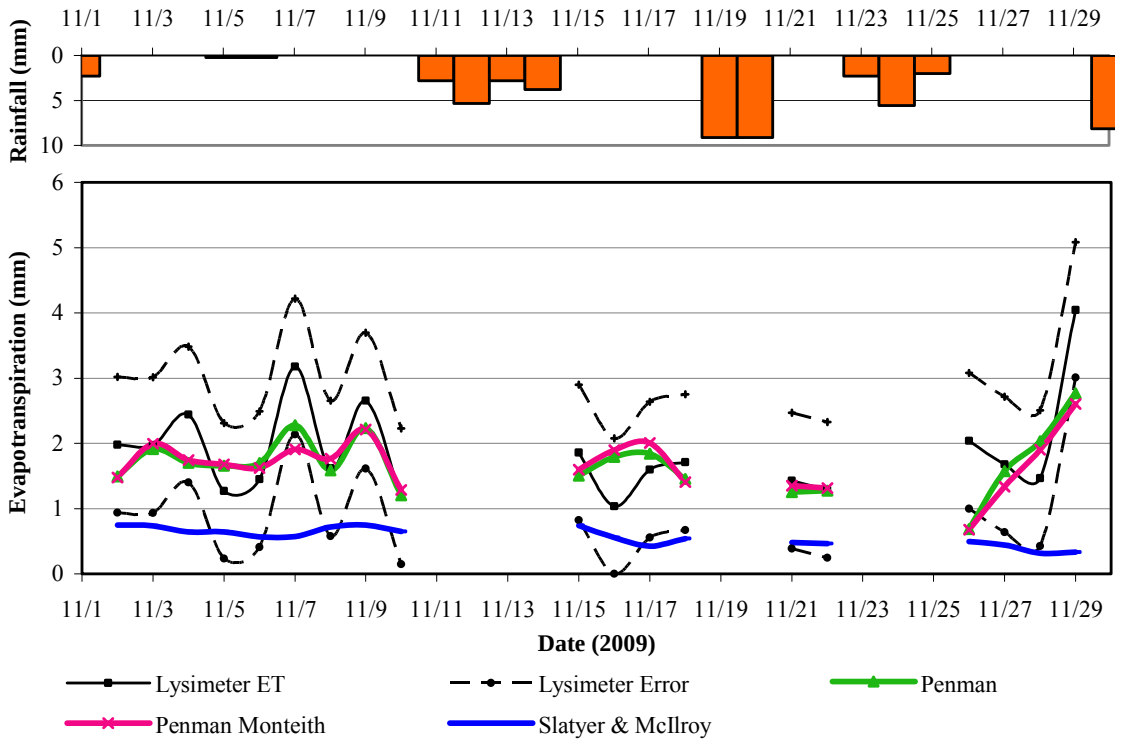

Figure 4.29. November 2009. "A" A comparison of measured and estimated ET

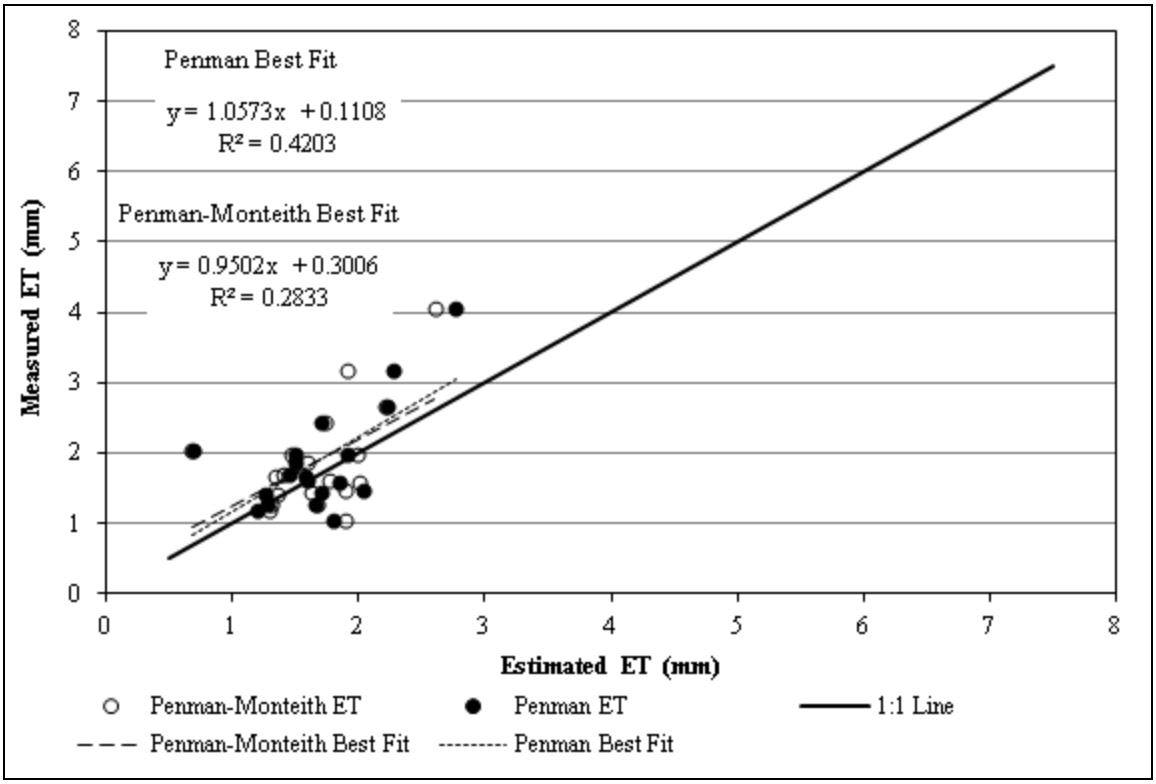

Figure 4.30. November 2009. "B" Penman and Penman-Monteith estimated versus lysimeter ET

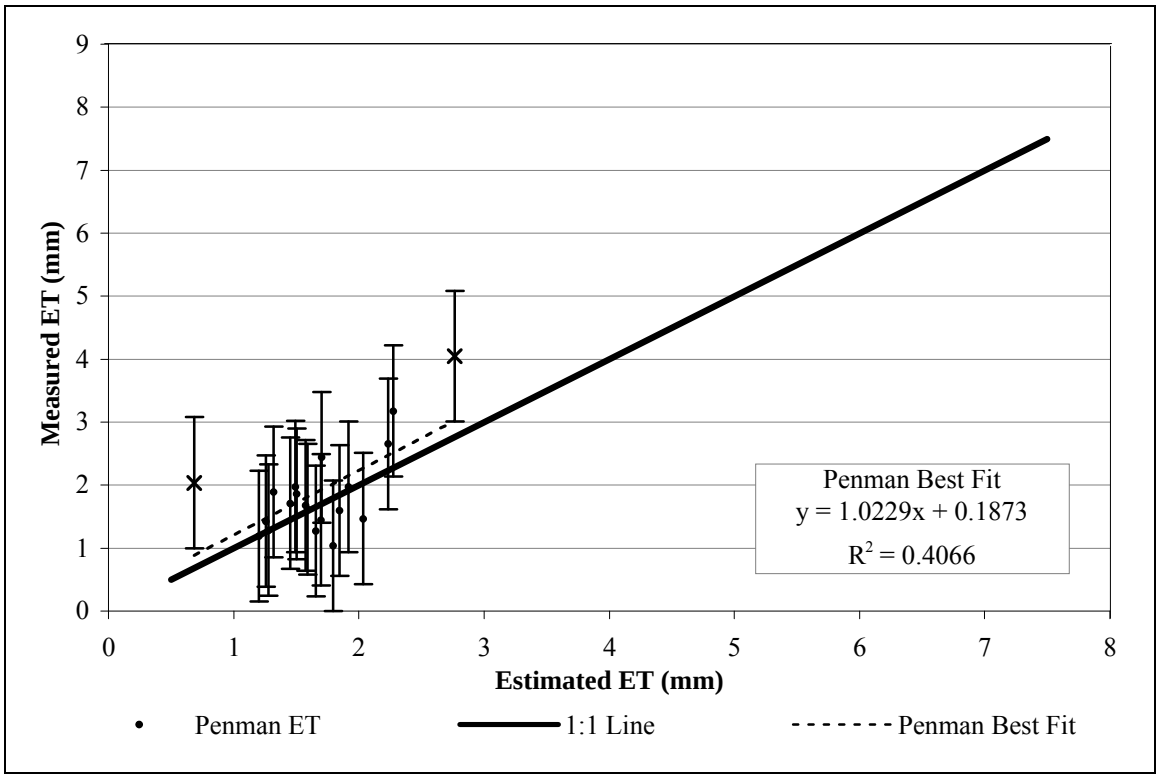

Figure 4.31. November 2009. "C" Measured versus Penman estimated ET

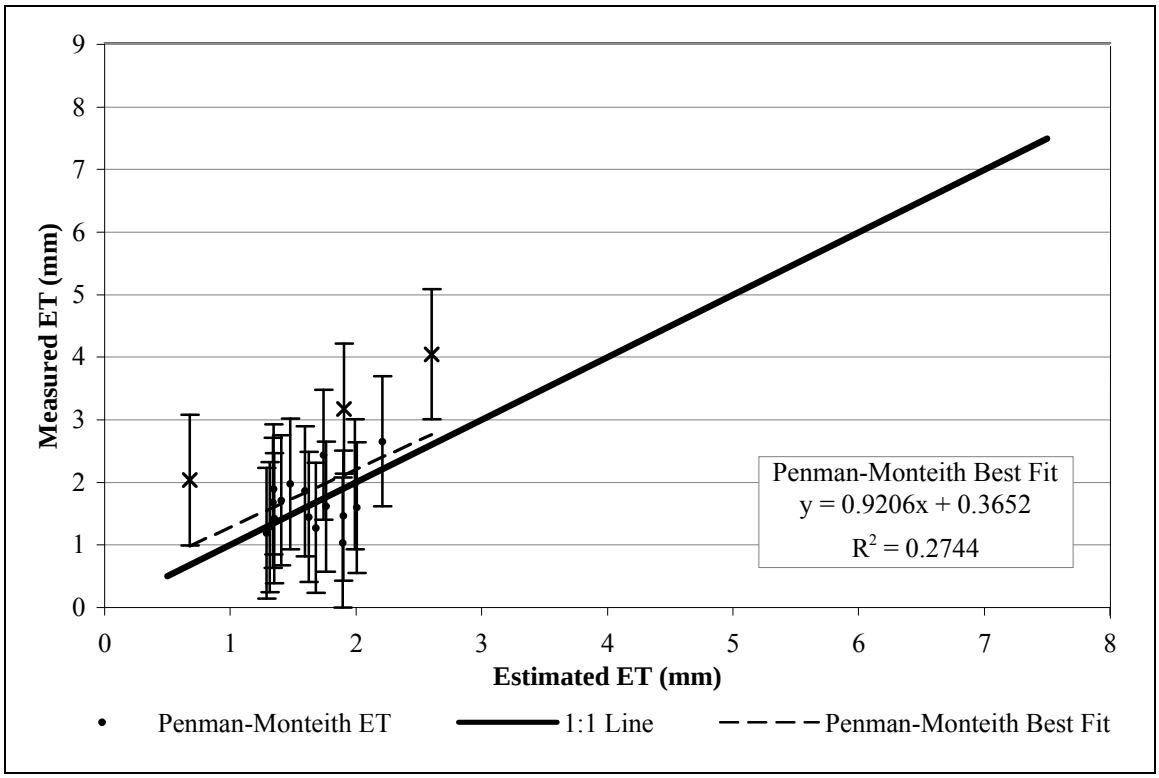

Figure 4.32. November 2009. "D" Measured versus Penman-Monteith estimated ET

4.2.2 *Numerical Evaluation of Predictive Equations*

A linear regression was used to evaluate the ability of the Penman and Penman-Monteith equations to accurately represent measured, lysimeter ET from the green roof lysimeter (as shown in Figure "B" above). The slope (m) and intercept (b) of the best fit line demonstrate how well the estimation equations predicted ET for a particular month while the coefficient of determination represents how much variability was accounted for by the regression, thus establishing a "goodness of fit". The results of this analysis are provided in Table 4.1.

Table 4.1. Linear Regression of the Penman and Penman-Monteith equations by month

Month	**Equation**	**Parameter**		
		m	**b**	**R^2**
APR	*Penman*	0.9509	0.189	0.7233
	Penman-Monteith	0.9502	0.526	0.7610
MAY	*Penman*	0.8233	0.1924	0.6625
	Penman-Monteith	0.8760	0.2179	0.6915
JUN	*Penman*	0.8997	0.0885	0.8620
	Penman-Monteith	0.9736	-0.0280	0.9067
JUL	*Penman*	0.8874	0.2275	0.3970
	Penman-Monteith	0.9184	0.1946	0.3657
AUG	*Penman*	1.0728	-0.4195	0.7122
	Penman-Monteith	1.0926	-0.5036	0.7025
SEP	*Penman*	0.9898	0.2080	0.6374
	Penman-Monteith	0.9885	0.2143	0.6612
OCT	*Penman*	1.0866	0.1610	0.5021
	Penman-Monteith	1.0144	0.3380	0.4527
NOV	*Penman*	1.0229	0.1873	0.4066
	Penman-Monteith	0.9206	0.3652	0.2744
ALL	*Penman*	0.8422	0.4937	0.7650
	Penman-Monteith	0.8890	0.4326	0.7757

The Penman-Monteith equation has a slightly higher correlation over the duration of the study (April through November). However, on a monthly basis, the results are variable, with the

Penman equation showing a stronger correlation than the Penman-Monteith for half of the months observed, despite calibration of the Penman-Monteith equation.

This occurrence is likely due to the differences in model structure from the Penman to the Penman-Monteith equation and the calibration methods applied in this study to evaluate the Penman-Monteith equation (i.e.. no consideration for seasonal or monthly variability) Since the Penman equation is an estimate of "potential" ET or ET that would occur if vegetation is not water-stressed and/or the evaporating surface is saturated, the equation tends to over predict ET under water-stressed conditions. The Penman-Monteith equation, on the other hand, is a calibrated estimation of ET, thus it is affected by any water stressed conditions that occurred throughout the calibration period. While this calibration allows for some accounting of water-stressed conditions, it is important to note that the equation is calibrated using the entire data set. Derived calibration coefficients are then applied uniformly across the entire data set, effectively estimating that these conditions do not vary by day, month or year, when the actual occurrence of water stressed conditions is highly variable at all of these time steps. This blanket application of correlation coefficients may account for a significant portion of the variability observed in the Penman-Monteith equation estimates of daily ET.

To further evaluate the effectiveness of the Penman and Penman-Monteith equations for prediction of ET, the regression equations presented in Table 4.1 were used to estimate daily ET for all days with negligible recorded rainfall. Monthly ET totals were then calculated by summing the values of daily ET for each predictive equation. Predicted values were compared to

the lysimeter measured total values of ET per month to evaluate the accuracy of each of the estimation methods. The Penman and Penman-Monteith monthly ET totals were also evaluated against the projected minimum and maximum values of lysimeter ET (a function of lysimeter measurement error described in Chapter 3 of this report). Results of this analysis are presented in Table 4.2.

Table 4.2. Comparison of monthly total ET measured to ET predicted by both the Penman and calibrated Penman-Monteith equations on days without rainfall

Month	Lysimeter* ET (cm)	Minimum* Lys. ET (cm)	Maximum* Lys. ET (cm)	Penman* ET (cm)	P-M* ET (cm)	Percent Difference (PENMAN) (%)	Percent Difference (P-M) (%)
April	8.87	6.79	10.95	8.93	8.23	0.68%	-7.24%
May	7.86	5.78	9.94	9.08	8.47	15.51%	7.82%
June	7.65	5.57	9.73	8.31	7.92	8.58%	3.46%
July	10.02	7.73	12.30	10.72	10.44	7.06%	4.23%
August	8.93	6.64	11.22	9.18	9.19	2.85%	2.88%
September	6.49	4.41	8.57	6.14	6.13	-5.44%	-5.51%
October	5.12	3.04	7.20	4.42	4.39	-13.75%	-14.42%
November	3.59	1.61	5.57	3.20	3.18	-10.97%	-11.51%
TOTAL	58.54	41.58	75.49	59.98	57.94	2.47%	1.01%

**Each monthly ET "total" only includes days without rainfall*

While both the Penman and Penman-Monteith Equations tend to over predict ET from May through August (as observed in plots "A" through "D" and Tables 4.1 and 4.2), the predicted monthly values of ET are well within the potential measurement error, as evidenced by Table 4.2 and Figure 4.33.

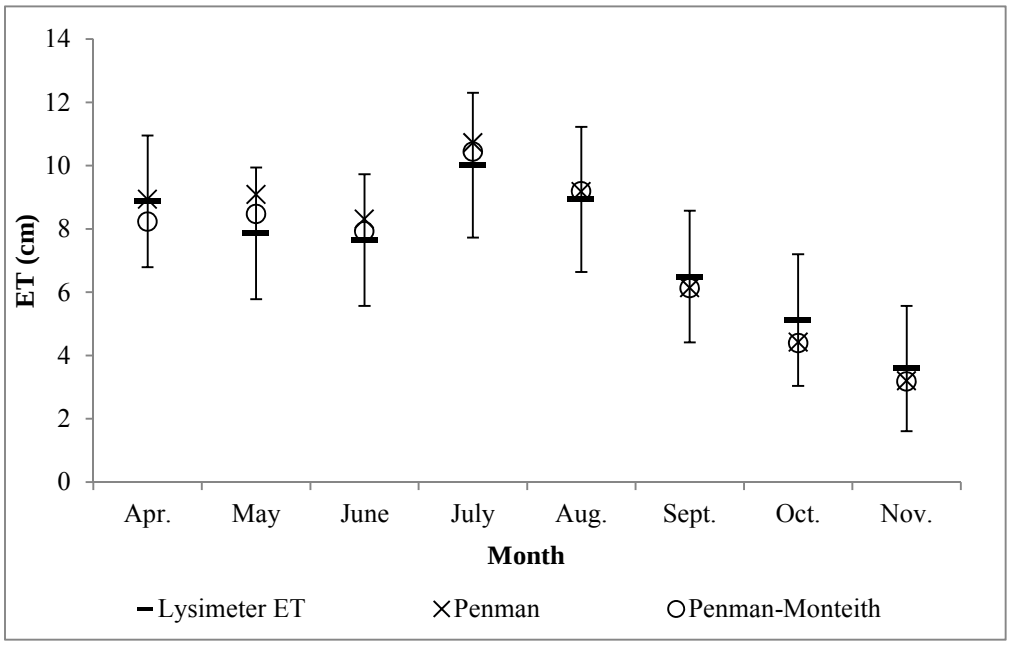

Figure 4.33. Monthly estimates of lysimeter, measured and Penman and Penman-Monteith, predicted values of ET for days without rainfall

On a monthly basis, slight over predictions in ET by the Penman and Penman-Monteith equations from May through August (although within the range of error of the lysimeter measured data) are likely a result of mild water-stressed conditions. This is particularly evident in the months of May and July where estimates from both predictive equations exceed the maximum lysimeter ET roughly 20% of the time. During both of these months, the lysimeter experiences prolonged periods with little or no rain followed by an observed over estimation of ET (see Figures 4.5 and 4.13 (Figure "A" for both May and July)). This is most likely due to the decrease in water availability in the soil and vegetation, restricting the export of water from the surface and preventing ET from meeting the atmospheric demand. This phenomenon is particularly evident in the first half of July (Figure 4.13) where the lysimeter is able to meet the Penman-predicted atmospheric demand for several days following a significant rain event, but was unable to maintain this level of ET for the duration of the eight-day dry period. However,

the 2009 calendar year, particularly the portion observed for this study, was unseasonably wet. As a result, it is difficult to establish a strong causal connection between extended dry periods and over prediction of ET. A complete breakdown of the percentage of days the maximum lysimeter ET is exceeded per month is provided in Table 4.3.

Table 4.3. Percentage of days the maximum lysimeter ET is exceeded per month

Month	(PENMAN) (%)	(P-M) (%)
April	10 %	5 %
May	25 %	20 %
June	5 %	0 %
July	23 %	18 %
August	5 %	5 %
September	5 %	0 %
October	0 %	0 %
November	0 %	0 %
TOTAL	9%	6%

4.3 **Applicability of Predictive Equations on Days with and without Rain**

While the green roof lysimeter data provides a method to measure ET, it only measures days without rain, thus neglecting ET that occurs on days with rainfall. This value may be negligible on days when it rains for the majority of the day, however, this may not be the case when a rainfall event occurs in the morning followed by an afternoon of sun, if rainfall occurs late in the evening, preceded by sun throughout the earlier part of the day, etc. To circumvent this problem, the Penman or calibrated Penman-Monteith equations have been applied using the respective models and calibrated to the entire dataset. For the purposes of this discussion, the calibrated Penman-Monteith equation is the preferred method for representation of average and total ET values. The Penman-Monteith equation was chosen over the Penman because, once calibrated, it yielded more accurate estimates of daily ET (Table 4.2).

4.3.1 *Monthly Averages and Totals*

To better understand the performance of the lysimeter, daily average ET, and total ET values for each month were calculated. From the calibrated Penman-Monteith equation, the daily average ET (April-November) was approximately 3.06 mm, with the month of July having the highest daily average (4.42 mm) and the month of November having the lowest (1.46 mm). Table 4.4 provides a daily average ET for each month based on lysimeter values as well as the Penman and calibrated Penman-Monteith Equations. The lysimeter ET data provided was calculated from dry days without rain only while the Penman and Penman-Monteith data includes all days (wet and dry). Since days with rain typically yielded lower values of ET, the averages displayed here are, and should be, lower than the lysimeter ET averages. Figure 4.34 is a comparison between the Penman and calibrated Penman-Monteith daily ET averages for each month (the lysimeter ET was eliminated from this plot since it does not account for days when it rains, resulting in a slight overestimation of the daily average per month).

Table 4.4. Daily average Lysimeter, Penman, and Penman-Monteith ET for per month.

Month	Lysimeter ET* (mm)	Penman ET (mm)	P-M ET (mm)
April	4.44	3.72	3.38
May	3.93	3.75	3.44
June	3.83	3.64	3.43
July	4.55	4.57	4.42
August	4.06	3.71	3.69
September	3.25	2.78	2.72
October	2.56	1.99	1.90
November	1.89	1.53	1.46
AVERAGE	3.59	3.22	3.06

**Lysimeter ET data is from days without rain.*

The calibrated Penman-Monteith equation was used again to represent total ET for the data set, thus 74.64 cm were estimated to have left the green roof from April to November 2009. The rainfall total for this same period was 112.88 cm, resulting in a capture percentage of 66.1%. Table 4.5 presents ET totals and capture percentages on a monthly basis for both the Penman and Penman-Monteith Equations.

Capture percentage on a monthly basis is subject to a degree of error. Rainfall that occurs in one month but does not evaporate until the next month results in an artificially low capture percentage in the first month, and an artificially high capture percentage in the second.

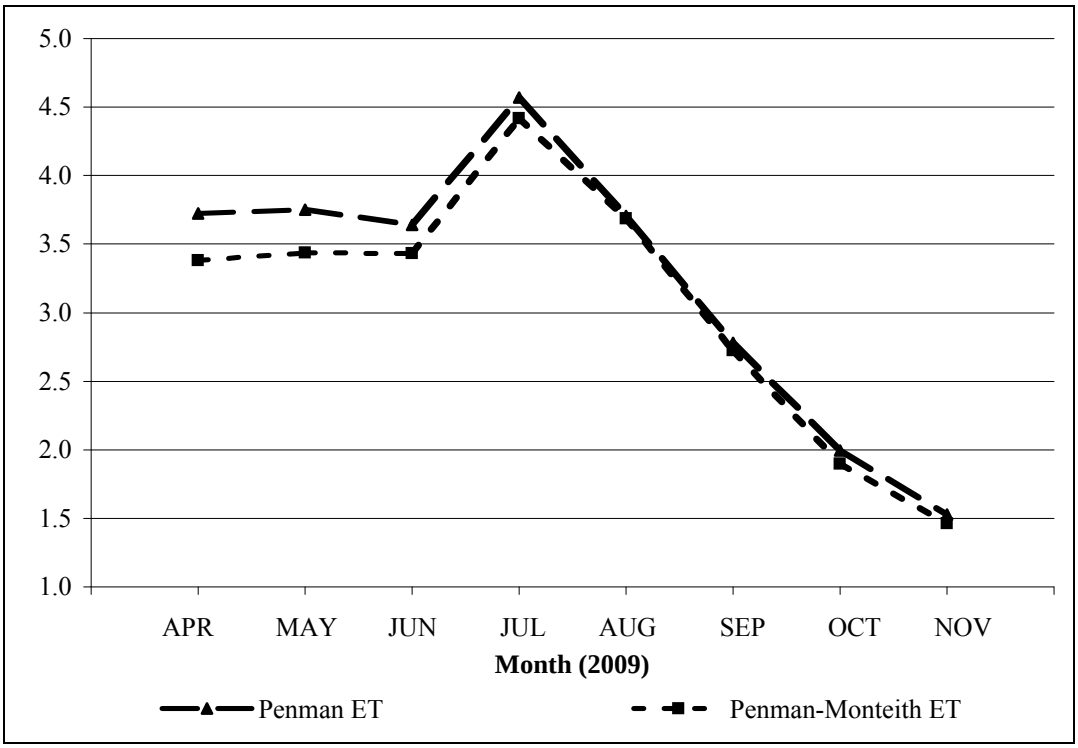

Figure 4.34. Comparison of Penman and calibrated Penman-Monteith daily ET averages per month

Table 4.5. Penman and Penman-Monteith Total ET and percent capture per month.

Month	Rainfall (cm)	Penman ET (cm)	P-M ET (cm)	Rainfall Excess (cm)	Capture Percent (PENMAN) (%)	Capture Percent (P-M) (%)
April	11.89	11.17	10.14	0.72	93.9%	85.3%
May	14.35	11.63	10.65	2.72	81.0%	74.2%
June	11.76	10.92	10.29	0.84	92.8%	87.5%
July	13.11	14.17	13.69	-1.07	108.1%	104.5%
August	26.80	11.49	11.43	15.31	42.9%	42.6%
September	12.95	8.34	8.17	4.62	64.3%	63.1%
October	16.64	6.17	5.88	10.46	37.1%	35.3%
November	5.38	4.58	4.38	0.81	85.0%	81.4%
TOTAL	112.88	78.46	74.64	34.42	69.5%	66.1%

5 CONCLUSIONS

As the science of stormwater management evolves to include green alternatives for mitigation and continuous flow modeling becomes the standard for SCM sizing and performance evaluation, the role of evapotranspiration becomes apparent, requiring accurate representation of the ET component in hydrologic models. One of the major challenges in evapotranspiration quantification is that the complexity of the process makes direct measurement extremely costly in terms of equipment and labor required. Because of this, the use of empirical or theoretical equations is critical to the advancement of this research.

5.1 Effectiveness of Predictive Equations in Estimating ET

Based on the findings presented in Chapter 4 of this document, both the Penman and Penman-Monteith equations provided reasonable estimations of measured lysimeter evapotranspiration. The Penman-Monteith equation yields slightly better results than its foundational counterpart (the Penman equation). This is expected since the Penman-Monteith equation is a product of a calibration routine that adjusts surface and aerodynamic parameters based on measured lysimeter ET. This calibration accounts for resistances (aerodynamic or vegetative) unique to the Villanova green roof. It does not, however, explicitly account for seasonal variability or water stressed conditions on a daily, or even monthly, basis. Rather it reflects resistances that are unique to the vegetation on the green roof and provides a modest correction for water-stressed

conditions[4]. The Penman equation, in comparison, accounts for aerodynamic resistances based on vegetation height (similar to the Penman-Monteith equation) but neglects any vegetative surface resistance that may occur.

For the duration of the study, the Penman equation over-predicted ET by a total of 1.44cm: a 2.47% difference from lysimeter-measured ET, while the Penman-Monteith under-predicted ET by a total of 0.6cm: a 1.01% difference from lysimeter measured ET. Both equations predicted total ET for the 8-month study will within the range of error of the measured weighing lysimeter. On a monthly basis, the maximum error in estimation from the Penman equation was an overestimate of ET by 1.22cm (15.51%) for the month of May while the maximum error in estimation from the Penman-Monteith equation was an underestimate of ET by 0.73cm (14.42%) for the month of October.

Although the Penman-Monteith Equation provides slightly better results, the significance of the Penman equation should not be neglected due to its ability to provide reasonable results without calibration. The Penman equation could prove particularly useful when a lysimeter in not economically, physically, or otherwise, a feasible solution, making calibration of the Penman-Monteith equation difficult. As more research is conducted on this green roof and others across the country and around the world, we will have a better idea of the broader applicability of both

[4] The correction for water-stressed conditions is a single value, established based on the entire dataset and applied uniformly to each daily estimate of ET. As a result, this method may produce over estimates of ET on water-stressed days and underestimates on non-water-stressed days.

of these equations and a more complete understanding of the calibration needs of the Penman-Monteith equation both seasonally and geographically.

5.2 **Role of ET in the Water Budget of a Green Roof**

This study also illustrates the significance of evapotranspiration as a component in the water budget of the Villanova green roof. Based on the observed lysimeter results in combination with several predictive equations (either the Penman or Penman-Monteith equation) the green roof lysimeter was able to capture over 65% of the rainfall for the duration of the study (April to November 2009). This estimate is likely slightly higher than what is actually occurring on the Villanova green roof on an annual basis since the lysimeter does not have an underdrain. In the absence of an underdrain, the lysimeter can store and release some additional water back into the atmosphere that would otherwise leave the roof in the form of discharge to the storm sewer. While overflow from the green roof was not monitored during this study, previous single storm event data, collected from the Villanova Green Roof in October 2007, supports the capture percentage observed during the ET study for the month of October (37.1% capture in October 2007 versus 37.1% and 35.3% for the Penman and Penman-Monteith estimates, respectively in October 2009).

Since January 2011, the Villanova Urban Stormwater Partnership has installed a low-flow monitor to measure discharge from the roof (primarily the water that leaves the roof via the underdrain (underflow)). This data should prove particularly useful in gauging the performance of the roof. In addition, a better understanding of the function of the Villanova green roof

relative to the function of the green roof lysimeter may also dictate future design of these facilities by quantifying the water quality and quantity effects of an underdrain. One observed benefit of a system without an underdrain is reduction in maintenance costs due to watering needs of the roof during extended dry periods. In the summer of 2010, the site experienced extended periods of time with little or no rain. As a result, many of the plants on the green roof were noticeably water-stressed and required periodic watering throughout this time. In comparison, the lysimeter (an underdrainless system) was able to survive and thrive on the additional water stored in the soil medium and synthetic storage layers without supplemental watering (Schneider 2010). While abandoning the underdrain all together may have other design implications (maintaining plant health or accommodating additional design loads), modifications to the traditional green roof design may be able to incorporate all of these design concerns while providing additional stormwater benefit.

5.3 **Research Limitations and Future Work**

While the preliminary results of this research are promising, there are several limitations pertaining to both the measured ET and predictive equations that should be noted. hese limitations should also be seen as opportunities for future research. Opportunities include the examination of an entire year of data plus subsequent years to observe seasonal and annual trends in evapotranspiration and determine if seasonal coefficients are required for Penman-Monteith correction. Additional data would likely allow for some observation and analysis of water-stressed conditions on the roof providing a basis for estimating these conditions (e.g. water budget approach to roughly estimate volume of water in the soil). This is particularly significant

because the current predictive equations do not account for water stressed conditions. Additionally, since the Penman-Monteith equation is a product of a calibration routine, there is a potential for additional error from water-stressed conditions that skew the calibration. This error is less significant in a system without an underdrain since water-stressed conditions occur less frequently.

The predictive equations used in this study (the Penman and Penman-Monteith equations) rely on measured weather parameters to estimate ET from the green roof. The site layout (walls on two of the four sides of the roof) leads to uneven heating and cooling of the site as well as variable wind dynamics across the roof. The sensitivity of these weather inputs should be evaluated to determine if the observed errors in ET can be explained through correction or targeted calibration of one or more specific input parameters rather than the blanket calibration approach proposed in this research. Additionally, the sensitivity of current predictive equations to alternate sources of weather data (such as an offsite station) should be evaluated to determine the necessary resolution of weather data inputs to maintain the integrity of ET estimates.

Lastly, a comparison of the water quantity and quality performance of the lysimeter and the green roof would provide insight into the function and drawbacks to green roof systems with and without an underdrain. This may provide insight into the optimization of these systems for stormwater performance. A system without an underdrain (or a valve controlled underdrain) would likely provide some additional water quantity benefit (through the retention and evapotranspiration of more water) and may also increase water quality performance (by reducing pollutant export from these facilities).

REFERENCES

Allen, R.G., M.E. Jensen, J.L.Wright, R.L. Burman. (1989). "Operational Estimates of Reference Evapotranspiration." Journal of Agronomy **81**: 650-662.

Allen, R.G., L.S. Pereira, D. Raes, M. Smith. (1998). Crop Evapotranspiration - Guideline for Computing Crop Water Requirements - FAO Irrigation and Drainage Paper 56. Rome, Italy, FAO Food and Agriculture Organization of the United Nations.

Allen, R.G., W.O. Pruitt, et al. (1996). Chapter 4: "Evaporation and Transpiration". ASCE Handbook of Hydrology. New York, American Society of Civil Engineers**:** pp. 125-252.

Anderson, M. G. (2008). Part 4. Hydrometeorology. Encyclopedia of Hydrological Sciences. J. J. McDonnell, John Wiley & Sons, Inc. **1:** 3456.

ASTM Standard E2398 (2011a). "Standard Test Method for Water Capture and Media Retention of Geocomposite Drain Layers for Vegetative (Green) Roof Systems". ASTM International, West Conshohocken, PA. 2011. DOI: 10.1520/E2398-11. www.astm.org.

ASTM Standard E2399 (2011b). "Standard Test Method for Maximum Media Density for Dead Load Analysis of Vegetative (Green) Roof Systems". ASTM International, West Conshohocken, PA. 2011. DOI: 10.1520/E2399-11. www.astm.org

Ball, J. (2001). "Soil Water Relationships." Retrieved 24 March, 2009, from http://www.noble.org/AG/Soils/SoilWaterRelationships/Index.htm.

Berghage, R., A. Jarrett, et al. (2007). Quantifying Evapotranspiration and Transpirational Water Losses from Green Roofs and Green Roof Media Capacity for Neutralizing Acid Rain. National Decentralized Water Resources Capacity Development Project (NDWRCP).

Brunt, D. (1952). Physical and Dynamical Meteorology. Cambridge, University Press.

Brutsaert, W. (1982). Evaporation into the Atmosphere: Theory, History, and Applications. New York, Springer.

Brutsaert, W. (2005). Hydrology: an introduction. New York, Cambridge University Press.

Budikova, D., M. Hall-Beyer, et al. (2008). "Albedo." In: Encyclopedia of Earth. Eds. Cutler J. Cleveland (Washington, D.C.: Environmental Information Coalition, National Council for Science and the Environment). [First published in the Encyclopedia of Earth November 21, 2006; Last revised March 19, 2008; Retrieved March 24, 2009]. http://www.eoearth.org/article/Albedo.

Clawson, E. L. and S. Hribal (2009). Weighing Lysimeters Measure Crop Water Use. Louisiana Agriculture Magazine.

Crago, R. and R. Crowley (2005). "Complementary Relationships for Near-Instantaneous Evaporation." Journal of Hydrology **300**(1-4): 13.

Davie, T. (2002). Fundamentals of Hydrology (Fundamentals of Physical Geography), Routledge.

FFL (2002). Guideline for the Planning, Execution and Upkeep of Green-Roof Sites. Bonn, Forschungsgesellschaft Landschaftsentwicklung Landschaftsbau e. V. (FFL).

Gardner, W. R. (1960). "Dynamic Aspects of Water Availability to Plants." Soil Science **89**(2): 11.

Harrison, L. P. (1963). Fundamental Concepts and Definitions Relating to Humidity. Humidity and Moisture. Wexler. N.Y., Reinhold Publishing Co. **3**.

Kramer, P. J. and J. S. Boyer (1995). Water Relations of Plants and Soils, Academic Press, Inc.

Maidment, D. R. (1993). Handbook of Hydrology. New York, McGraw-Hill, Inc.

McCuen, R. H. (1979). "Downstream Effects of Stormwater Management Basins " Journal of the Hydraulics Division **105**(11): 14.

Nyvall, J. (2002). Soil Water Storage Capacity and Available Soil Moisture. F. a. F. Ministry of Agriculture. Abbotsford, BC.

Osmundson, T. (1999). Roof Gardens: History, Design, and Construction. New York, W.W. Norton & Company.

Parlange, M. B. and G. G. Katul (1992). "An Advection-Aridity Evaporation Model." Water Resources Research **28**(1): 6.

Penman, H. L. (1948). "Natural Evaporation from Open Water, Bare Soil and Grass." Proceedings of the Royal Society of London, Series A **193**(1032): 26.

Perlman, H. (2008). "The Water Cycle: Evaporation." Retrieved 4 March 2009, 2009, from http://ga.water.usgs.gov/edu/watercycleevaporation.html.

Perlman, H. (2008). "The Water Cycle: Transpiration." Retrieved 4 March 2009, 2009, from http://ga.water.usgs.gov/edu/watercycletranspiration.html.

Pidwirny, M. (2006). "Infiltration and Soil Water Storage." Fundementals of Physical Geography 2nd Edition. Retrieved 24 March, 2009, from http://www.physicalgeography.net/fundamentals/8l.html.

Priestley, C. H. B. and R. J. Taylor (1972). "On the Assessment of Surface Heat Flux and Evaporation Using Large-Scale Parameters." Monthly Weather Review **100**(2).

Qualls, R. J. and H. Gultekin (1997). "Influence of Components of the Advection-Aridity Approach on Evapotranspiration Estimation." Journal of Hydrology **199**(1-2): 10.

Rudwick, P. (2008). CEER Green Roof Project (follow-up), Villanova University Civil and Environmental Engineering Department.

Sauer, T. J. and R. Horton (2005). Chapter 7: Soil Heat Flux. Micrometeorology in Agricultural Systems. J. L. Hatfield. Madison, WI, American Society of Agronomy, Crop Science Society of America, Soil Science Society of America.

Schneider, D. (2010). Personal Communication.

Slatyer, R. O. and I. C. McIlroy (1961). Practical Microclimatology: with Special Reference to the Water Factor in the Soil-Plant-Atmosphere Relationships, UNESCO.

Smith, M., R. G. Allen, et al. (1991). Report of the Expert Consultation on Procedures for Revision of FAO Guidelines for Prediction of Crop Water Requirements. Rome, Italy, United Nations-Federal Agriculture Organization**:** 54.

Snodgrass, E. C. (2010). "Green Roofs: New Homes for Sedums and Other Hardy Succulents." Retrieved March 28, 2010, 2010, from http://www.bbg.org/gar2/topics/plants/handbooks/cacti/greenroof.html.

Stewart, B. A. and T. A. Howell (2003). Encyclopedia of Water Science, Marcel Dekker Inc.

Tetens, V. O. (1930). "Uber Einige Meteorologische." Begriffe Zeitschrift fur Geophysik: 12.

Tokarz, E. (2006). CEER Green Roof Project, Villanova University Department of Civil and Environmental Engineering.

Viessman, W., Jr. and G. L. Lewis (2003). Introduction to Hydrology. Upper Saddle River, NJ, Pearson Education, Inc.

Villarreal, E. L. and L. Bengtsson (2005). "Response of a Sedum Green-Roof to Individual Rain Events." Ecological Engineering **25**: 1-7.

Ward, A. W. and S. W. Trimble (2004). Environmental Hydrology, CRC Press.

APPENDIX A

Rooflite Roof Media Specifications and Analysis of Performance

rooflite® extensive mc Specifications

rooflite® extensive mc is a growing medium for extensive green roofs in multi-course construction. The material is a mixture of mineral light weight aggregates like HydRocks® and premium organic components complying with the following requirements:

Particle Size Distribution		
Proportion of silting components (d < 0.063 mm)	Mass %	≤ 15
Density Measurements		
Bulk Density (dry weight basis)	g/cm^3	0.70 - 0.85
Bulk Density (dry weight basis)	lb/ft^3	44 - 53
Bulk Density (at max. water-holding capacity)	g/cm^3	1.15 - 1.35
Bulk Density (at max. water-holding capacity)	lb/ft^3	72 - 85
Water/Air Measurements		
Total Pore Volume	Vol. %	≥ 65
Maximum water-holding capacity	Vol. %	35 - 65
Air-filled porosity at max water-holding capacity	Vol. %	≥ 10
Water permeability (saturated hydraulic conductivity)	cm/sec	0.001 – 0.12
Water permeability (saturated hydraulic conductivity)	in/min	0.024 – 2.83
pH and Salt Content		
pH (in $CaCl_2$)		6.0 - 8.5
Soluble salts (water extract)	g/L	< 3.5
Soluble salts (gypsum extract)	g/L	< 2.5
Organic Measurements		
Organic matter content	g/L	< 65
Nutrients		
Phosphorus, P_2O_5 (CAL)	mg/L	≤ 200
Potassium, K_2O (CAL)	mg/L	≤ 700
Magnesium, Mg (CaCl2)	mg/L	≤ 200
Nitrate + Ammonium (CaCl2)	mg/L	≤ 80

Supplier: Skyland USA LLC, phone: 1.877.268.0017, www.skylandusa.us

All values are based on compacted materials according to laboratory standards and testing methods defined by the Forschungsgesellschaft Landschaftsentwicklung Landschaftsbau e.V. (FLL) Landscape Development and Landscaping Research Society, Guidelines for the Planning Construction and Maintenance of Green-Roofing, Green Roofing Guideline, 2008

rooflite®
Certified Green Roof Media

Typical Green Roof Media Analysis for rooflite® extensive mc

Results on dry weight basis unless specified otherwise

Analysis	Units	Results*	FLL** Requirements
Particle Size Distribution (See accompanying graph)			
Proportion of silting components (d < 0.063 mm)	mass %	5 - 10	< 15
Density Measurements*			
Bulk Density (dry weight basis)	g/cm^3	0.70 – 0.85	
Bulk Density (dry weight basis)	lb/ft^3	44 - 53	
Bulk Density (at max. water-holding capacity)	g/cm^3	1.15 – 1.35	
Bulk Density (at max. water-holding capacity)	lb/ft^3	72 - 85	
Water/Air Measurements			
Total Pore Volume	Vol. %	65 - 75	
Maximum water-holding Capacity	Vol. %	40 - 55	$\geq$ 35 $\leq$ 65
Air-Filled Porosity (at max water-holding capacity)	Vol. %	15 - 25	$\geq$ 10
Water permeability (saturated hydraulic conductivity)	cm/sec	0.02 – 0.08	0.001 – 0.12
Water permeability (saturated hydraulic conductivity)	in/min	0.47 – 1.89	0.024 – 2.83
pH and Salt Content			
pH ($CaCl_2$)		7.5 – 8.5	6.0 - 8.5
Soluble salts (water extract)	g /L	1.5 – 3.0	< 3.5
Organic Measurements			
Organic matter content	g/L	30 - 45	< 65
Nutrients			
Phosphorus, P_2O_5 (CAL)	mg/L	150 - 200	$\leq$ 200
Potassium, K_2O (CAL)	mg/L	400 - 700	$\leq$ 700
Magnesium, Mg (CaCl2)	mg/L	150 - 200	$\leq$ 200
Nitrate + Ammonium (CaCl2)	mg/L	10 - 40	$\leq$ 80

* *Listed range of values is typical for the Mid Atlantic region*

** *All values are based on compacted materials according to laboratory standards and testing methods defined by the Forschungsgesellschaft Landschaftsentwicklung Landschaftsbau e.V.(FLL) Landscape Development and Landscaping Research Society e.V. Guidelines for the Planning Construction and Maintenance of Green Roofing, Green Roofing Guideline, 2008*

rooflite®
Certified Green Roof Media

Typical Particle Size Distribution for rooflite® extensive mc

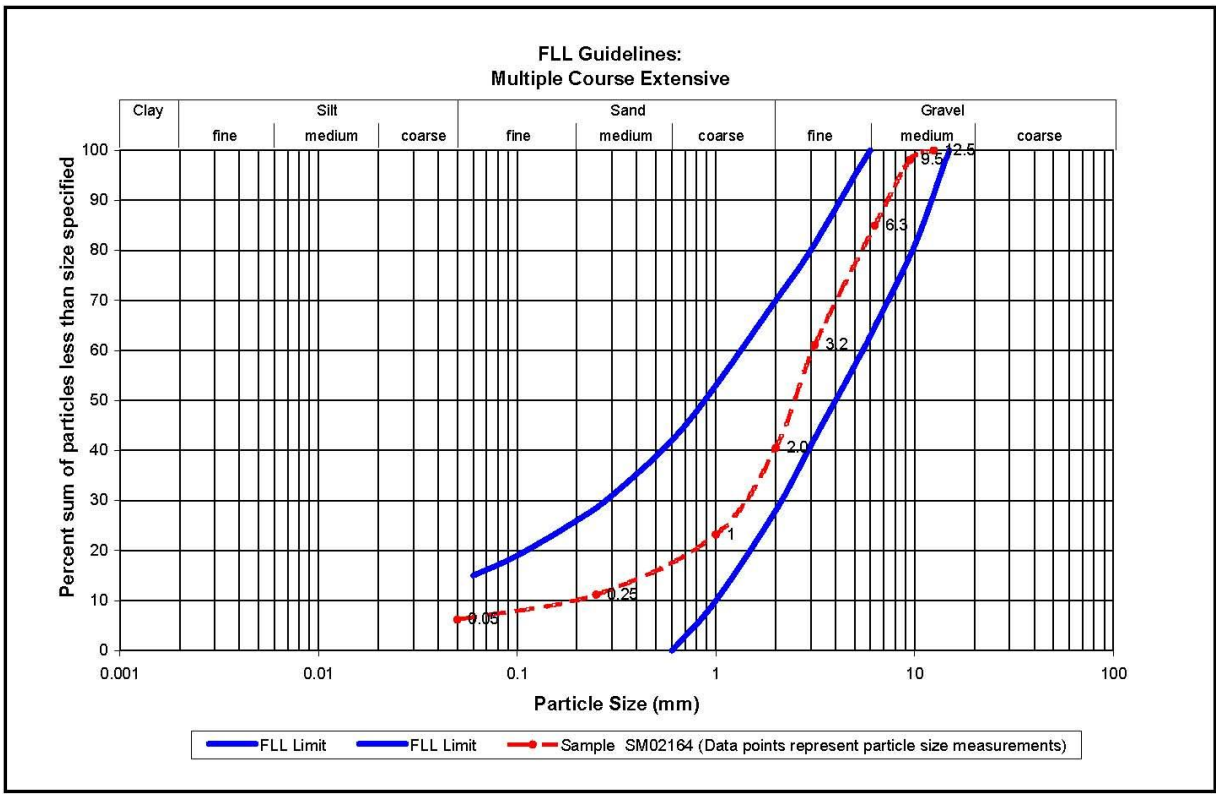

APPENDIX B

Sentran, LLC Load Cell Information

SENTRAN

PF

PRECISION LOW PROFILE LOAD CELL

applications

- Laboratory Measurements
- Materials Testing
- Dynamic Measurements
- Process Control
- Weighing

features

- 100 to 5000 lbs. Capacities
- Compact Low Profile Design
- 500% Overload Capability
- Stainless Steel Construction
- 0.1% Accuracy Class
- High Frequency Response
- IP66/IP67 Environmental Sealing
- Low Sensitivity to Side Load and Off-Center Loading
- Two Year Warranty

Application Tip: *The PF Series is designed for applications requiring excellent performance in an compact, rugged low profile load cell.*

The PF Series is a high performance, low profile, bonded foil strain gage load cell constructed of electro-polished stainless steel (PF3). To achieve sealing ratings of IP66 and IP67 (thoroughly sealed against airborne particles, strong jets of water and the effects of immersion up to 1 meter.) proprietary, multi-redundant environmental barriers are incorporated, including VITON® Fluorelastomer O-ring seals to protect sensitive areas. The PF Series is designed to accurately measure compression forces in capacities ranging from 100 lbs. to 5,000 lbs. The integrated sensing diaphragm and precision ground base combine to produce excellent performance, superior environmental integrity and reduced sensitivity to off-center and side loading effects. Integral overload protection permits compression loads of 500% of rated capacity to be applied without adverse effects. Side loads of 50% of rated capacity can be tolerated, simultaneously. The low deflection of the PF Series yields a high dynamic response for applications in structural analysis and materials testing. The durable polyurethane jacketed cable, features a braided, tinned-copper shield for mechanical protection and to minimize the effects of common industrial electrical noise, e.g. RFI and EMI. The attributes of the PF Series make it an ideal choice for measurements in the laboratory, manufacturing and process applications, and for general force measurements and weighing situations where an extraordinarily rugged, low profile precision load cell solution is needed.

SENTRAN, LLC
California Commerce Center
4355 Lowell Street
Ontario, CA 91761-2225

Toll Free: 1(888) 545-8988
Phone: 1(909) 605-1544
Fax: 1(909) 605-6305
Email: mail@sentranllc.com
URL: www.sentranllc.com

Innovative Measurement Solutions

specifications

PF

performance

Rated capacities [1] (lbs.)	100, 250, 500, 1K, 2K, 3K, 4K, & 5K
Rated output (FSO)	2 mV/V ± 0.25%
Combined error	= 0.25 % FSO
Non-linearity	= 0.10 % FSO
Hysteresis	= 0.10 % FSO
Non-repeatability	= 0.05 % FSO
Creep (30 minutes)	= 0.03 % of load
Zero balance	= 10 % FSO
Zero Return (30 minutes)	Better than 0.03 % FSO

[1] ("K" = thousand)

mechanical

Material:	17-4PH Stainless steel
Finish:	Electro-polished
Safe overload	Compression: 500% FSO
	Tension: N/A
	Side load: 50% FSO
Ultimate overload	Compression: 1000% FSO
	Tension: N/A
	Side load: 100% FSO
Deflection	0.005" (.13mm) nominal
Weight	1 lbs.

electrical

Input impedance	400 ohms (nominal)
Output impedance	350 ohms (nominal)
Insulation resistance	>5000 Megohms @ 50VDC
Excitation Voltage	10 V AC/DC (15 V maximum)
Cable Color code:	+ Excitation (red)
	- Excitation (black)
	+ Output (green)
	- Output (white)
	Shield (bare)
Cable type	4-conductor, 22 AWG, tin-copper braided shield, polyurethane jacket
Cable termination	Finished conductors

environmental

Temperature, operating	-20 to +180 °F (-29 to +82°)
Temperature, compensated	+40 to +140 °F (-10 to +60°C)
Temperature effects:	Zero < 0.002% FSO/°F
	< 0.0036% FSO/°C
	Output < 0.002% of Rdg./°F
	< 0.0036% Rdg./°C
Sealing	IP66/IP67; redundant

options

Shunt calibration, Special cable lengths, High Temperature operation, MS connectors and Control Instrumentation.

dimensions

Bottom View Showing Mounting Stud

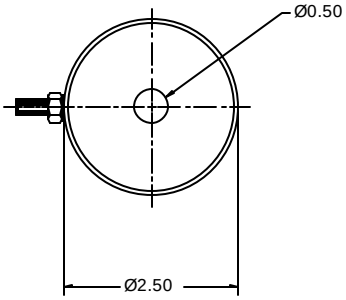

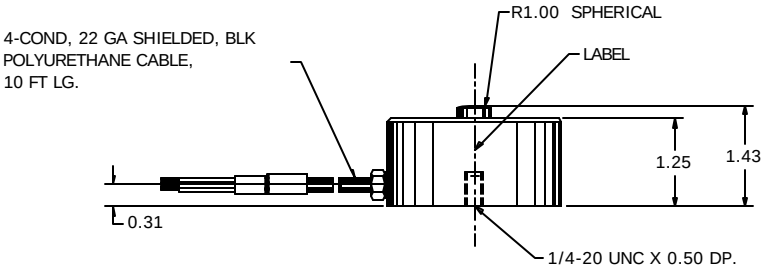

SENTRAN periodically introduces product enhancements. Specifications are subject to change without notice. Certified drawings are available upon request.

PF B&W.02-0505

APPENDIX C

Daily Weather Data (April through November 2009)

APPENDIX C

Daily Weather Data (April 2009 through November 2009)

Date	T_{min}	T_{avg}	T_{max}	RH_{min}	RH	RH_{max}	$u_{z\ avg}$	R_n	Rainfall
	(C)	(C)	(C)	(C)	(C)	(C)	(m/s)	MJ/m2/day	(in)
4/1/2009	4.410	8.089	10.95	73.84	89.75	96.10	2.120	3.097	0.18
4/2/2009	8.300	13.227	19.43	60.29	83.91	97.20	1.535	6.508	0.01
4/3/2009	11.330	14.382	19.99	54.39	81.30	97.10	2.551	3.624	1.49
4/4/2009	10.600	14.544	17.88	30.50	37.88	62.00	2.330	6.257	0
4/5/2009	8.750	14.082	19.43	23.49	34.95	46.16	1.593	1.535	0
4/6/2009	7.342	11.102	14.40	43.93	74.70	95.10	1.606	2.551	0.22
4/7/2009	1.800	5.042	9.49	35.65	52.32	69.96	1.690	2.330	0
4/8/2009	0.884	6.383	10.64	29.37	47.92	69.35	1.883	6.300	0
4/9/2009	3.397	11.331	18.15	21.10	36.17	58.20	1.334	8.673	0
4/10/2009	7.335	12.568	18.94	32.86	59.13	79.16	1.512	5.603	0
4/11/2009	3.847	8.228	10.60	42.28	77.04	95.60	1.721	3.304	0.68
4/12/2009	1.444	6.046	11.12	22.02	35.11	51.28	1.834	8.974	0
4/13/2009	0.787	8.025	13.71	22.37	37.80	92.30	1.339	8.659	0.13
4/14/2009	5.364	7.945	11.50	77.11	90.86	97.80	1.765	2.843	0.65
4/15/2009	4.345	7.245	10.91	66.64	83.41	92.00	1.672	3.286	0.49
4/16/2009	3.577	10.898	19.11	25.50	52.59	93.90	1.611	9.589	0
4/17/2009	3.531	13.573	21.67	19.65	39.60	77.41	1.258	9.563	0
4/18/2009	10.240	18.809	26.06	19.92	27.55	39.51	1.419	9.227	0
4/19/2009	8.680	14.780	21.21	30.55	41.91	50.19	1.840	7.660	0
4/20/2009	7.447	8.101	9.50	45.91	86.91	96.80	2.222	3.004	0.61
4/21/2009	8.840	13.104	19.08	45.80	79.55	96.60	1.428	5.750	0.11
4/22/2009	6.662	10.015	15.27	47.63	71.27	90.90	1.507	4.764	0.01
4/23/2009	5.594	10.226	15.10	35.33	52.48	85.80	1.384	7.909	0.02
4/24/2009	5.847	15.298	23.96	24.93	44.88	71.72	2.000	9.816	0
4/25/2009	11.370	22.587	32.16	25.04	52.68	89.70	1.626	8.997	0
4/26/2009	20.100	26.912	34.35	20.31	38.20	60.68	1.368	10.027	0
4/27/2009	20.030	26.744	33.78	24.92	39.38	57.21	2.317	10.124	0
4/28/2009	18.740	25.036	32.27	26.97	42.02	61.94	2.321	10.115	0
4/29/2009	8.930	14.068	19.96	30.82	61.31	90.40	1.736	6.595	0.08
4/30/2009	9.410	13.764	18.54	35.35	59.24	91.60	2.034	7.247	0
5/1/2009	13.550	17.383	21.73	75.22	90.04	93.90	2.665	4.623	0.14
5/2/2009	13.670	16.158	18.80	61.57	80.55	94.20	1.401	5.437	0.11
5/3/2009	11.750	13.428	15.06	89.40	92.97	94.80	0.988	3.021	0.8
5/4/2009	9.720	11.362	12.35	91.80	94.53	95.80	1.368	2.825	0.93
5/5/2009	10.000	11.725	14.02	84.40	93.19	96.00	1.151	3.631	0.75
5/6/2009	10.600	13.814	19.08	68.37	87.18	97.20	1.609	5.607	0.69
5/7/2009	11.940	18.023	23.58	66.07	85.63	97.40	1.487	5.942	0.5
5/8/2009	13.260	20.204	27.26	43.02	64.75	84.60	1.327	8.778	0.01
5/9/2009	17.200	22.812	27.79	37.06	65.68	94.30	1.802	8.787	0

Date	T_{min}	T_{avg}	T_{max}	RH_{min}	RH	RH_{max}	$u_{z\ avg}$	R_n	Rainfall
	(C)	(C)	(C)	(C)	(C)	(C)	(m/s)	MJ/m2/day	(in)
5/10/2009	12.040	17.131	22.44	32.77	43.69	60.70	1.789	11.305	0
5/11/2009	10.860	14.174	21.35	38.79	55.39	80.20	1.098	7.766	0
5/12/2009	9.540	14.449	21.68	28.39	50.81	87.80	0.899	8.564	0
5/13/2009	7.868	15.654	22.28	24.54	49.21	78.02	1.985	9.507	0
5/14/2009	12.820	16.919	22.14	53.42	76.06	96.00	3.194	5.079	0.8
5/15/2009	16.380	20.848	27.21	53.76	80.08	96.40	1.197	7.631	0.01
5/16/2009	17.140	20.622	25.55	66.63	85.86	96.70	2.297	5.690	0.02
5/17/2009	10.960	14.806	19.63	37.98	62.90	93.60	1.510	6.490	0.04
5/18/2009	6.598	11.300	17.38	33.09	47.12	74.51	1.203	8.697	0
5/19/2009	4.512	14.162	22.92	22.84	49.41	82.90	1.051	12.138	0
5/20/2009	8.770	19.290	30.12	21.13	48.64	86.30	1.541	11.925	0
5/21/2009	11.360	21.115	30.76	20.25	47.28	85.30	1.630	12.166	0
5/22/2009	13.880	21.759	29.21	37.95	63.46	95.70	1.687	9.727	0
5/23/2009	16.970	24.349	31.26	36.72	63.46	93.10	1.793	12.396	0
5/24/2009	18.310	23.797	29.84	52.29	72.83	93.40	1.807	9.282	0
5/25/2009	18.990	23.825	30.64	29.63	61.64	93.70	1.101	11.440	0
5/26/2009	10.050	13.229	19.85	41.83	69.35	92.60	2.133	4.731	0.06
5/27/2009	10.210	16.685	23.32	64.89	82.66	94.80	1.238	5.863	0
5/28/2009	13.670	18.962	24.08	69.42	85.39	95.80	1.650	6.311	0
5/29/2009	13.370	18.129	25.87	64.58	88.34	97.00	1.071	6.365	0.79
5/30/2009	13.870	20.203	27.81	35.57	58.77	91.70	0.875	10.925	0
5/31/2009	14.180	20.595	29.61	31.62	45.19	66.12	1.242	11.404	0
6/1/2009	9.460	17.335	25.34	27.29	49.14	84.00	1.736	12.784	0
6/2/2009	14.960	21.839	31.55	39.63	69.95	89.40	1.113	10.204153	0.03
6/3/2009	13.300	19.414	26.49	52.48	77.28	95.60	1.158	9.175081	0.78
6/4/2009	12.610	14.888	17.26	83.10	91.43	95.70	0.946	4.7437094	0.47
6/5/2009	13.110	14.246	15.48	92.80	94.21	95.40	1.341	3.3519915	0.85
6/6/2009	13.840	19.128	25.16	57.64	78.09	94.90	0.978	8.0423978	0
6/7/2009	16.060	22.823	31.08	35.90	66.70	92.20	1.628	13.013885	0
6/8/2009	18.000	23.097	30.58	54.64	75.86	92.20	1.445	9.5699779	0
6/9/2009	17.950	20.278	25.44	70.41	88.31	96.40	1.505	5.3566166	0.52
6/10/2009	16.730	21.310	26.17	61.86	79.71809	93	1.139	8.6882137	0
6/11/2009	17.350	18.252	19.25	90.1	94.27847	96.3	1.475	3.8951798	0.37
6/12/2009	19.020	24.328	31.15	48.65	74.225	96.4	1.058	9.7375897	0
6/13/2009	16.630	20.980	29.77	55.02	81.73573	95.2	1.282	7.2120278	0.3
6/14/2009	15.960	20.625	28.33	42.95	75.20736	94.8	1.146	9.8647506	0
6/15/2009	15.090	19.263	27.32	50.63	77.59965	94	1.555	9.902223	0.11
6/16/2009	14.100	16.904	19.84	66.79	79.69417	91.8	1.637	5.075172	0
6/17/2009	12.570	15.725	20.51	54.91	81.69382	95	1.873	7.4046355	0.14
6/18/2009	15.380	17.922	19.67	94.1	95.45694	96.3	2.387	2.966979	0.36
6/19/2009	17.180	20.800	25.75	54.06	78.04722	95.4	0.795	7.625579	0
6/20/2009	16.960	19.659	23.22	80.4	90.22014	95.8	1.321	3.5916004	0.45
6/21/2009	18.010	21.269	26.87	52.63	74.79319	92.4	1.423	6.2386993	0.02

Date	T_{min}	T_{avg}	T_{max}	RH_{min}	RH	RH_{max}	$u_{z\ avg}$	R_n	Rainfall
	(C)	(C)	(C)	(C)	(C)	(C)	(m/s)	MJ/m2/day	(in)
6/22/2009	17.880	22.866	28.53	50.39	70.66528	94.7	1.073	8.9470958	0.1
6/23/2009	17.600	23.116	29.38	49.38	66.53948	85.7	0.910	9.3233812	0
6/24/2009	19.010	23.600	29.24	49.75	70.23281	88.9	0.812	8.308311	0
6/25/2009	20.060	24.917	32.32	46.56	72.43792	91.7	1.155	9.6511327	0
6/26/2009	19.570	24.785	33.43	44.23	73.64913	93.6	1.144	7.762194	0
6/27/2009	17.860	23.305	29.51	40.48	65.67368	93.2	1.142	11.776412	0
6/28/2009	17.870	23.880	32.27	38.7	61.46802	86.5	1.069	13.264804	0
6/29/2009	17.550	24.078	31	33.56	58.13	89.5	1.183	11.843647	0
6/30/2009	18.330	23.028	31.97	34.74	70.44969	92.2	1.527	11.234886	0.13
7/1/2009	18.460	23.947	31.9	38.37	70.09858	94.7	1.076	10.54494	0.03
7/2/2009	18.550	22.623	29.57	50.46	76.36743	95.8	1.062	9.4504358	0.88
7/3/2009	17.310	22.318	28.64	46.8	66.79972	89.1	1.098	10.79491	0
7/4/2009	17.280	22.959	29.12	36.85	55.43889	79.99	1.167	12.54701	0
7/5/2009	15.360	21.662	28.12	36.32	57.16319	81.4	1.022	10.711983	0
7/6/2009	16.020	23.480	31.21	28.28	57.21608	88	0.868	12.805593	0
7/7/2009	17.090	24.118	32.52	33.55	55.85382	87.8	1.183	10.168563	0
7/8/2009	15.450	21.673	28.98	35.07	56.68708	82.8	0.957493	11.699437	0
7/9/2009	15.110	20.857	27.89	42.68	63.39208	80.2	1.469438	10.604819	0
7/10/2009	15.160	21.820	29.68	38.73	63.27333	88.1	1.319264	11.40268	0
7/11/2009	16.300	22.241	28.62	46.47	71.01003	95.1	2.547351	10.551278	1.62
7/12/2009	17.890	23.468	31.02	32.84	63.10177	95.7	1.007163	12.602288	0.1
7/13/2009	15.930	22.665	30.27	31.26	54.42361	74.46	0.720392	10.499186	0
7/14/2009	14.980	22.163	30.01	27.35	48.80903	73.76	0.890858	12.238722	0
7/15/2009	15.210	23.713	31.63	30.67	52.90573	78.87	1.401319	12.824684	0
7/16/2009	20.280	25.477	34.38	40.55	63.99354	84.2	1.734236	9.1849509	0
7/17/2009	19.720	24.788	34.01	35.61	72.4417	94.2	0.916979	8.136148	0.27
7/18/2009	18.410	22.872	29.97	37.43	65.49566	95	0.980833	12.275204	0
7/19/2009	15.080	22.899	31.16	31.09	55.81635	84.1	0.870604	12.202179	0
7/20/2009	17.480	23.910	30.68	35.38	56.97944	85.7	1.051403	9.7241008	0
7/21/2009	18.030	19.566	21.23	63.91	89.49611	95	0.879951	3.1435244	0.29
7/22/2009	18.220	23.123	31.43	51.31	79.58858	95.7	1.232139	7.184582	0
7/23/2009	18.300	21.250	24.62	81.1	89.96736	94.4	1.484868	4.3237241	0.26
7/24/2009	17.080	21.834	30.55	50.84	77.57007	93.4	0.871972	8.7528174	0.04
7/25/2009	16.570	24.356	31.02	47.25	69.02128	92	1.909604	11.609152	0.01
7/26/2009	20.510	24.695	31.8	48.32	75.25587	94.1	1.667931	8.7351007	0.35
7/27/2009	20.940	25.200	31.16	52.87	75.87667	95.1	1.627292	9.6547192	0.01
7/28/2009	19.920	25.668	32.8	52.89	74.65441	94.8	1.581031	8.8690112	0
7/29/2009	22.280	25.259	31.05	60.01	84.83257	95.6	2.376556	6.4815817	0.15
7/30/2009	21.680	26.286	33.03	44.76	70.22729	95.2	1.225677	11.085305	0
7/31/2009	19.970	24.141	31.72	59.05	83.93938	95.3	1.557688	6.8666519	1.15
8/1/2009	18.750	24.762	31.6	48.43	73.3366	94.9	1.461125	10.250481	0
8/2/2009	20.100	22.219	24.49	80.4	91.51563	95.9	1.382604	3.8451719	2.96
8/3/2009	19.750	24.637	31.78	37.86	68.86979	95.1	0.795698	11.036609	0

Date	T_{min}	T_{avg}	T_{max}	RH_{min}	RH	RH_{max}	$u_{z\ avg}$	R_n	Rainfall
	(C)	(C)	(C)	(C)	(C)	(C)	(m/s)	MJ/m2/day	(in)
8/4/2009	19.270	25.433	32.68	43.84	68.08396	93.3	1.582135	10.190508	0
8/5/2009	21.650	26.009	31.77	50.07	73.41396	94.6	0.916247	9.1771356	0
8/6/2009	17.930	21.287	25.54	48.97	68.52465	89.6	0.800799	5.5176847	0.03
8/7/2009	16.500	22.455	29.32	36.17	59.43205	79.98	0.890497	10.475481	0
8/8/2009	17.610	23.474	31.61	29.81	61.05354	91.4	1.078583	10.961938	0.02
8/9/2009	19.740	22.711	28.46	72.14	90.2283	96.6	1.013049	4.4448691	1.8
8/10/2009	20.590	28.096	36.11	49.21	69.61771	94.2	0.945101	10.615765	0
8/11/2009	23.110	27.270	33.28	48.36	66.45378	81.2	0.926132	10.214692	0
8/12/2009	21.620	24.486	31.41	56.8	78.36538	93.9	1.060969	6.135537	0.13
8/13/2009	19.360	21.830	24.91	79.75	90.36163	94.5	0.888156	4.4704504	0.73
8/14/2009	18.780	23.689	30.71	54.49	78.47594	95.7	0.610521	8.1695878	0
8/15/2009	19.620	26.195	34.79	38.97	70.43278	94.9	1.090569	11.039096	0
8/16/2009	20.560	27.081	35.34	37.6	67.27437	93.2	0.825354	10.833437	0
8/17/2009	20.460	27.311	36.78	34.74	63.26486	88.4	1.069118	10.083046	0
8/18/2009	21.460	26.781	34.66	47.69	71.16285	88.7	1.527014	10.464501	0.02
8/19/2009	21.630	27.336	35.14	43.83	72.15351	93.6	1.026632	9.5800069	0.01
8/20/2009	22.840	26.944	31.95	57.69	77.24149	95.1	1.601177	7.215491	0
8/21/2009	21.190	26.002	32.67	58.24	82.28444	95.2	1.982122	7.881945	1.8
8/22/2009	21.300	23.878	28.12	71.08	88.73684	96.2	0.761649	4.6952459	1.34
8/23/2009	21.830	25.344	32.53	52.22	78.61163	95.2	0.613128	7.3342158	0
8/24/2009	19.530	23.789	31.16	44.35	71.52955	91.7	0.77726	8.9640688	0
8/25/2009	18.390	24.443	32.82	37.44	66.26809	87.5	1.007326	9.7042187	0
8/26/2009	20.010	25.905	33.25	40.45	66.17326	86.6	1.173674	9.4622274	0
8/27/2009	20.410	23.630	29.13	49.2	67.3033	81.2	1.066774	8.0763906	0
8/28/2009	19.610	20.833	23.8	74.42	89.90035	96.1	1.218309	4.0328301	0.4
8/29/2009	19.600	22.854	28.33	66.13	89.14295	96.7	0.975972	4.7012686	1.31
8/30/2009	16.910	23.237	31.29	37.33	67.46955	95.5	0.851823	8.6921577	0
8/31/2009	14.250	18.281	25.56	42.74	66.81233	81.7	0.955285	7.1817764	0
9/1/2009	11.490	18.092	25.91	33.52	60.16684	83.9	0.964128	8.6973948	0
9/2/2009	12.200	19.516	28.21	33.41	63.75576	92.2	0.755038	8.6975485	0
9/3/2009	13.790	20.233	28.54	33.91	61.80149	92.7	0.908292	8.455931	0
9/4/2009	15.730	22.983	29.77	37.95	60.54569	84.4	0.845354	8.3543237	0
9/5/2009	17.790	23.434	31.48	30.14	53.71035	78.55	0.868382	8.3873428	0
9/6/2009	17.510	20.912	28.47	46.45	70.56993	83.6	1.584406	8.6697539	0
9/7/2009	16.620	19.697	23.74	65.02	76.72628	86.4	1.244965	4.5930323	0
9/8/2009	16.070	19.793	23.8	58.78	77.00715	90.8	0.737132	5.1676419	0
9/9/2009	17.080	19.835	23.49	64.07	82.11795	93.5	0.843792	4.3005279	0.23
9/10/2009	13.900	16.550	22.42	52.46	73.48688	93.7	1.672205	5.7615692	0.13
9/11/2009	12.810	15.149	17.44	93	95.575	96.5	2.055181	2.6438968	2.26
9/12/2009	15.960	17.803	20.24	79.38	91.44035	96.8	0.846493	3.6707074	0.23
9/13/2009	17.510	21.525	29.18	39.25	73.77875	96	0.851337	7.0706189	0
9/14/2009	15.690	21.137	28.68	43.63	71.30563	93.7	0.670986	7.8775794	0
9/15/2009	16.840	21.558	29.63	41.29	70.74601	90.5	0.680979	7.559838	0

Date	T_{min}	T_{avg}	T_{max}	RH_{min}	RH	RH_{max}	$u_{z\ avg}$	R_n	Rainfall
	(C)	(C)	(C)	(C)	(C)	(C)	(m/s)	MJ/m2/day	(in)
9/16/2009	15.540	17.162	19.55	69.31	81.98087	93.9	1.410795	2.9327748	0.27
9/17/2009	12.440	15.306	17.27	68.02	82.68806	92.8	0.970413	3.9958133	0.01
9/18/2009	12.950	17.967	25.65	50.97	77.7876	90.7	0.846986	5.0830463	0
9/19/2009	11.000	16.373	23.49	30.34	59.41347	86.1	0.812757	7.426601	0
9/20/2009	9.170	16.868	25.86	32.17	64.22618	93.7	0.931462	7.3315144	0
9/21/2009	11.620	18.472	25.91	50.69	76.07903	95.2	1.185153	6.7748214	0
9/22/2009	17.580	20.891	25.06	62.2	80.65774	96.2	1.604542	4.9736326	0
9/23/2009	19.530	23.008	27.96	63.9	83.28885	95.2	1.478892	4.9180897	0.73
9/24/2009	19.710	23.827	29.47	56.31	75.92677	95.7	0.860142	6.1618554	0.09
9/25/2009	12.080	18.385	25.86	35.44	56.66413	71.26	1.244646	6.2454844	0
9/26/2009	11.130	14.590	19.69	45.55	72.56747	96	1.710618	5.2302256	0.34
9/27/2009	14.070	17.659	22.7	71.01	89.06233	97.4	1.532493	3.5589959	0.58
9/28/2009	12.320	17.202	24.72	49.51	77.6042	94.7	1.868847	6.6999137	0.23
9/29/2009	10.660	15.218	21.84	38.82	63.44868	82.9	1.608653	5.7376377	0
9/30/2009	8.430	13.581	18.06	56.73	72.14868	87.2	0.814934	3.9075758	0
10/1/2009	6.294	10.719	17.61	37.84	68.82472	91.7	0.672306	5.3501219	0
10/2/2009	8.220	14.276	18.37	55.65	74.26486	95.2	2.245948	3.7174434	0.06
10/3/2009	15.250	18.732	23.62	65.38	85.27941	96.8	1.183003	4.2016118	0.02
10/4/2009	11.800	17.230	26.41	31.12	62.12003	93.5	0.81074	5.7916639	0
10/5/2009	10.270	14.644	21.48	37.34	60.0008	81.2	0.938215	5.8282482	0
10/6/2009	7.769	14.978	22.57	35.34	65.22545	88	1.373896	5.8856372	0
10/7/2009	12.010	16.921	22.76	34.6	62.87913	95.3	2.504535	5.7029243	0.06
10/8/2009	8.120	14.917	20.95	38.88	61.84552	87.8	0.964712	5.4482363	0
10/9/2009	13.430	19.058	24.55	49.95	73.78809	93	2.193052	4.4641615	0.03
10/10/2009	9.410	15.843	19.21	50.81	73.97882	92.3	0.976747	3.4401608	0.05
10/11/2009	6.004	12.546	20.63	37.25	63.37469	91.8	0.708514	5.2077222	0
10/12/2009	5.655	8.814	12.08	47.69	62.94024	85.2	1.00958	3.3496622	0
10/13/2009	7.408	12.662	20.81	42.84	65.04934	88.2	1.109438	4.3142708	0
10/14/2009	4.302	8.814	13.29	43.65	61.38552	78.8	0.746635	4.30698	0
10/15/2009	3.084	5.633	8.58	64.67	88.25139	98.8	1.424944	2.5349134	0.85
10/16/2009	2.955	4.286	5.398	91.5	96.62569	98.3	1.557174	2.6900552	0.38
10/17/2009	3.965	5.479	7.883	85.8	93.42326	98	1.558684	2.904894	1.02
10/18/2009	3.322	6.088	8.82	65.06	85.26274	96.7	1.307403	3.0978426	0.27
10/19/2009	2.583	7.843	15.15	35.48	63.07024	94.4	0.804493	4.5887673	0
10/20/2009	4.724	12.360	21.39	31.92	59.41931	77.87	0.657458	4.0460623	0
10/21/2009	9.860	16.587	25.04	30.46	54.08691	76.81	0.715816	4.2060835	0
10/22/2009	11.530	16.667	21.97	27.95	62.05122	80.9	1.375872	3.3823749	0
10/23/2009	10.730	13.731	16.18	63.55	80.40476	97.7	1.869684	2.8815029	0.3
10/24/2009	14.750	18.421	20.69	66.2	91.76719	98	3.1245	2.6520631	1.35
10/25/2009	8.500	12.952	18.17	40.52	56.1384	70.6	1.077868	3.985255	0
10/26/2009	7.100	11.651	17.91	38.74	63.12455	86	1.115434	3.7705146	0
10/27/2009	8.880	11.852	14.32	82	94.26076	97.1	0.982337	2.3675273	0.92
10/28/2009	11.270	13.643	16.69	81.7	92.01771	97.3	1.293177	2.5219758	1.13

Date	T_{min}	T_{avg}	T_{max}	RH_{min}	RH	RH_{max}	$u_{z\ avg}$	R_n	Rainfall
	(C)	(C)	(C)	(C)	(C)	(C)	(m/s)	MJ/m2/day	(in)
10/29/2009	9.560	11.569	14.75	68.8	82.86656	94.3	1.213444	2.8261933	0
10/30/2009	9.460	11.955	13.79	69.3	79.67889	96.8	1.98134	2.7567999	0
10/31/2009	12.250	15.780	20.02	72.65	93.77625	98.2	3.054375	2.2911837	0.11
11/1/2009	8.550	10.647	13.24	55.03	74.20236	92.2	0.852736	2.5818557	0.09
11/2/2009	7.004	10.285	15.66	55.44	70.05486	87.7	0.992142	3.3066479	0
11/3/2009	5.547	10.899	18.44	34.71	61.52427	93.9	1.02374	3.1849358	0
11/4/2009	3.267	8.302	13.58	35.35	53.9033	76.46	1.013483	3.0036175	0
11/5/2009	4.103	8.575	14.43	39.82	63.63993	84.7	1.044681	2.9791738	0.01
11/6/2009	0.633	5.302	10.61	37.24	57.40476	80.4	1.250205	2.9003973	0.01
11/7/2009	-0.454	6.177	12.05	41.9	65.75802	85.5	1.997896	2.8276103	0
11/8/2009	5.804	13.801	21.98	39.15	64.85243	90.6	0.711215	2.9200634	0
11/9/2009	9.940	15.380	20.72	48.53	67.89295	86.6	1.546802	2.9173148	0
11/10/2009	11.270	14.707	18.89	57.56	70.79378	85.6	0.710056	2.5805229	0
11/11/2009	6.782	9.969	13.05	50.38	64.30455	86.1	1.723052	2.4632927	0.11
11/12/2009	5.228	7.250	9.61	49.02	70.69931	87.9	2.212139	2.4388169	0.21
11/13/2009	8.880	10.129	11.98	55.18	80.49885	95.5	2.548257	2.3511069	0.11
11/14/2009	10.800	12.384	13.59	94.5	95.67847	96.8	1.419361	2.2265444	0.15
11/15/2009	12.740	16.194	22.31	54.69	73.51497	94.4	0.895194	2.8391658	0
11/16/2009	8.055	13.111	17.03	37.19	57.4284	82.1	1.189451	2.2803526	0
11/17/2009	6.459	9.844	15	28.15	45.24542	63.65	1.079649	1.9010628	0
11/18/2009	5.136	9.697	14.87	56.82	74.47563	88.2	1.311323	2.4166553	0
11/19/2009	9.920	12.331	15.5	86.4	93.76319	97.7	1.408639	2.196015	0.36
11/20/2009	7.153	12.050	15.76	44.48	66.67531	97.8	1.360233	2.2594942	0.36
11/21/2009	6.089	9.501	15.06	48.95	64.43448	78.82	0.859677	2.1554611	0
11/22/2009	4.603	8.872	14.63	50.85	71.78469	89.1	1.037483	2.1218053	0
11/23/2009	6.388	7.980	9.69	67.29	82.59903	97.6	1.66926	2.2549553	0.09
11/24/2009	7.627	9.872	12.86	79	92.535	98	1.05399	2.198855	0.22
11/25/2009	9.070	10.269	11.46	92.1	95.85382	97.3	0.945563	2.1353537	0.08
11/26/2009	8.690	10.309	12.22	74.03	87.99507	96.5	0.55717	2.1980606	0
11/27/2009	4.139	6.494	8.99	49.76	67.93097	92.3	1.894288	2.1728853	0
11/28/2009	3.039	7.408	12.27	37.78	57.30361	74.92	1.753483	1.5214074	0
11/29/2009	2.354	10.119	18.04	34.17	54.69889	78.68	1.948431	1.4679008	0
11/30/2009	2.259	9.008	12.4	60.84	75.82358	93.5	1.764535	2.2589785	0.32
12/1/2009	0.877	5.306	10.55	40.03	60.23444	80.2	1.163677	1.5610691	0